TECHNISCHE
UNIVERSITÄT
WIEN
Vienna University of Technology

DIPLOMARBEIT

Collective behavior of an ultrarelativistic plasma in an anisotropically expanding geometry

ausgeführt am

Institut für Theoretische Physik
der Technischen Universität Wien

unter der Anleitung von

Univ. Prof. DI Dr. Anton Rebhan

durch

Dominik Steineder
Steinbrechergasse 24/13
A-1220 Wien
steineder@hep.itp.tuwien.ac.at

Wien, 4.12.2009   Unterschrift

Acknowledgements

Contents

Chapter 1

Introduction

Quantum chromodynamics (QCD) is nowadays the well established theory to describe the strong interaction. As quantum electrodynamics (QED), it is a gauge field theory, however with important differences. While QED is an Abelian theory with gauge group $U(1)$, QCD has $SU(3)$ as gauge group and is non-Abelian. In QED the gauge boson associated with $U(1)$ is the photon, which is uncharged. Contrary to this for the color group $SU(3)$ there exist 8 gluons that carry color themselves. Both, QED and QCD, are renormalizable theories and the coupling constant turns out to be a function of the energy scale. But here we find once more a remarkable difference between QCD and QED. While the coupling for the latter increases for larger energy scales, non-Abelian gauge theories have the property that the coupling constant decreases for increasing energy scales. This is called asymptotic freedom and has been tested experimentally by deep inelastic scattering of leptons on nucleons. On the other side, at low energies quarks, which are the matter particles of QCD, are confined in hadrons and these are then the relevant degrees of freedom.

However, according to standard cosmology there existed a gas of almost free quarks and gluons until $10^{-6} - 10^{-5}$s after the Big Bang. This unusual state of matter is called quark-gluon plasma (QGP), in analogy to the conventional electromagnetic plasma, where atoms are split in electrons and ions. The QGP might also occur in the core of heavy neutron stars and it is believed to be produced fleetingly on earth at the Relativistic Heavy Ion Collider (RHIC) at Brookhaven National Laboratory. The conditions under which a QGP may exist are either very hot, with a temperature above a critical temperature T_C of the order of 160 MeV, or extremely dense (or both). At RHIC the required temperatures are achieved by letting ultrarelativistic heavy ions collide. In the following we want to sketch such a collision.

The two heavy nuclei are accelerated nearly to the speed of light and are
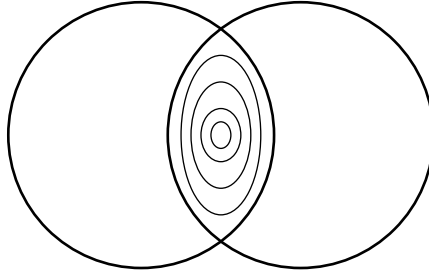
Figure 1.1: Illustration of the almond shaped collision region for a non-central heavy ion collision. The beam line is perpendicular to the plane of the drawing.

therefore strongly Lorentz contracted. They most probably do not collide perfectly head on, so that there is an almond shaped collision region. If nothing interesting happens and the nucleons simply collide independently the detector will show an isotropic distribution of transverse momenta. But in the experiments an anisotropic distribution is detected. This can be explained, if we assume that the products of nucleon-nucleon collisions can not fly out freely but collide themselves with the products of other nucleon-nucleon collisions and therefore come to approximate local thermal equilibrium (e.g. locally thermalized QGP). A short time after the collision of the Lorentz contracted nuclei the almond shaped collision region is filled up into an almond shaped cylinder. There is some central pressure and no pressure outside the cylinder, such that there exists an anisotropic pressure gradient (the pressure gradient must be larger along the shorter diameter of the almond). Due to this pressure gradient the particles are accelerated more along the shorter diameter, which results in an anisotropic momentum distribution. This is called elliptic flow and it is one indication beside others that the QGP has been produced.

However, when simulations of ideal hydrodynamics are matched to experimental data, it is found that the data is described well only if the QGP thermalizes very rapidly on a time scale of the order of or perhaps smaller than 1 fm/c. One way to describe this fast thermalization is to assume a strongly coupled plasma. Actually the data harvested at RHIC seems to indicate that the produced QGP is indeed not weakly coupled. This means that at center of mass energies achieved at RHIC the QCD coupling constant is not sufficiently small such that perturbative methods could be used. Strongly coupled systems have been investigated analytically by making use of the AdS/CFT conjecture in the recent past. However, soon the experiments at the LHC at CERN will study heavy ion collision at much higher

center of mass energies and therefore it might be possible that the plasma shows specific perturbative features there. But even if it turns out that the LHC can not reach high enough energies, a better understanding of the weakly coupled QGP is still desireable, since already in the case of RHIC physics the actual truth will most probably be somewhere in between the strong and weak coupling asymptotics.

In this thesis we want to examine the weakly coupled QGP and there a key issue in the context of the fast thermalization is the understanding of the collective behavior of the plasma and especially of the instabilities that arise in non-equilibrium situations present in the early stage after the collision. To be able to describe such systems, we need to take into account that the QGP expands into the vacuum after the collision and this makes a non-stationary treatment inevitable.

We only investigate the theoretically clean limit at asymptotically weak coupling and additionally we consider the linear approximation, which is valid for sufficiently weak gauge fields, where non-Abelian self-interactions are negligible. Therefore we are dealing with an effectively Abelian theory in the following. This thesis is organized as follows: In chapter 2 we present some basics of thermal quantum field theory, that we use to obtain the collective behavior of an isotropic plasma in chapter 3. In chapter 4 we analyze the implications of anisotropic momentum distributions of the particles in the plasma in stationary situations. We also discuss the presence of instabilities before we turn to the investigation of anisotropically expanding plasmas in chapter 5. Eventually we present our results for the time evolution of the gauge fields in chapter 6, where we examine the collective modes in detail.

We use natural units ($c = \hbar = k_B = 1$) and the Minkowski signature $(+, -, -, -)$ throughout this thesis.

Chapter 2

Basics of thermal QFT

In this introductory chapter we want to establish some concepts of quantum field theory at finite temperature. The discussion presented here is mainly concerned with aspects we will need later. We will skip many important facets of the theory and the interested reader is referred to the textbooks [1, 2] and to [3, 4].

2.1 Partition function as functional integral

2.1.1 Quantum statistical mechanics

We start by recalling some important facts from quantum statistical mechanics. In equilibrium statistical mechanics it is possible to work in different ensembles depending on the characteristics of the system:

microcanonical ensemble: energy E, particle number N and volume V fixed

canonical ensemble: temperature T, N and V fixed; E variable

grand canonical ensemble: T, chemical potential μ and V fixed; E and N variable

$\beta = T^{-1}$ and μ can be thought of as Lagrange multipliers, which determine the mean energy and the mean particle number in the canonical and grand canonical ensemble. In general, every conserved observable $\hat{N}_i$, like charge or baryon number, can be associated with a chemical potential μ_i.

In equilibrium the fundamental quantity in statistical mechanics is the statistical density matrix $\hat{\rho}$, which is defined as

$$\hat{\rho} = e^{-\beta(\hat{H} - \mu_i \hat{N}_i)} \tag{2.1}$$

4

and the partition function Z is given by

$$Z = \text{Tr}\hat{\rho} = \text{Tr}e^{-\beta(\hat{H}-\mu_i\hat{N}_i)}. \tag{2.2}$$

With the knowledge of the partition function the other thermodynamic properties, such as pressure, entropy or energy can be obtained from it. The thermal expectation value of any observable $\hat{A}$ can be obtained from

$$\langle\hat{A}\rangle = \frac{1}{Z}\text{Tr}(\hat{\rho}\hat{A}). \tag{2.3}$$

2.1.2 Transition amplitude

After this short reminder of quantum statistical mechanics we want to rewrite the partition function as a functional integral. Before we can do this, we first want to calculate the transition amplitude. To be accurate, we consider bosonic fields and will remark on fermions later.

In conventional quantum mechanics the projection of an eigenstate $\langle\mathbf{x}|$ of the position operator $\hat{\mathbf{x}}$ onto the eigenstate $|\mathbf{p}\rangle$ of the momentum operator $\hat{\mathbf{p}}$ is given by

$$\langle\mathbf{x}|\mathbf{p}\rangle = e^{i\mathbf{p}\cdot\mathbf{x}} \tag{2.4}$$

In QFT we have an infinite number of degrees of freedom and therefore the discrete sum $\sum_i p_i x_i$ becomes an integral,

$$\langle\phi|\pi\rangle = e^{i\int d^3x\pi(\mathbf{x})\phi(\mathbf{x})}. \tag{2.5}$$

In the above expression $\phi(\mathbf{x})$ and $\pi(\mathbf{x})$ are eigenfunctions of the field operator $\phi(t,\mathbf{x})$ and the conjugate momentum operator $\pi(t,\mathbf{x})$ at $t=0$, respectively. The completeness and orthogonality conditions are

$$\int d\phi(\mathbf{x})|\phi\rangle\langle\phi| = 1, \tag{2.6}$$

$$\int \frac{d\pi(\mathbf{x})}{2\pi}|\pi\rangle\langle\pi| = 1, \tag{2.7}$$

$$\langle\phi_a|\phi_b\rangle = \delta[\phi_a(\mathbf{x}) - \phi_b(\mathbf{x})], \tag{2.8}$$

$$\langle\pi_a|\pi_b\rangle = \delta[\pi_a(\mathbf{x}) - \pi_b(\mathbf{x})] \tag{2.9}$$

and the Hamiltonian $\hat{H}$ can be written as an integral of the Hamilton density $\mathcal{H}$, which depends on the field operators

$$\hat{H} = \int d^3x\mathcal{H}(\pi(\mathbf{x}),\phi(\mathbf{x})). \tag{2.10}$$

We want to find the transition amplitude for identical initial and final states ϕ. The reason for this will be clear in a moment. We divide the time interval $[t_i = 0, t_f = t]$ into N pieces of length Δt and let $N \to \infty$

$$
\begin{aligned}
\langle \phi | e^{-i\hat{H}t} | \phi \rangle &= \lim_{N \to \infty} \langle \phi | e^{-i\hat{H}\Delta t} e^{-i\hat{H}\Delta t} \ldots e^{-i\hat{H}\Delta t} | \phi \rangle \quad (2.11) \\
&= \lim_{N \to \infty} \int \prod_{i=1}^{N} \frac{d\pi_i}{2\pi} d\phi_i \langle \phi | \pi_N \rangle \langle \pi_N | e^{-i\hat{H}\Delta t} | \phi_N \rangle \langle \phi_N | \pi_{N-1} \rangle \times \\
&\quad \langle \pi_{N-1} | e^{-i\hat{H}\Delta t} | \phi_{N-1} \rangle \times \ldots \times \langle \phi_2 | \pi_1 \rangle \langle \pi_1 | e^{-i\hat{H}\Delta t} | \phi_1 \rangle \langle \phi_1 | \phi \rangle.
\end{aligned}
$$

Here, we inserted each of the completeness relations N times alternatingly. Looking at the terms involving the Hamiltonian, we can write these as

$$
\begin{aligned}
\langle \pi_i | e^{-i\hat{H}\Delta t} | \phi_i \rangle &= e^{-i\Delta t \int d^3 x \mathcal{H}(\pi_i, \phi_i)} \langle \pi_i | \phi_i \rangle \\
&= e^{-i\Delta t \int d^3 x \mathcal{H}(\pi_i, \phi_i)} e^{i \int d^3 x \pi_i \phi_i}. \quad (2.12)
\end{aligned}
$$

This is allowed since Δt is infinitesimally small and when we expand the exponential we can neglect all terms of $O(\Delta t^2)$. Finally for the last factor in (2.12) we get, according to the orthonormality condition $\langle \phi_1 | \phi \rangle = \delta(\phi - \phi_1)$. Putting the pieces together we find

$$
\begin{aligned}
\langle \phi | e^{i\hat{H}t} | \phi \rangle &= \lim_{N \to \infty} \int \prod_{i=1}^{N} \frac{d\pi_i}{2\pi} d\phi_i \delta(\phi - \phi_1) \times \\
&\quad \exp \left\{ i\Delta t \sum_{j=1}^{N} \int d^3 x \left[\pi_j \frac{\phi_{j+1} - \phi_j}{\Delta t} - \mathcal{H}(\pi, \phi) \right] \right\}. \quad (2.13)
\end{aligned}
$$

where $\phi_{N+1} = \phi$. Finally we take the limit $N \to \infty$ and obtain

$$
\langle \phi | e^{i\hat{H}t} | \phi \rangle = \int \mathcal{D}\pi \int_{\phi(0,\mathbf{x})=\phi}^{\phi(t,\mathbf{x})=\phi} \mathcal{D}\phi \exp \left\{ i \int_0^{t_f} dt \int d^3 x \left[\pi \partial_t \phi - \mathcal{H}(\pi, \phi) \right] \right\},
$$
$$(2.14)$$

where we denoted the continuum limit of the functional integration as

$$
\int \prod_{i=1}^{N} \frac{d\pi_i}{2\pi} d\phi_i \to \int \mathcal{D}\pi \int \mathcal{D}\phi. \quad (2.15)
$$

We emphasize that the fields ϕ and π in (2.14) depend on time and space coordinates.

Finally we want to compare the partition function (2.2) with the result for the transition amplitude (2.14)

$$
\begin{aligned}
Z &= \mathrm{Tr} e^{-\beta(\hat{H} - \mu_i \hat{N}_i)} \\
&= \int d\phi \langle \phi | e^{-\beta(\hat{H} - \mu_i \hat{N}_i)} | \phi \rangle \\
&= \int \mathcal{D}\pi \int_{periodic} \mathcal{D}\phi \exp \left\{ - \int_0^\beta d\tau \int d^3 x (\mathcal{H} - \mu_i \mathcal{N}_i - i\pi \partial_\tau \phi) \right\}.
\end{aligned}
\tag{2.16}
$$

Now it should be obvious why we calculated the transitions amplitude for identical initial and final states. Here, we identify the inverse temperature with "imaginary time" $\tau = it$ [1], such that the integration over τ goes from 0 to $1/T$. "Periodic" in the above expression means that all ϕ's have to satisfy $\phi(0, \mathbf{x}) = \phi(\beta, \mathbf{x})$, hence they must be periodic in imaginary time.

It is possible to write the partition function in the form of the usual path integrals known in conventional quantum mechanics, in terms of the Lagrangian instead of the Hamiltonian. After a shift of the conjugate momenta (e.g. $\tilde{\pi} = \pi - \partial_t \phi$ for a real non-interacting scalar field), the integral over the π's, which turns out to be a Gaussian integral, factorizes and gives a constant. Therefore we obtain

$$
Z = const. \int_{periodic} \mathcal{D}\phi \exp \left\{ \int_0^\beta d\tau \int d^3 x \mathcal{L} \right\}.
\tag{2.17}
$$

Actually the situation is different for fermions, since they are anticommuting objects. This manifests in the partition function such that

$$
Z = \mathrm{Tr} e^{-\beta \hat{H}} = \int d\eta^* d\eta e^{-\eta^* \eta} \langle -\eta | e^{-\beta \hat{H}} | \eta \rangle,
\tag{2.18}
$$

where η is an anticommuting number. Note the different sign convention for the trace. Finally it turns out that for fermions we need antiperiodic boundary conditions in (2.16) and (2.17) instead of periodic ones[2].

2.2 Matsubara frequencies

We will exclusively consider the so called "imaginary time" or "Matsubara formalism" (ITF). Since we will only use diagrammatic methods in equilibrium situations, ITF is convenient for our purpose[3].

---

[1]This can also be interpreted as going from Minkowski to Euclidean space, where τ is real, since the Minkowski metric transforms into a Euclidean metric ($t^2 - \mathbf{x}^2 \to -(\tau^2 + \mathbf{x}^2)$).

[2]More details on this are given in [1, 2, 3].

[3]The "real time formalism" is treated in [2].
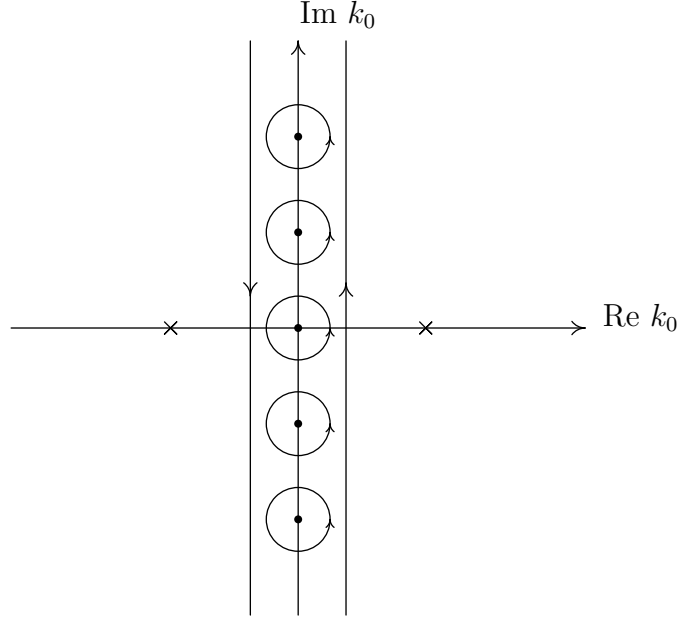
Figure 2.1: The integration contour in the complex k_0 plane

2.2.1 Bosons

In 2.1.2 we met the condition for the bosonic field to be periodic in imaginary time with periodicity β. This translates to discrete frequencies, the so called bosonic Matsubara frequencies ω_n, in momentum space. To see this, we Fourier transform the field

$$\phi(X) = \sqrt{\frac{\beta}{V}} \sum_K e^{-iK\cdot X}\phi(K) = \sqrt{\frac{\beta}{V}} \sum_K e^{i(\omega_n\tau + \mathbf{k}\cdot\mathbf{x})}\phi(K). \tag{2.19}$$

The normalization is chosen such, that the Fourier-transformed field $\phi(K)$ is dimensionless. Capital letters denote four-momenta

$$X \equiv (t, \mathbf{x}) = (-i\tau, \mathbf{x}), \qquad K \equiv (k_0, \mathbf{k}) = (-i\omega_n, \mathbf{k}) \tag{2.20}$$

and by $K\cdot X = k_0 t - \mathbf{k}\cdot\mathbf{x}$ we mean the Minkowski scalar product. Demanding $\phi(0, \mathbf{x}) = \phi(\beta, \mathbf{x})$, we need that $e^{i\omega_n\beta} = 1$ and therefore

$$\omega_n = \frac{2\pi n}{\beta} = 2\pi nT, \qquad n \in \mathbb{Z}. \tag{2.21}$$

Next we present a method to calculate Matsubara sums making use of contour integration. We assume $g(\omega = i\omega_n)$ is regular along the imaginary

axis. We can rewrite the sum over ω_n

$$T \sum_{n=-\infty}^{n=+\infty} g(\omega = i\omega_n) = \frac{1}{2\pi i} \oint_{\mathcal{C}} d\omega g(\omega) \frac{1}{2} \coth \frac{\omega}{2T}, \qquad (2.22)$$

where the contour $\mathcal{C}$ encircles all the poles along the imaginary axis coming from $\coth \frac{\omega}{2T}$, but none of the possible poles of $g(\omega)$ away from the imaginary axis. In figure 2.1 the dots refer to poles of $\coth \frac{\omega}{2T}$, which are located where the denominator $e^{\omega/2T} - e^{-\omega/2T} = 0$, hence at $\omega = i\omega_n$. Therefore (2.22) simply follows from the residue theorem[4]

$$\frac{1}{2\pi i} \oint_{\mathcal{C}} h(z) = \sum_n \text{Res } h(z)|_{z=z_n}. \qquad (2.23)$$

To solve the contour integral we can deform the contour into vertical lines as shown in figure 2.1 and substitute $\omega \to -\omega$ for one integral. We then obtain

$$T \sum_{n=-\infty}^{n=+\infty} g(\omega = i\omega_n) = \frac{1}{2\pi i} \int_{-i\infty+\epsilon}^{i\infty+\epsilon} dk_0 \left[g(\omega) + g(-\omega) \right] \frac{1}{2} \coth \frac{\omega}{2T}, \qquad (2.24)$$

with $\epsilon \to 0^+$. To evaluate (2.24) we can close the path with a large half circle which allows us to pick up the poles of $g(\omega)$ (indicated by crosses in figure 2.1) and then use the residue theorem a second time. Finally we can use an identity, which can be derived easily,

$$\frac{1}{2} \coth \frac{x}{2T} = \frac{1}{2} + f_B(x), \qquad (2.25)$$

where $f_B(x) = (e^{\beta x} - 1)^{-1}$ is the Bose-Einstein distribution.

A simple example is

$$T \sum_{n=-\infty}^{n=+\infty} \frac{1}{\omega_n^2 + p^2} = \frac{1}{2p} \left[1 + 2f_B(p) \right]. \qquad (2.26)$$

2.2.2 Fermions

For fermions we will repeat the procedure taking into account the antiperiodicity of the fields. The Fourier transformed expression with ω_n again being the Matsubara frequency, but this time for fermions, is given by

$$\psi(X) = \frac{1}{\sqrt{V}} \sum_K e^{-iK \cdot X} \psi(K) = \frac{1}{\sqrt{V}} \sum_K e^{i(\omega_n \tau + \mathbf{k} \cdot \mathbf{x})} \psi(K). \qquad (2.27)$$

---

[4]If we can write the function h as $h(z) = \phi(z)/\psi(z)$, with analytic functions $\phi(z)$ and $\psi(z)$, the residues are $\text{Res } h(z)|_{z=z_n} = \phi(z_n)/\psi'(z_n)$.

Noting that $\psi(0, \mathbf{x}) = -\psi(\beta, \mathbf{x})$, which implies that $e^{i\omega_n\beta} = -1$, we find for the fermionic Matsubara frequencies

$$\omega_n = \frac{(2n+1)\pi}{\beta} = (2n+1)\pi T, \qquad n \in \mathbb{Z}. \tag{2.28}$$

Matsubara sums for fermions can be done by contour integration, just as for bosons, if we replace the coth $\frac{\omega}{2T}$ by a tanh $\frac{\omega}{2T}$ (The requirements for $g(\omega)$ are the same.)

$$T\sum_{n=-\infty}^{n=+\infty} g(\omega = i\omega_n) = \frac{1}{2\pi i}\oint_{\mathcal{C}} d\omega g(\omega)\frac{1}{2}\tanh\frac{\omega}{2T}. \tag{2.29}$$

The contour $\mathcal{C}$ encloses only the poles from tanh $\frac{\omega}{2T}$, which are given by the zeros of $e^{\omega/2T} + e^{-\omega/2T}$ and hence for $\omega = i\omega_n$. After deforming the contour and making use of $\omega \to -\omega$ we obtain

$$T\sum_{n=-\infty}^{n=+\infty} g(\omega = i\omega_n) = \frac{1}{2\pi i}\int_{-i\infty+\epsilon}^{i\infty+\epsilon} dk_0 \left[g(\omega) + g(-\omega)\right]\frac{1}{2}\tanh\frac{\omega}{2T}. \tag{2.30}$$

This can again be calculated by closing the contour with a large half circle, such that the poles of $g(\omega)$ are encircled and then using the residue theorem. Note that we can rewrite

$$\frac{1}{2}\tanh\frac{x}{2T} = \frac{1}{2} - f_F(x), \tag{2.31}$$

with $f_F(x) = (e^{x/T} + 1)^{-1}$ being the Fermi-Dirac distribution function.

The simplest Matsubara sum in the fermionic case is given by

$$T\sum_n \frac{1}{\omega_n^2 + p^2} = \frac{1}{2p}[1 - 2f_F(p)]. \tag{2.32}$$

Examples of fermionic Matsubara sums we will need for the calculation of the photon self-energy, which are related to loop diagrams, are

$$T\sum_n \frac{1}{(\omega_n^2 + E_1^2)((\omega_n - \nu_m)^2 + E_2^2)} =$$
$$-\sum_{s_1,s_2=\pm 1} \frac{s_1 s_2}{4E_1 E_2}\frac{1 - f_F(s_1 E_1) - f_F(s_2 E_2)}{i\nu_m - s_1 E_1 - s_2 E_2}, \tag{2.33}$$

$$T\sum_n \frac{\omega_n}{(\omega_n^2 + E_1^2)((\omega_n - \nu_m)^2 + E_2^2)} =$$
$$\sum_{s_1,s_2=\pm 1} \frac{is_2}{4E_2}\frac{1 - f_F(s_1 E_1) - f_F(s_2 E_2)}{i\nu_m - s_1 E_1 - s_2 E_2}. \tag{2.34}$$

Here ω_n and ν_m are fermionic and bosonic Matsubara frequencies, respectively.

2.3 Gauge theories

To conclude this chapter we want to add some brief remarks on gauge theories. At first we state some facts of non-Abelian gauge theories such as QCD, but we will keep it general and consider the gauge group $SU(N)$ ($N = 3$ for QCD). The generators of the group are denoted by T_a. The index a runs in integral steps from 1 to $N^2 - 1$. The generators satisfy the commutation relation

$$[T_a, T_b] = if_{abc}T_c, \tag{2.35}$$

where the f_{abc} are the totally antisymmetric structure constants of the group. The generators are normalized such that

$$\text{Tr}[T_aT_b] = \frac{1}{2}\delta_{ab}. \tag{2.36}$$

The gauge fields and the field strength tensor can be expanded in terms of T_a

$$A_\mu = A_\mu^a T_a, \quad F_{\mu\nu} = F_{\mu\nu}^a T_a, \quad F_{\mu\nu}^a = \partial_\mu A_\nu^a - \partial_\nu A_\mu^a + gf^{abc}A_\mu^b A_\nu^c, \tag{2.37}$$

with g being the coupling constant. Infinitesimal gauge transformations of the gauge fields read[5]

$$\delta A_\mu^a(x) = D_\mu^{ab}(x)\omega^b(x) = (\partial_\mu\delta^{ab} + gf^{abc}A_\mu^c(x))\omega^b(x), \tag{2.38}$$

where D_μ^{ab} is the covariant derivative and $\omega^b(x)$ are infinitesimal scalar functions which parametrize the gauge transformation. The Lagrangian of the pure gauge theory is given by

$$\mathcal{L} = -\frac{1}{4}F_{\mu\nu}^a F_a^{\mu\nu}. \tag{2.39}$$

After this general remarks on non-Abelian gauge theories we want to find the appropriate partition function. This is done in detail for electromagnetic fields in [1, 2]. Here we simply want to give the main idea of the calculation and state the final result for both, Abelian and non-Abelian gauge theories.

If one naively writes down the partition function as in (2.17), there is a redundancy in the path integral. The reason for this is that we sum over

---

[5]The gauge fields transform under a gauge transformation $U(x) = e^{ig\omega^a(x)T_a} \in SU(N)$ according to $A_\mu \rightarrow UA_\mu U^{-1} + \frac{i}{g}U\partial_\mu U^{-1}$.

physically equivalent configurations where the gauge fields only differ by a gauge transformation, hence they belong to the same gauge orbit. We want to pick out only one configuration of each gauge orbit, which can be done by the so called "Faddeev-Popov trick" that is well known in zero temperature field theory [5, 6, 7]. Using a gauge fixing condition $f^a(A^b_\mu(x)) = 0$ we can insert

$$1 = \Delta_f(A)\Delta_f^{-1}(A), \quad \text{with} \quad \Delta_f^{-1}(A) = \int \prod_x dh(x) \prod_{x,a} \delta[f^a(^hA(x))] \quad (2.40)$$

into the path integral. $h(x)$ is the x-dependent group element and $^hA(x)$ is the gauge transform of $A(x)$. It is then possible to integrate over $h(x)$, hence over gauge orbits, to obtain for the partition function

$$Z = \int_{periodic} \mathcal{D}A^a_\mu \Delta_f(A) \prod_{x,a} \delta[f^a(A(x))] \exp\left\{\int_0^\beta d\tau \int d^3x \mathcal{L}\right\}. \quad (2.41)$$

$\Delta_f(A)$ is the Faddeev-Popov determinant

$$\Delta_f(A) = \det\left(\frac{\delta f^a(^\omega A(x))}{\delta\omega^b(y)}\right) = \det\left(\frac{\partial f^a}{\partial A^c_\mu(x)} D^{cb}_\mu(x)\delta^{(4)}(x-y)\right). \quad (2.42)$$

For Abelian electromagnetism a takes only one value and $D^{ab}_\mu \to \partial_\mu$. $\Delta_f(A)$ does not play a role in zero temperature QED since there it is not field dependent. However, we must keep it at finite temperatures even for QED because the determinant depends on temperature through the boundary conditions.

Finally we can write the Faddeev-Popov determinant as a functional integral over anticommuting Grassmann fields $\eta(x)$ and $\bar\eta(x)$ by

$$\Delta_f(A) = \int_{periodic} \mathcal{D}(\eta, \bar\eta) \exp\left\{\int_0^\beta d\tau \int d^3x \bar\eta_a \left(\frac{\partial f^a}{\partial A^c_\mu} D^{cb}_\mu\right)\eta_b\right\}. \quad (2.43)$$

Despite of their fermionic character $\eta(x)$ and $\bar\eta(x)$ obey periodic boundary conditions. These fields are called Faddeev-Popov ghosts. In QED it can be shown that the ghost fields do not interact with any other fields[6] but serve only to eliminate the unphysical degrees of freedom of the photon in the partition function. The situation is different for non-Abelian gauge theories, where, in general, the ghost fields have interaction terms with physical fields and therefore Feynman graphs containing ghost lines must be taken into account.

---

[6]This can be seen already in (2.43), because this expression has no dependence on A^μ for QED.

Chapter 3

Collective excitations in an isotropic plasma

In a medium the properties of elementary particles get modified due to inter-actions. We then speak about quasi-particles or collective modes, which can be characterized by a dispersion law $\omega(\mathbf{q})$. If we consider a weakly coupled plasma ($g \ll 1$), we can define a hierarchy of scales in the system. The energy scale T is characteristic of individual particles, since their average energy is $\sim T$ and the distance between two neighboring particles is $\sim T^{-1}$. We are now interested in the energy scale gT (with g replaced by the electron charge e for QED) at which collective motion of particles takes place over distances $\sim 1/gT$.

We will calculate the polarization tensor for photons and gluons, from which we can obtain the dispersion relation of collective modes, in the Hard Thermal Loop (HTL) approximation. At the end we will show, that we can obtain the same results from kinetic theory, which can be understood since the typical wavelength of the collective excitation ($\lambda \sim 1/gT$) is much larger than the thermal wavelength ($\lambda \sim 1/T$) and thus a semi-classical treatment might be appropriate.

3.1   Why Hard Thermal Loops?

Before we come to the actual calculation of the photon polarization tensor, we will briefly describe the HTL approximation. HTLs are the dominant one-loop diagrams in the limit of high temperature. They are generated by a small part of the integration region, where the loop momentum K^μ is "hard", which means it is of order the temperature. In our terminology a momentum Q^μ is "soft" if every component of Q is of order gT. The reason why we need
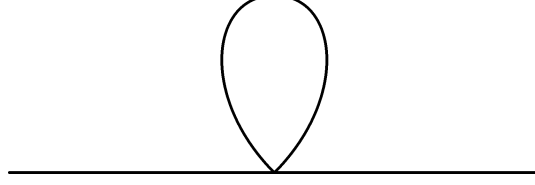
Figure 3.1: Self-energy in $\lambda\phi^4$-theory

HTLs can be illustrated by an example from scalar $\lambda\phi^4$-theory [1, 8].

Let us consider the one-loop self-energy (fig. 3.1)

$$\Pi = 12g^2 T \sum_n \int \frac{d^3k}{(2\pi)^3} \frac{1}{\omega_n^2 + \epsilon_k^2} = 12g^2 \int \frac{d^3k}{(2\pi)^3} \frac{1}{2\epsilon_k} \left(1 + 2f_B(\epsilon_k)\right), \quad (3.1)$$

with $\epsilon_k = \sqrt{\mathbf{k}^2 + m^2}$. The term independent of T is ultraviolet divergent and must be removed by zero-temperature renormalization (here we simply drop it). The thermal part is finite and in the high temperature limit (where all masses are negligible) the integral is dominated by momenta $k \sim T$. The leading term contribution, which is the HTL, is proportional to T^2

$$\Pi \simeq g^2 T^2. \quad (3.2)$$

The effective propagator is given by $\Delta^{-1} = \Delta_0^{-1} + \Pi$ and can be written in momentum space as

$$\Delta(K) = \frac{1}{\omega_n^2 + q^2 + g^2 T^2}. \quad (3.3)$$

When the momentum Q is hard, the self energy contribution is simply a small perturbative correction. However, if the momentum is soft, the correction will be as large as the inverse propagator and hence definitely not negligible. We see that conventional perturbation theory, which counts the loop order, breaks down when we calculate corrections at soft scales. This is because the HTL contributions to one-loop vertex functions are of the same order of magnitude as their tree-level counterparts for external momenta $Q \sim gT$ [1], which is the energy scale we want to consider in what follows.

---

[1]for details see [9]
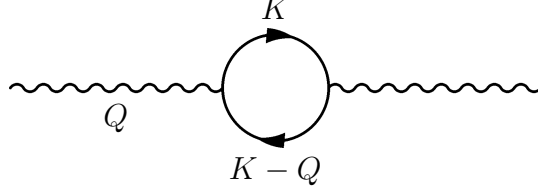
Figure 3.2: Photon self-energy

3.2   The polarization tensor

The photon polarization tensor $\Pi_{\mu\nu}$ (figure 3.2) is given by

$$\Pi_{\mu\nu}(Q) = e^2 T \sum_n \int \frac{d^3 k}{(2\pi)^3} \text{Tr}[\gamma_\mu \slashed{K} \gamma_\nu (\slashed{K} - \slashed{Q})] \tilde{\Delta}(K) \tilde{\Delta}(K - Q), \qquad (3.4)$$

where $\tilde{\Delta}(K) = (\omega_n^2 + k^2)^{-1}$ and $\tilde{\Delta}(K - Q) = ((\omega_n - \nu_m)^2 + (\mathbf{k} - \mathbf{q})^2)^{-1}$, with ω_n being a fermionic Matsubara frequency. We point out that since the external momentum Q belongs to the photon, the Matsubara frequency ν_m is bosonic [2]. In the HTL approximation we can neglect the soft external momentum $\slashed{Q}$ with respect to $\slashed{K}$ in the numerator, because we expect the main contribution to the loop integration coming from $K \sim T$.

The trace gives

$$\text{Tr}[\gamma_\mu \slashed{K} \gamma_\nu \slashed{K}] = 8 K_\mu K_\nu - 4 K^2 g_{\mu\nu}. \qquad (3.5)$$

For the polarization tensor we find

$$\begin{aligned}
\Pi_{\mu\nu}(Q) =& 8 e^2 T \sum_n \int \frac{d^3 k}{(2\pi)^3} K_\mu K_\nu \tilde{\Delta}(K) \tilde{\Delta}(K - Q) \\
&+ 4 e^2 g_{\mu\nu} T \sum_n \int \frac{d^3 k}{(2\pi)^3} \tilde{\Delta}(K - Q) \\
=& I_{\mu\nu} - g_{\mu\nu} \frac{e^2 T^2}{6},
\end{aligned} \qquad (3.6)$$

[2]Here our convention is $k_0 = i\omega_n$ and $q_0 = i\nu_n$.

where we used that $\tilde{\Delta}(K) = -1/K^2$ and evaluated [3]

$$T\sum_n \int \frac{d^3k}{(2\pi)^3} \tilde{\Delta}(K-Q) = T\sum_n \int \frac{d^3k}{(2\pi)^3} \tilde{\Delta}(K)$$

$$= \int \frac{d^3k}{(2\pi)^3} \frac{1}{2k}(1 - 2f_F(k)) \simeq -\frac{T^2}{24}. \qquad (3.7)$$

The Matsubara sum was performed according to (2.32) and the $\simeq$ means that we keep only the T^2 part of the result. It remains to calculate $I_{\mu\nu}$, which can be done by making use of (2.33) and (2.34). With $-\omega_m^2 = k_0^2 = K^2 + k^2$ we obtain for I_{00}

$$I_{00} = \frac{e^2 T^2}{3} + 2e^2 \int \frac{d^3k}{(2\pi)^3} \frac{k^2}{E_1 E_2} \times$$

$$\left[\left(\frac{1}{q_0 + E_1 + E_2} - \frac{1}{q_0 - E_1 - E_1} \right)(1 - f_F(E_1) - f_F(E_2)) + \right.$$

$$\left. \left(\frac{1}{q_0 + E_1 - E_2} - \frac{1}{q_0 - E_1 + E_2} \right)(f(E_1) - f(E_2)) \right], \qquad (3.8)$$

with $E_1 = k$ and $E_2 = |\mathbf{k} - \mathbf{q}|$. We note that $q_0 = i\nu_m$ is a discrete bosonic Matsubara frequency. In the HTL approximation, with $k \sim T$ and $q \sim eT \ll T$, we find for the denominators

$$q_0 \pm E_1 \pm E_2 \simeq \pm 2k, \qquad q_0 \pm E_1 \mp E_2 \simeq q_0 \pm \mathbf{q} \cdot \hat{\mathbf{k}}, \qquad (3.9)$$

and for the distribution functions

$$1 - f_F(E_1) - f_F(E_2) \simeq 1 - 2f_F(k), \qquad f_F(E_1) - f_F(E_2) \simeq \mathbf{q} \cdot \hat{\mathbf{k}} \frac{\partial f_F(k)}{\partial k}. \qquad (3.10)$$

The first term in square brackets of (3.8) turns out to be of the same form as (3.7). Finally after merging all contributions to Π_{00} the only term that survives is the second term in the square bracket above and we thus obtain

$$\Pi_{00}(Q) = 2e^2 \int \frac{d^3k}{(2\pi)^3} \left(\frac{1}{q_0 + \mathbf{q} \cdot \hat{\mathbf{k}}} - \frac{1}{q_0 - \mathbf{q} \cdot \hat{\mathbf{k}}} \right) \mathbf{q} \cdot \hat{\mathbf{k}} \frac{\partial f_F(k)}{\partial k}$$

$$= 4e^2 \int \frac{d^3k}{(2\pi)^3} \left(1 - \frac{q_0}{q_0 - \mathbf{q} \cdot \hat{\mathbf{k}}} \right) \frac{\partial f_F(k)}{\partial k}, \qquad (3.11)$$

---

[3]The divergent term independent of T must be again removed by zero temperature renormalization.
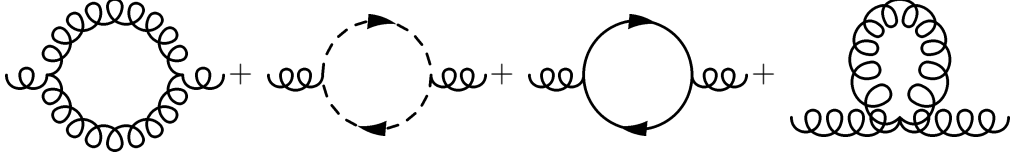
Figure 3.3: Feynman diagrams contributing to the gluon self-energy. Curly lines: gluons. Dashed lines: ghosts. Solid lines: quarks.

where we used that the angular integral gives the same result for both terms. Finally we can perform the k-integral exactly,

$$\int_0^\infty k^2 dk \frac{\partial f_F(k)}{\partial k} = -T^2 \int_0^\infty dx \frac{x^2 e^x}{(e^x+1)^2} = -\frac{T^2\pi^2}{6}, \qquad (3.12)$$

and find for the considered component of the polarization tensor

$$\Pi_{00}(Q) = -2m^2 \left(1 - \int \frac{d\Omega}{4\pi} \frac{q_0}{q_0 - \mathbf{q}\cdot\hat{\mathbf{k}}} \right). \qquad (3.13)$$

In the last step we defined the photon thermal mass m by [2]

$$m^2 = \frac{e^2 T^2}{6}. \qquad (3.14)$$

The remaining components can also be obtained by making use of the fermionic Matsubara sums (2.33) and (2.34). Eventually we get

$$\Pi_{0i}(Q) = 2m^2 \int \frac{d\Omega}{4\pi} \frac{q_0 \hat{k}_i}{q_0 - \mathbf{q}\cdot\hat{\mathbf{k}}}, \qquad (3.15)$$

$$\Pi_{ij}(Q) = 2m^2 \int \frac{d\Omega}{4\pi} \frac{q_0 \hat{k}_i \hat{k}_j}{q_0 - \mathbf{q}\cdot\hat{\mathbf{k}}}. \qquad (3.16)$$

To obtain the gluon self-energy we need to compute the Feynman graphs shown in figure 3.3. In [1, 2] it is shown that in the HTL limit we will obtain the same result as for QED, if we write the correct gluon mass m_g instead of the photon mass m

$$m_g^2 = \frac{g^2 T^2}{6} \left(N_c + \frac{1}{2} N_f \right), \qquad (3.17)$$

with N_c being the number of colors and N_f being the number of quark flavors. This is a rather surprising result, since it follows that the functional form of the dispersion relation will be the same for photons and gluons at least to lowest order in the coupling constants.

3.3   Dispersion relations

The HTL self-energy is a symmetric second-rank tensor and can, in general, be written as a linear combination of $g_{\mu\nu}$, $Q_\mu Q_\nu$, $U_\mu U_\nu$ and $Q_\mu U_\nu + Q_\nu U_\mu$. Here U_μ is the four-velocity of the heat bath, which we choose $U_\mu = \delta_\mu^0$. Furthermore it can be proven that the HTL polarization tensor obeys the Ward identity

$$Q^\mu \Pi_{\mu\nu}(Q) = 0 \qquad (3.18)$$

and therefore it is transverse. With this additional requirement we can decompose it making use of projection operators

$$P_T^{ij} = \delta^{ij} - \hat{q}^i \hat{q}^j, \qquad P_T^{00} = P_T^{0i} = P_T^{i0} = 0, \qquad (3.19)$$

$$P_L^{\mu\nu} = \frac{Q^\mu Q^\nu}{Q^2} - g^{\mu\nu} - P_T^{\mu\nu}, \qquad (3.20)$$

that are both 4-transverse to Q. Furthermore the projector P_T is also 3-transverse, while P_L is 3-longitudinal. Hence we call the term of the self-energy proportional to P_T "transverse" and the part proportional to P_L "longitudinal". The HTL self-energy written in terms of the projectors is now given by

$$\Pi_{\mu\nu}(Q) = F(Q) P_{L,\mu\nu} + G(Q) P_{T,\mu\nu}. \qquad (3.21)$$

It remains to calculate the functions $F(Q)$ and $G(Q)$. We assume that the external momentum vector $\mathbf{q}$ points in the z direction. We then find

$$\begin{aligned}
F(Q) &= \frac{Q^2}{q_0 q} \Pi_{0z}(Q) = \frac{2m^2 Q^2}{q} \int \frac{d\Omega}{4\pi} \frac{\cos\theta}{q_0 - q\cos\theta} \\
&= -\frac{2m^2 Q^2}{q^2} \left(1 - \frac{q_0}{2q} \ln \frac{q_0 + q}{q_0 - q} \right)
\end{aligned} \qquad (3.22)$$

and

$$\begin{aligned}
G(Q) &= \Pi_{xx}(Q) = 2m^2 \int \frac{d\Omega}{4\pi} \frac{q_0 \sin^2\theta \cos^2\phi}{q_0 - q\cos\theta} \\
&= m^2 \frac{q_0}{q} \left(\frac{q_0}{q} - \frac{Q^2}{2q^2} \ln \frac{q_0 + q}{q_0 - q} \right) = \\
&= m^2 - \frac{1}{2} F(Q).
\end{aligned} \qquad (3.23)$$

We emphazise that q_0 was originally a discrete bosonic Matsubara frequency. To allow for soft $q_0 \ll T$ not being restriceted to zero[4], we need to analytically continue the frequency yielding $q_0 \to \omega + i\epsilon$ for retarded boundary conditions.

---

[4]The only case where $\omega_n = 2\pi n T \ll T$ is for $n = 0$.
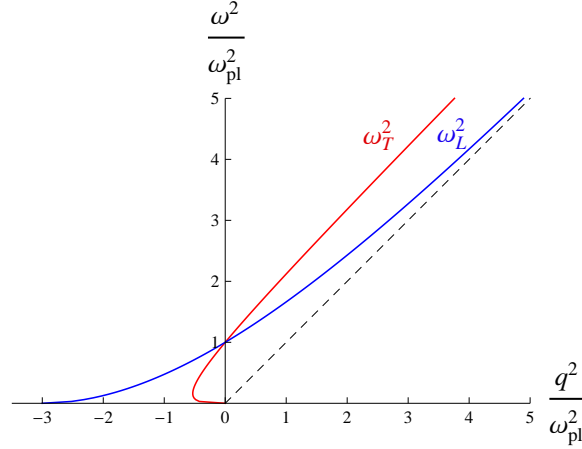
Figure 3.4: Dispersion relations for gauge bosons in quadratic scales.

The logarithm in (3.22) and (3.23) has a cut from $-q$ to $+q$ in the complex ω-plane. It is real for time-like Q^2 ($Q^2 = \omega^2 - q^2 > 0$) and complex for space-like Q^2:

$$\ln\left(\frac{\omega + q}{\omega - q}\right) = \ln\left|\frac{\omega + q}{\omega - q}\right| - i\pi\theta(q^2 - \omega^2). \tag{3.24}$$

After finding $F(Q)$ and $G(Q)$, we eventually obtain the retarded gauge boson propagator in a covariant gauge with gauge fixing parameter ρ from $\Delta^{-1} = \Delta_0^{-1} + \Pi$ [1]

$$\Delta_{\mu\nu}^R = \frac{1}{G - Q^2}P_{T,\mu\nu} + \frac{1}{F - Q^2}P_{L,\mu\nu} + \rho\frac{Q_\mu Q_\nu}{Q^4}. \tag{3.25}$$

From the poles of the transverse and longitudinal parts of the propagator we derive the dispersion laws for transverse and longitudinal waves in the plasma, which are the collective excitations we are looking for. The dispersion relations are presented in figure 3.4, in a quadratic plot.

Above a common frequency, which we call plasma frequency, $\omega_{pl} = \sqrt{2/3}m$, there are propagating modes. The transverse modes tend to a mass hyperboloid with asymptotic mass $m_\infty^2 = m^2$, while the longitudinal branch approaches the lightcone exponentially. The longitudinal mode has no analog in zero temperature theory and is a purely collective phenomenon. The spatially transverse mode can be thought of as the physical polarizations of gauge bosons modified by the medium.

For $\omega < \omega_{pl}$ we find that the wavevector q is imaginary, hence there exist no propagating modes. But there is still a collective behavior, which corresponds to collective screening in both, the electric and magnetic sector

for $\omega > 0$. In the static limit ($\omega = 0$) the inverse screening length $|\mathbf{q}|$ reaches the Debye mass $m_D^2 = 3\omega_{pl}^2$ in the longitudinal case (electrostatic screening) but it vanishes for the transverse branch (absence of magnetostatic screening) [10].

For $\omega^2 < q^2$ we find an imaginary part in the structure function coming from (3.24), which corresponds to the possibility of Landau damping. This is the collisionless transfer of energy from soft fields to hard plasma constituents moving in phase with the fields.

3.4 Kinetic theory

At the end of this chapter we want to show that it is possible to obtain the HTL polarization tensor from kinetic theory. We neglect collisions in our discussion, since the distance scales in the soft regime are still small compared to the mean free path ($\sim 1/g^2T$). The distribution function $f(\mathbf{p}, \mathbf{x}, t)$ describes the time dependent distribution of particles in the phase space. We start by examining the Boltzmann equation for a QED plasma

$$[\partial_t + \mathbf{v} \cdot \nabla_{\mathbf{x}} + e(\mathbf{E} + \mathbf{v} \times \mathbf{B}) \cdot \nabla_{\mathbf{p}}] f(\mathbf{p}, \mathbf{x}, t) = 0. \qquad (3.26)$$

Since the particles are charged, we need to solve the Boltzmann equation and Maxwell's equation for the soft fields self-consistently. The latter is

$$\partial_\mu F^{\mu\nu} = J_{ind}^\nu = e \int \frac{d^3p}{(2\pi)^3} V^\mu f(\mathbf{p}, \mathbf{x}, t), \qquad (3.27)$$

with $V^\mu = (1, \mathbf{p}/p^0)$. The current is given by the hard particles. These equations are known as Boltzmann-Vlasov equations. We want to consider small fluctuations δf around a neutral thermal background distribution function f_0, which is position independent.

$$f(\mathbf{p}, \mathbf{x}, t) = f_0(\mathbf{p}) + \delta f(\mathbf{p}, \mathbf{x}, t). \qquad (3.28)$$

The linearized version of the equations is given by

$$(\partial_t + \mathbf{v} \cdot \nabla_{\mathbf{x}})\delta f(\mathbf{p}, \mathbf{x}, t) = -e(\mathbf{E} + \mathbf{v} \times \mathbf{B}) \cdot \nabla_{\mathbf{p}} f_0(\mathbf{p}), \qquad (3.29)$$

$$\partial_\mu F^{\mu\nu} = e \int \frac{d^3p}{(2\pi)^3} V^\mu \delta f(\mathbf{p}, \mathbf{x}, t). \qquad (3.30)$$

For QCD the distribution function becomes a color density matrix and space-time derivatives become covariant derivatives D_μ. We find in the adjoint

representation

$$V \cdot D\delta f_a(\mathbf{p}, \mathbf{x}, t) = -g(\mathbf{E}_a + \mathbf{v} \times \mathbf{B}_a) \cdot \nabla_{\mathbf{p}} f_0(\mathbf{p}) = gV_\mu F_a^{\mu\nu} \partial_\nu^{(p)} f_0(\mathbf{p}), \quad (3.31)$$

$$D_\mu F_a^{\mu\nu} = J_{a,ind}^\nu = \frac{g}{2} \int \frac{d^3 p}{(2\pi)^3} V^\mu \delta f_a(\mathbf{p}, \mathbf{x}, t). \quad (3.32)$$

We will only consider the linear approximation, which is valid as long as the gauge fields are weak enough such that we can neglect them in the covariant derivative ($\partial_\mu \sim gT \gg gA_\mu$). To leading order in the coupling constant the Boltzmann-Vlasov equations for QED and QCD are the same, since $D_\mu \to \partial_\mu$ and $F_{\mu\nu} \to \partial_\mu A_\nu - \partial_\nu A_\mu$. If we perform a Fourier transformation, we will find an expression for δf from (3.31). Inserting it into (3.32), we can obtain the induced current. In momentum space and with retarded boundary conditions it reads [5]

$$J_{a,ind}^\mu(Q) = \frac{g^2}{2} \int \frac{d^3 p}{(2\pi)^3} V^\mu \partial_{(p)}^\beta f_0(\mathbf{p}) \left(g_{\gamma\beta} - \frac{V_\gamma Q_\beta}{q_0 - \mathbf{q} \cdot \mathbf{v} + i\epsilon} \right) A^\gamma(Q). \quad (3.33)$$

The HTL gauge boson self-energy is obtained as functional derivative of the induced current with respect to A_a^ν

$$\Pi_{\mu\nu}(Q) = \frac{g^2}{2} \int \frac{d^3 p}{(2\pi)^3} V_\mu \partial_{(p)}^\beta f_0(\mathbf{p}) \left(g_{\nu\beta} - \frac{V_\nu Q_\beta}{q_0 - \mathbf{q} \cdot \mathbf{v} + i\epsilon} \right). \quad (3.34)$$

In the isotropic case we find the same result we obtained by diagrammatic methods in section 3.2 [6]. We note that in the kinetic theory approach it is straight forward to consider non-isotropic momentum-space distribution functions. Therefore we will follow this procedure for our studies of non-equilibrium situations in the next chapters.

Finally we want to find the equation of motion for the A fields. We do this by expressing the induced current in terms of the polarization tensor

$$J_{ind}^\mu(Q) = \Pi^{\mu\nu}(Q) A_\nu(Q). \quad (3.35)$$

If we plug this into Maxwell's equation, we will find in momentum space

$$-iQ_\mu F^{\mu\nu}(Q) = J_{ind}^\nu(Q) + J_{ext}^\nu(Q), \quad (3.36)$$

where we have taken a possible external current into account. Rearranging things a bit, we eventually obtain

$$[Q^2 g^{\mu\nu} - Q^\mu Q^\nu + \Pi^{\mu\nu}(Q)] A_\mu(Q) = -J_{ext}^\nu(Q). \quad (3.37)$$

---

[5]For QED we replace $g^2/2 \to e^2$.

[6]A more detailed discussion of the kinetic theory approach is presented for example in [11]

It is possible to rewrite this in terms of physical electric fields by choosing a particular gauge[7]. In temporal axial gauge defined by $A_0 = 0$ we obtain

$$[(q^2 - \omega^2)\delta^{ij} - q^i q^j + \Pi^{ij}(Q)]E^j(Q) = (\Delta^{-1}(Q))^{ij}E^j(Q) = i\omega J^i_{ext}(Q). \quad (3.38)$$

For a non-vanishing frequency ω there is also a magnetic field present due to the law of induction, which is given by $\mathbf{q} \times \mathbf{E} = \omega \mathbf{B}$ in momentum space. The collective behavior can again be obtained from the poles of the propagator $\Delta(Q)$.

---

[7]$\Pi^{\mu\nu}$ is gauge invariant [12].

Chapter 4

The anisotropic plasma

After we discussed collective modes of the isotropic ultrarelativistic plasma in the last chapter, we want to examine anisotropic momentum-space distribution functions. We consider a special class of distribution functions, where we simply stretch or contract an isotropic distribution along one direction denoted by $\hat{\mathbf{n}}$

$$f(\mathbf{p}) = N(\xi) f_{iso}\big(\mathbf{p}^2 + \xi(\mathbf{p} \cdot \hat{\mathbf{n}})^2\big). \tag{4.1}$$

ξ is the anisotropy parameter, which can range from -1 to ∞. $N(\xi)$ is a normalization constant that can depend on the anisotropy parameter. We set it equal to one for simplicity. For $-1 < \xi < 0$ we have a prolate distribution function (distribution is elongated along $\hat{\mathbf{n}}$) and for $0 < \xi < \infty$ it is oblate (distribution is contracted along $\hat{\mathbf{n}}$). This class of distribution functions was studied by Romatschke and Strickland in [13, 14]. After a general discussion of the collective behavior in the anisotropic case, which will follow [13] closely, we want to consider in some detail the appearance of instabilities. We will study these instabilities in particular for an extremely oblate distribution function [15].

4.1   Self-energy structure functions

We have already stated that the polarization tensor is symmetric and transverse. Therefore not all components of $\Pi^{\mu\nu}$ are independent. We can restrict this discussion to the spatial part of the self-energy, because $(Q = (\omega, \mathbf{q}))$

$$\Pi^{0\nu}(Q) = \frac{q_i \Pi^{i\nu}(Q)}{\omega}, \qquad \Pi^{00}(Q) = \frac{q_i \Pi^{ij}(Q) q_j}{\omega^2}. \tag{4.2}$$

The space-like components can be written as[1]

$$\Pi^{ij}(Q) = -\frac{g^2}{2} \int \frac{d^3p}{(2\pi)^3} v^i \partial_l^{(p)} f(\mathbf{p}) \left(\delta^{jl} + \frac{v^j q^l}{Q \cdot V + i\epsilon} \right). \tag{4.3}$$

With our choice of the distribution function (4.1) we can simplify this expression by changing the coordinates to

$$\tilde{p}^2 = p^2 \big(1 + \xi(\mathbf{v} \cdot \mathbf{n})^2 \big). \tag{4.4}$$

After this change we can integrate out the $|\tilde{p}|$ dependence and obtain

$$\Pi^{ij}(Q) = m_D^2 \int \frac{d\Omega}{4\pi} v^i \frac{v^l + \xi(\mathbf{v} \cdot \mathbf{n})n^l}{(1 + \xi(\mathbf{v} \cdot \mathbf{n})^2)^2} \left(\delta^{jl} + \frac{v^j q^l}{Q \cdot V + i\epsilon} \right), \tag{4.5}$$

with

$$m_D^2 = -\frac{g^2}{(2\pi)^2} \int_0^\infty d\tilde{p}\tilde{p}^2 \frac{df_{iso}(\tilde{p}^2)}{d\tilde{p}}. \tag{4.6}$$

To find the self-energy structure functions for the anisotropic case we need to establish a tensor basis for a symmetric 3-tensor that depends on the momentum vector $\mathbf{q}$ and a fixed anisotropy vector $\hat{\mathbf{n}}$. The projector to the transverse direction of $\mathbf{q}$ is given by

$$A^{ij} = \delta^{ij} - \frac{q^i q^j}{q^2}. \tag{4.7}$$

This can be used to define $\tilde{n}^i = A^{ij}n^j$, with which we can construct the remaining tensors

$$B^{ij} = \frac{q^i q^j}{q^2}, \tag{4.8}$$

$$C^{ij} = \frac{\tilde{n}^i \tilde{n}^j}{\tilde{n}^2}, \tag{4.9}$$

$$D^{ij} = q^i \tilde{n}^j + q^j \tilde{n}^i. \tag{4.10}$$

We can decompose any symmetric 3-tensor $\mathbf{T}$ into the basis spanned by $\mathbf{A}$, $\mathbf{B}$, $\mathbf{C}$ and $\mathbf{D}$

$$\mathbf{T} = a\mathbf{A} + b\mathbf{B} + c\mathbf{C} + d\mathbf{D} \tag{4.11}$$

---

[1]In our conventions the parton distribution function for the QGP can be decomposed as $f(p) = 2N_f \big(n(p) + \bar{n}(p) \big) + 4N_c n_g(p)$, where n, $\bar{n}$ and n_g are the distribution functions of quarks, anti-quarks and gluons, respectively [16].

and the inverse is given by [13]

$$\mathbf{T}^{-1} = a^{-1}\mathbf{A} + \frac{(a+c)\mathbf{B} - a^{-1}(bc - \tilde{n}^2 q^2 d^2)\mathbf{C} - d\mathbf{D}}{b(a+c) - \tilde{n}^2 q^2 d^2}. \qquad (4.12)$$

We can apply this tensor decomposition to the self-energy and find

$$\Pi^{ij} = \alpha A^{ij} + \beta B^{ij} + \gamma C^{ij} + \delta D^{ij}, \qquad (4.13)$$

where α, β, γ and δ are the structure functions, which depend on m_D, ω, q, ξ and $\hat{\mathbf{q}} \cdot \hat{\mathbf{n}} = \cos\theta$. They can be extracted from the polarization tensor by the contractions

$$q^i \Pi^{ij} q^j = q^2 \beta, \qquad (4.14)$$
$$\tilde{n}^i \Pi^{ij} q^j = \tilde{n}^2 q^2 \delta, \qquad (4.15)$$
$$\tilde{n}^i \Pi^{ij} \tilde{n}^j = \tilde{n}^2 (\alpha + \gamma), \qquad (4.16)$$
$$\mathrm{Tr}\Pi^{ij} = 2\alpha + \beta + \gamma. \qquad (4.17)$$

The resulting integral expressions can be found in [13, 14].

In the isotropic limit, where $\xi \to 0$, γ and δ vanish and

$$\alpha(Q) = \Pi_T(Q) = \frac{m_D^2 \omega}{2q} \left(\frac{\omega}{q} - \frac{Q^2}{2q^2} \ln \frac{\omega+q}{\omega-q} \right), \qquad (4.18)$$

$$\beta(Q) = \frac{\omega^2}{q^2} \Pi_L(Q) = \frac{m_D^2 \omega^2}{q^2} \left(\frac{\omega}{2q} \ln \frac{\omega+q}{\omega-q} - 1 \right), \qquad (4.19)$$

which is the same result we obtained in section 3.3 [2].

As in the isotropic case the collective behavior is found by examining the propagator, whose inverse can be written as

$$\mathbf{\Delta}^{-1}(Q) = (q^2 - \omega^2 + \alpha)\mathbf{A} + (\beta - \omega^2)\mathbf{B} + \gamma\mathbf{C} + \delta\mathbf{D}. \qquad (4.20)$$

Applying the inversion formula (4.12) we obtain

$$\mathbf{\Delta} = \Delta_A \mathbf{A} + (q^2 - \omega^2 + \alpha + \gamma)\Delta_G \mathbf{B} + [(\beta - \omega^2)\Delta_G - \Delta_A]\mathbf{C} - \delta\Delta_G \mathbf{D}, \quad (4.21)$$

with

$$\Delta_A^{-1} = q^2 - \omega^2 + \alpha, \qquad (4.22)$$
$$\Delta_G^{-1} = (q^2 - \omega^2 + \alpha + \gamma)(\beta - \omega^2) - q^2 \tilde{n}^2 \delta^2. \qquad (4.23)$$

---

[2]We note that $m_D^2 = 2m^2$.

4.2 Collective modes

To find the dispersion relations which characterize the collective modes in an anisotropic plasma, we look for the zeros in (4.22) and (4.23). We first examine the stable modes and then turn to the unstable ones.

4.2.1 Stable modes

Stable modes can be determined by the poles of the propagator with real $\omega > q$. For Δ_G we find that we can factorize the denominator

$$\Delta_G^{-1} = (\omega^2 - \Omega_+^2)(\omega^2 - \Omega_-^2), \tag{4.24}$$

where

$$2\Omega_\pm^2 = \bar{\Omega}^2 \pm \sqrt{\bar{\Omega}^4 - 4((\alpha + \gamma + q^2)\beta - q^2\tilde{n}^2\delta^2)}, \tag{4.25}$$

and

$$\bar{\Omega}^2 = \alpha + \beta + \gamma + q^2. \tag{4.26}$$

The quantity under the square root can be written as $(\alpha - \beta + \gamma + q^2)^2 + 4q^2\tilde{n}^2\delta^2$, which is always positive for real $\omega > q$. Therefore there are at most two stable modes coming from Δ_G, whose dispersion relations can be obtained by finding the solutions to

$$\omega_\pm = \Omega_\pm^2(\omega_\pm). \tag{4.27}$$

Another stable mode is coming from Δ_A, which has its pole at

$$\omega_\alpha^2 = q^2 + \alpha(\omega_\alpha). \tag{4.28}$$

In the isotropic limit ($\xi \to 0$) we discover again a transversal branch with $\omega_\alpha = \omega_+ = \omega_T$ and a longitudinal branch with $\omega_- = \omega_L$. For a finite anisotropy parameter ξ we get 3 stable collective modes, whose dispersion relations depend on the angle between $\mathbf{q}$ and $\hat{\mathbf{n}}$

4.2.2 Unstable modes

Additionally to the stable modes we just discussed there exist unstable modes as well. For $\xi \neq 0$ the propagators have poles at imaginary ω. To obtain the dispersion relations we substitute $\omega = i\Gamma$ and solve for real $\Gamma(q)$. This gives the following factorization for Δ_G^{-1}

$$\Delta_G^{-1} = (\Gamma^2 + \Omega_+^2)(\Gamma^2 + \Omega_-^2). \tag{4.29}$$

This time there is only one solution since in [13] it was found that $\Omega_+^2 > 0$ for all $\Gamma > 0$.

For $\xi > 0$, which corresponds to the oblate distribution function, there is also an unstable mode coming from Δ_A so that in total we find

$$\Gamma_-^2 = -\Omega_-^2\,(i\Gamma_-), \tag{4.30}$$

$$\Gamma_\alpha = -q^2 - \alpha(i\Gamma_\alpha). \tag{4.31}$$

Finally we remark that in both cases there are solutions with positive and negative growth rates. The exponentially growing solutions are studied in some detail in the next section.

4.3 Instabilities

In the preceding discussion, which was based on [13], we found that in an anisotropic plasma there exist instabilities. These instabilities may lead to a faster isotropization in the early stage of a heavy ion collision and are therefore of interest phenomenologically. They are also well known phenomena in conventional plasma physics, where several different types are known [17, 18, 19]. Usually plasma instabilities are divided into "hydrodynamic instabilities", caused by coordinate space inhomogeneities, and "kinetic instabilities" due to non-equilibrium momentum distribution of plasma particles. While the first group plays no prominent role in quark-gluon plasma physics the latter does and we intend to study these in the following. We want to follow [15] by Arnold, Lenaghan and Moore in this section in order to gain more insight qualitatively and quantitatively.

4.3.1 Categorization of instabilities

Let us write down the linearized effective equation for soft gauge fields with no external current

$$[(\omega^2 - q^2)g^{\mu\nu} - Q^\mu Q^\nu + \Pi^{\mu\nu}(Q)]A_\nu = 0. \tag{4.32}$$

For a given wave vector $\mathbf{q}$ we find an instability if there are solutions for ω with Im $\omega > 0$. In the case of parity symmetric distribution functions ($f(\mathbf{p} = f(-\mathbf{p}))$) there exist sufficient conditions for the existence of unstable growing modes[3] [15]. They are motivated in appendix A.

---

[3]Our class of distribution functions given in (4.1) satisfies this condition.

CONDITION 1: There is an instability with a given wavevector $\mathbf{q}$ for each negative eigenvalue of the 3×3 matrix $q^2 \delta^{ij} - q^i q^j + \Pi^{ij}(0, \mathbf{q})$

Instabilities which satisfy condition 1 are called magnetic[4], because the condition itself involves the self energy for $\mathbf{A}(\omega = 0)$ and thus magnetic and not electric fields. However when the magnetic fields grow there will also be growing electric fields due to the law of induction.

Actually following [15] condition 1 can be used to obtain a necessary and sufficient condition for magnetic instabilities in an ultrarelativistic plasma

CONDITION 1-b: Magnetic instabilities exist for a given (parity symmetric) distribution $f(\mathbf{p})$, if

$$\mathcal{M}(\hat{\mathbf{p}}) \equiv \frac{g^2}{4\pi^2} \int_0^\infty p\,dp\,f(p\hat{\mathbf{p}}) \tag{4.33}$$

is anisotropic in $\mathbf{p}$.

There exists another type of instabilities that is of interest to us, which we call electric or longitudinal. They can be discovered by

CONDITION 2: There is an instability for a given wave vector $\mathbf{q}$ if

$$q^2 - \Pi^{00}(0, \hat{\mathbf{q}}) + \Pi^{0i}(0, \hat{\mathbf{q}})[q^2 + \mathbf{\Pi}(0, \mathbf{q})]_{ij}^{-1}\Pi^{j0}(0, \hat{\mathbf{q}}) < 0, \tag{4.34}$$

where $[q^2 + \mathbf{\Pi}(0, \mathbf{q})]^{-1}$ denotes the inverse of the 3×3 matrix $q^2 \delta^{ij} + \Pi^{ij}(0, \mathbf{q})$.

We note that this categorization as "magnetic" and "electric" instabilities is not always physically significant and in this chapter we simply use this terminology to distinguish whether the instability is indicated by condition 1 or 2. We should also mention that the polarization of the actual growing modes can differ from what we would expect by the conditions given above. The reason for this is that these modes have non-zero (imaginary) frequency ω and it turns out that the eigen-directions can change as one varies ω from $i\epsilon$ (with $\epsilon \to 0^+$) to the actual location of the unstable solution [15]. Nevertheless we will only present the calculations in the static limit for simplicity. Before we discuss unstable modes associated with condition 1 and 2 we want to gain some qualitative insight into the mechanisms leading to the instability.

---

[4]They are also known as Weibel [20] or transverse instabilities and are studied in the context of heavy ion collisions for example in [21, 22] too.
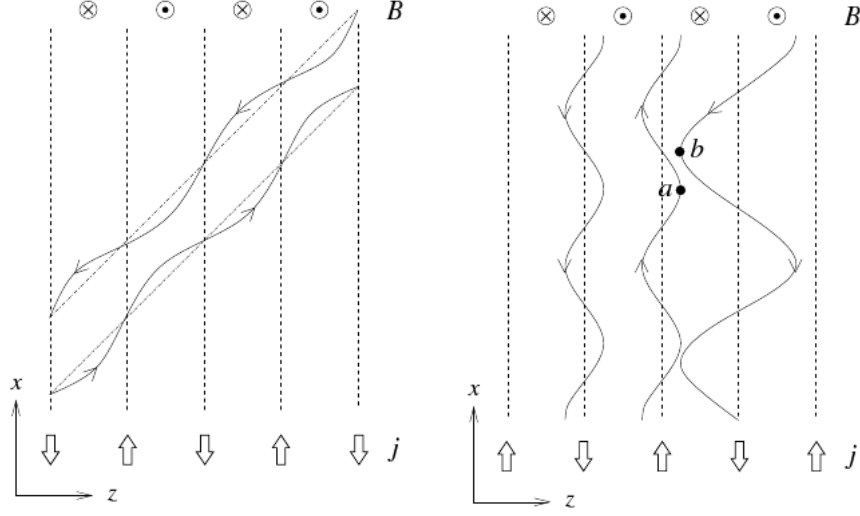
Figure 4.1: Untrapped (left panel) and trapped (right panel) particles travelling in the background of a magnetic field $\mathbf{B} = B\mathbf{e}_y \sin(qz)$ (taken from [15]). The arrows of the trajectories show the direction of the momentum for positively charged particles. The direction ($\pm y$) of the magnetic field is shown at the top. The big arrows in the bottom line indicate the average current $\mathbf{j}(z)$ pointing in the $\pm x$ direction.

4.3.2   Qualitative origin of instabilities

We start by examining magnetic instabilities. We consider a gas of non-interacting charged particles in zero field. Because we restricted this treatment to parity symmetric distribution functions, there is no current. For every particle going in one direction there is another particle going in the opposite direction. We fix the wave vector to point in the z direction for now and turn on a small magnetic field

$$\mathbf{B} = \mathcal{B}\mathbf{e}_y \sin(qz), \tag{4.35}$$

with $\mathbf{e}_y$ being the unit vector in the y direction. It is easy to check that one can choose a vector field $\mathbf{A}$ which points in the x direction and which is given by

$$\mathbf{A} = \mathcal{A}\mathbf{e}_x \cos(qz). \tag{4.36}$$

Due to the magnetic field the charged particles wiggle around their straight line trajectories, which they would have in zero field.

Let us first discuss the situation in the left panel of figure 4.1. Because of the wiggles, at certain z coordinates there are more particles moving in one x direction than in the opposite. This causes an average current in the

$\pm x$ direction indicated by the big arrows in the bottom line. The current produces a magnetic field in the opposite direction of the original one and thus this contribution is stabilizing. Also the velocity of particles traveling in the z direction is larger in certain regions and smaller in others. This leads again to a current pointing in the same direction as before and therefore is stabilizing too.

To find a destabilizing contribution we should consider particles with a small velocity component v_z such that they get trapped in the z direction by the magnetic field. This is illustrated in the right panel of figure 4.1. Consider a pair of particles located initially at a and b that move in opposite directions in zero field. As soon as we turn on the magnetic field the particle starting from a will stay quite close to its initial z coordinate. Since it is moving upwards there will be a contribution to the current in the positive x direction. Contrary to this the particle initially located at b wiggles stronger and travels within a bigger z region. Therefore even though the current was canceled in zero field, it does not cancel any longer after turning on the magnetic field. However this time the resulting current points in the correct direction to amplify the original magnetic field and thus the situation is potentially unstable leading to the instability we were looking for.

We summarize that untrapped particles are stabilizing while trapped particles are destabilizing. From our qualitative discussion we can conclude whether there are magnetic instabilities in certain simple situations or not. For example there is no instability in the isotropic limit. If we contract the distribution function in the direction of the wave vector $\mathbf{q}$, we will add more trapped particles, which will lead to an instability. On the other side for a stretched distribution along $\mathbf{q}$ we do not expect a magnetic instability since the number of untrapped particles increased.

Finally we consider an electric instability caused by charge fluctuations. This instability can be associated with a destabilizing contribution of Π^{00} ($\Pi^{00}(0, \hat{\mathbf{q}}) > 0$) according to condition 2. We assume we have a small static electric potential

$$A^0 = \phi \cos(qz) \tag{4.37}$$

and the corresponding electric field is

$$\mathbf{E} = \mathcal{E}\mathbf{e}_z \sin(qz). \tag{4.38}$$

Particles with a velocity component v_z in the z direction will be trapped, if v_z is too small so that they can not move over the electric potential barriers. Trapped positively charged particles then accumulate in regions with a negative electric field and are therefore stabilizing in contrast to the situation before. However, particles with v_z large enough to overcome the electric
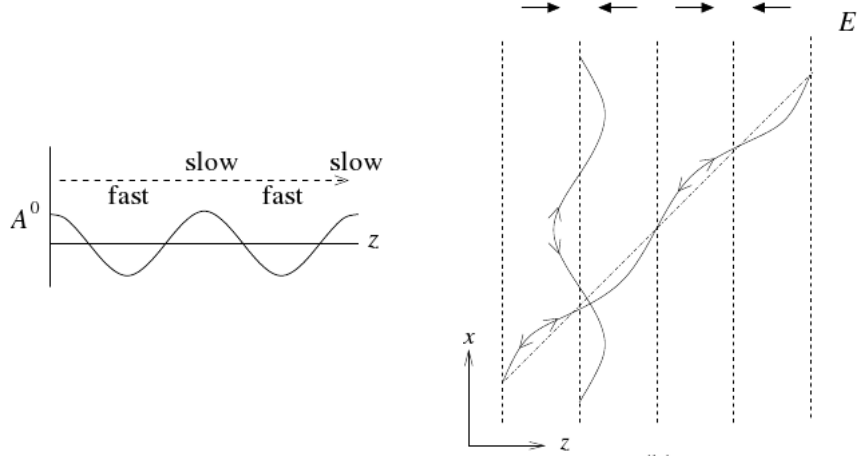
Figure 4.2: In the left panel the z component of the motion of an untrapped particle in a sinusoidal electric field is shown. In the right panel untrapped and trapped particles with respect to their z direction are illustrated. (Both taken from [15].)

potential barriers are destabilizing. This can be seen by noting that, because of energy conservation, positively charged particles move slower at the maxima of A^0 and faster at the minima. Thus they spend more time near the maxima and so their contribution to the average charge density will be greatest there. This leads to an enhancement of the magnitude of A^0. This is illustrated in figure 4.2. Eventually we repeat that for electric instabilities the trapped particles are stabilizing while the untrapped particles are destabilizing, which is contrary to the magnetic case.

4.3.3 Magnetic instability for planar momentum distribution

After the qualitative discussion of instabilities we want to do a stability analysis[5] for an extremely oblate distribution function

$$f(\mathbf{p}) = F(p_\perp)\delta(p_z) \tag{4.39}$$

corresponding to $\xi \to \infty$ in (4.1) with the direction of the anisotropy in the z direction. We choose the wave vector $\mathbf{q}$ to lie in the xz plane without loss of generality due to the axial symmetry of the distribution. We emphasize that

---

[5]We will not consider growth rates here, but are only interested whether there is an instability or not. Therefore it turns out to be sufficient to consider the static limit. For details on growth rates we refer to [13, 15].
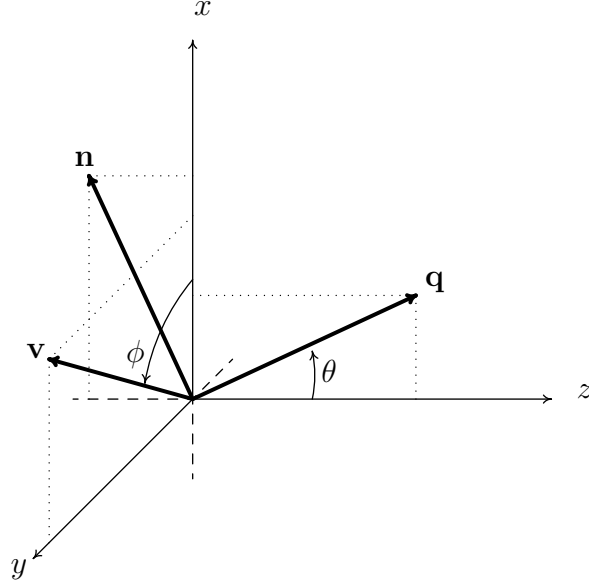
Figure 4.3: Directions of $\mathbf{q}$, $\mathbf{n}$ and $\mathbf{v}$. $\mathbf{q}$ and $\mathbf{n}$ lie in the xz plane and $\mathbf{v}$ lies in the xy plane. The anisotropy is in the z direction.

for the present discussion the vector $\hat{\mathbf{n}}$ will not be the anisotropy vector, which is simply the unit vector in the z direction, but the vector in the xz plane perpendicular to the wave vector. To check for evidence of an instability we only need to consider the static limit. After an integration by parts of the spatial components of the self energy (4.3) we find

$$\Pi^{ij}(\omega = 0, \mathbf{q}) = \frac{g^2}{2} \int \frac{d^3p}{(2\pi)^3} \frac{f(\mathbf{p})}{p} \left[\delta^{ij} - \frac{v^i \hat{q}^j + \hat{q}^i v^j}{\hat{\mathbf{q}} \cdot \mathbf{v} - i\epsilon} + \frac{v^i v^j}{(\hat{\mathbf{q}} \cdot \mathbf{v} - i\epsilon)^2} \right].$$
(4.40)

The distribution function $f(\mathbf{p})$ has support only in the $p_x p_y$ plane and is independent of the direction in the plane. We can introduce a parameter $m^2 > 0$

$$m^2 = \frac{g^2}{2} \int \frac{d^3p}{(2\pi)^3} \frac{f(\mathbf{p})}{p}$$
(4.41)

and find

$$\Pi^{ij}(0, \mathbf{q}) = m^2 \left\langle \delta^{ij} - \frac{v^i \hat{q}^j + \hat{q}^i v^j}{\hat{\mathbf{q}} \cdot \mathbf{v} - i\epsilon} + \frac{v^i v^j}{(\hat{\mathbf{q}} \cdot \mathbf{v} - i\epsilon)^2} \right\rangle_{p \in p_x p_y \text{ plane}},$$
(4.42)

where we factored out the angular dependence. In our treatment θ will be the angle $\mathbf{q}$ makes with the z axis and ϕ the angle $\mathbf{v}$ makes with the x axis (see figure 4.3).

For $\sin\theta \neq 0$ we find

$$\Pi^{\hat{\mathbf{q}}\hat{\mathbf{q}}}(0, \mathbf{q}) = 0 \tag{4.43}$$

$$\Pi^{\hat{\mathbf{n}}\hat{\mathbf{n}}}(0, \mathbf{q}) = m^2 \int_0^{2\pi} \frac{d\phi}{2\pi} \left[1 + 0 + \frac{\cos^2\theta}{\sin^2\theta} \right] = \frac{m^2}{\sin^2\theta} \tag{4.44}$$

$$\Pi^{yy}(0, \mathbf{q}) = m^2 \int_0^{2\pi} \frac{d\phi}{2\pi} \left[1 + 0 + \frac{\sin^2\phi}{(\sin\theta\cos\phi - i\epsilon)^2} \right]$$

$$= m^2 \left(1 - \frac{1}{\sin^2\theta} \right) = -m^2 \cot^2\theta \tag{4.45}$$

These components can be shown to be the eigenvalues of $\Pi^{ij}(0, \hat{\mathbf{q}})$ [6] [15]. According to condition 1 there exists an instability for each negative eigenvalue of $q^2\delta^{ij} - q^i q^j + \Pi^{ij}(0, \hat{\mathbf{q}})$. This is clearly only the case for Π^{yy} associated with A^y, where we find an instability for

$$q < q_{max}(\theta) = m \cot\theta. \tag{4.46}$$

The corresponding magnetic field points in the $\hat{\mathbf{n}}$ direction. This instability corresponds to the poles of Δ_A for $\xi \to \infty$. We see that there is no instability at all for a wave vector perpendicular to the anisotropy direction. There is also no instability associated with $\Pi^{\hat{\mathbf{n}}\hat{\mathbf{n}}}$ and a magnetic field in the y direction. We want to give an instructive explanation for this. Transversal instabilities are caused by trapped particles with $\mathbf{v}$ orthogonal to $\mathbf{q}$. In our geometry this means we must consider the case when $\mathbf{v}$ is pointing in the y direction. If the magnetic field is in the y direction as well, there will be no trapped particles and hence no instability. The situation will change, if we consider a distribution function with a certain small but finite thickness in the z direction. In [15] it is argued that then there are two unstable growing modes for $\sin\theta \leq \Delta\theta$ with $\Delta\theta \sim p_z/p$ being the angular width of the distribution function. The second unstable mode corresponds to $A^{\hat{\mathbf{n}}}$. For $\sin\theta > \Delta\theta$ there is again only the instability we already found in the planar case.

By symmetry for $\sin\theta = 0$ (wave vector parallel to the anisotropy direction) the behavior of Π^{xx} must be equal to that of Π^{yy} and we always find two magnetically unstable modes.

4.3.4 Electric instability for planar momentum distribution

We want to repeat the stability analysis, but now we check for condition 2. This time we integrate Π^{00} by parts which gives for an ultrarelativistic

---

[6]For example one can show that all non diagonal elements vanish.

plasma in the static limit

$$\Pi^{00}(0,\mathbf{q}) = \frac{g^2}{2} \int \frac{d^3p}{(2\pi)^3} \frac{f(\mathbf{p})}{p} \left(\frac{1}{(\hat{\mathbf{q}} \cdot \mathbf{v} - i\epsilon)^2} - 1 \right). \qquad (4.47)$$

The first term in the bracket gives no contribution since it integrates to zero and we end up finding

$$\Pi^{00}(0,\mathbf{q}) = -m^2. \qquad (4.48)$$

According to condition 2 this is stabilizing. But we still have to compute Π^{0i} which is once more obtained after a partial integration

$$\Pi^{0i}(0,\mathbf{q}) = \frac{g^2}{2} \int \frac{d^3p}{(2\pi)^3} \frac{f(\mathbf{p})}{p} \frac{v^i - \hat{q}^i \hat{\mathbf{q}} \cdot \mathbf{v}}{(\hat{\mathbf{q}} \cdot \mathbf{v} - i\epsilon)^2}. \qquad (4.49)$$

It is easy to check that the only non vanishing contribution is

$$\Pi^{0\hat{n}}(0,\mathbf{q}) = \frac{g^2}{2} \int \frac{d^3p}{(2\pi)^3} \frac{f(\mathbf{p})}{p} \frac{\cos\theta \cos\phi}{(\sin\theta \cos\phi - i\epsilon)^2}. \qquad (4.50)$$

Performing the angular integral first and then taking the limit $\epsilon \to 0$ gives

$$\Pi^{0\hat{n}}(0,\mathbf{q}) = -im^2 \frac{\cos\theta}{\sin^2\theta}. \qquad (4.51)$$

All we still need to check for condition 2 is $\Pi^{\hat{n}\hat{n}}(0,\mathbf{q})$, but this has been found already in the last section. Therefore we have the required terms. There is an electric or longitudinal instability for each wave vector which satisfies

$$q^2 - \Pi^{00}(0,\mathbf{q}) + \Pi^{0\hat{n}}(0,\mathbf{q})[q^2 + \mathbf{\Pi}(0,\mathbf{q})]^{-1}_{\hat{n}\hat{n}}\Pi^{\hat{n}0}(0,\mathbf{q}) < 0. \qquad (4.52)$$

This means we find an electrically unstable mode if

$$q^2 + m^2 - \frac{m^4 \cot^2\theta}{q^2 \sin^2\theta + m^2} < 0. \qquad (4.53)$$

The expression is minimized for $q = 0$ and the inequality gives

$$1 - \cot^2\theta < 0. \qquad (4.54)$$

This shows that there can only be an electric instability, if its wave vector lies within 45 degrees of the z axis. For a given θ the maximal q can be written as

$$q_{max}(\theta) = m \left[\frac{\cos\theta(4\cos^2\theta)^{1/2} - \sin^2\theta - 1}{2\sin^2\theta} \right]^{1/2}. \qquad (4.55)$$

This instability corresponds to the poles of Δ_G for $\xi \to \infty$.

However, a more detailed analysis beyond the static limit given in the appendix of [15] reveals that in the case of $\sin\theta = 0$ this instability is not associated with a longitudinal polarization, but points in the $\hat{\mathbf{x}}$ direction. This is an example, where the simple conclusion that condition 2 indicates longitudinally polarized instabilities may be misleading for the actual values of ω for the unstable modes, as mentioned in section 4.3.1.

Finally we should emphasize that the instability found here can not be described by our qualitative discussion of the origin of electrically unstable modes, because the contribution from Π^{00} turned out to be stabilizing. However, this instability arises due to $\Pi^{0\hat{n}}$, which refers to the coupling of charge and current fluctuations as the responsible mechanism.

4.3.5 Remarks on prolate momentum distributions

To conclude this chapter we briefly discuss prolate momentum distributions. We concentrate on another extreme case, namely the line momentum distribution (see the appendix of [15])

$$f(\mathbf{p}) = F(\mathbf{p}_z)\delta^{(2)}(\mathbf{p}_\perp), \tag{4.56}$$

with $F(-p_z) = F(p_z)$. For the current treatment we do not set $\omega = 0$ from the beginning, but we specialize to the static limit only later. The general form of the polarization tensor is

$$\Pi^{ij}(\omega, \mathbf{q}) = \frac{g^2}{2} \int \frac{d^3p}{(2\pi)^3} \frac{f(\mathbf{p})}{p} \left[\delta^{ij} - \frac{q^i v^j + q^j v^i}{-\omega + \mathbf{q} \cdot \mathbf{v} - i\epsilon} + \frac{(q^2 - \omega^2)v^i v^j}{(-\omega + \mathbf{q} \cdot \mathbf{v} - i\epsilon)^2} \right]. \tag{4.57}$$

Using the δ functions in (4.56) to do all but the p_z integral, we find

$$\Pi^{ij}(\omega, \mathbf{q}) = \frac{m^2}{2} \sum_{\pm} \left[\delta^{ij} \mp \frac{q^i \delta^{jz} + q^j \delta^{iz}}{-\omega \pm q\cos\theta - i\epsilon} + \frac{(q^2 - \omega^2)\delta^{iz}\delta^{jz}}{(-\omega \pm q\cos\theta - i\epsilon)^2} \right], \tag{4.58}$$

where the sum is over contributions from $p_z < 0$ and $p_z > 0$ and m^2 is given by

$$m^2 = \frac{g^2}{2} \int \frac{d^3p}{(2\pi)^3} \frac{f(\mathbf{p})}{p} = \frac{g^2}{(2\pi)^3} \int_0^\infty dp_z \frac{F(p_z)}{p_z}. \tag{4.59}$$

At this point we emphasize that if $F(0) \neq 0$ the expression above has a logarithmic small p_z divergence. However, a small width $\Delta p_\perp$ of the δ function

would cut off the divergence when $p_z \sim \Delta p_\perp$.[7] Here we are only interested in leading order results and therefore we can proceed with (4.58). For the y direction we easily obtain

$$\Pi^{yy}(\omega, \mathbf{q}) = m^2 \qquad (4.60)$$

and hence there is no instability associated with this polarization. The remaining directions give

$$\Pi^{\hat{q}\hat{q}}(\omega, \mathbf{q}) = \eta^2 \Pi^{00}(\omega, \mathbf{q}) = m^2 \eta^2 \sin^2 \theta \frac{\eta^2 + \cos^2 \theta}{(\eta^2 - \cos^2 \theta)^2}, \qquad (4.61)$$

$$\Pi^{\hat{q}\hat{n}}(\omega, \mathbf{q}) = \eta \Pi^{0\hat{n}}(\omega, \mathbf{q}) = m^2 \eta^2 \sin \theta \cos \theta \frac{\eta^2 - 2 + \cos^2 \theta}{(\eta^2 - \cos^2 \theta)^2}, \qquad (4.62)$$

$$\Pi^{\hat{n}\hat{n}}(\omega, \mathbf{q}) = m^2 \frac{(\eta^2 - 1)^2 \cos^2 \theta + \eta^2 \sin^4 \theta}{(\eta^2 - \cos^2 \theta)^2}, \qquad (4.63)$$

where $\eta = \omega/q$ and additionally we absorbed the $i\epsilon$ prescription in the denominator into η such that $\eta \to \eta + i\epsilon$.

In the static limit ($\omega = 0$) we find $\Pi^{00}(0, \mathbf{q}) = m^2 \tan^2 \theta$ and $\Pi^{0\hat{n}}(0, \mathbf{q}) = 0$, which indicates an electric instability according to condition 2 for

$$q < q_{max} = m \tan \theta. \qquad (4.64)$$

Furthermore we note that $\Pi^{\hat{n}\hat{n}}(0, \mathbf{q}) = m^2/\cos^2 \theta$. This implies that there exists no magnetic instability for $\theta \neq \pi/2$. Qualitatively this can be understood, because for $\hat{\mathbf{q}}$ not in the xy plane there are no trapped particles for the distribution given in (4.56). However, from condition 1-b we conclude that there must be a magnetic instability associated with $\theta = \pi/2$.

---

[7]This is a reasonable assumption for physical situations.

Chapter 5

The anisotropically expanding plasma

In the last chapter we found that for anisotropic momentum distribution functions there exist exponentially growing modes, which we studied in some detail. They have been studied numerically for Abelian and non-Abelian plasmas (for example in [23, 24, 25]). We also pointed out that these instabilities may be of interest in order to understand the fast equilibration of the quark-gluon plasma after a heavy ion collision. However, to be able to describe a system after a heavy ion collision we must take into account that the quark-gluon plasma produced by the colliding nuclei is expanding into the vacuum. This expansion modifies the dynamics of the system and was considered semi-analytically in the Abelian limit in [26]. The situation for non-Abelian fields is discussed in [27].

The aim of this chapter is to set the framework to be able to discuss the behavior of collective modes in an ultrarelativistic and anisotropically expanding plasma. The expansion takes place in the z direction in our consideration. We solve the Boltzmann-Vlasov equations in an appropriate coordinate system and eventually find integro-differential equations that describe the time evolution of the soft gauge fields. The solution of this equations will then be the topic of the next chapter. We will mainly follow the discussion presented in [26], but we intend to generalize it in some aspects.

5.1 Boltzmann-Vlasov equations for a non-stationary plasma

In the discussion of an isotropic plasma in section 3.4 we found the Boltzmann-Vlasov equations

$$V \cdot D\delta f_a(\mathbf{p}, \mathbf{x}, t) = gV_\mu F_a^{\mu\nu} \partial_\nu^{(P)} f_0(\mathbf{p}) \tag{5.1}$$

$$D_\mu F_a^{\mu\nu} = J_{a,ind}^\nu = \frac{g}{2} \int \frac{d^3p}{(2\pi)^3} \frac{P^\mu}{p^0} \delta f_a(\mathbf{p}, \mathbf{x}, t), \tag{5.2}$$

with $V^\mu = (1, p^i/p^0)$. For (5.1) to be valid in a non-stationary plasma as well, we need to assume a color neutral background distribution function $f_0(\mathbf{p}, \mathbf{x}, t)$ that satisfies

$$V \cdot \partial f_0(\mathbf{p}, \mathbf{x}, t) = 0. \tag{5.3}$$

In a stationary plasma f_0 only depends on the momenta and therefore the condition is satisfied trivially. The situation is different for a plasma that expands in the direction of the anisotropy (here $\hat{\mathbf{z}}$), which we want to consider in the following. This is assumed to be a good approximation for a parton gas in the initial stage after a heavy ion collision as long as the dimension of the system perpendicular to the z direction is sufficiently large [28]. Additionally we assume the distribution to be boost invariant in rapidity and isotropic in the xy plane. This leads to [26]

$$f_0(\mathbf{p}, \mathbf{x}, t) = f_0(p_\perp, tp^z - zp^0) = f_0(p_\perp, p'^z, \tau) \tag{5.4}$$

which can be shown to satisfy (5.3). According to special relativity the transformed momentum p'^z is given by

$$p'^z = \gamma(p^z - \beta p^0), \qquad \beta = \frac{z}{t}, \qquad \gamma = \frac{t}{\tau} \tag{5.5}$$

where $\tau = \sqrt{t^2 - z^2}$ is the proper time and for ultrarelativistic particles $p^0 = \sqrt{p_\perp^2 + (p_z)^2}$.

5.2 Comoving coordinates

To describe the dynamics of fluctuations around a boost invariant background it is useful to change to convenient coordinates, which are proper time τ and space-time rapidity $\eta = \operatorname{atanh}\frac{z}{t}$. The cartesian coordinates are then

$$t = \tau \cosh \eta, \qquad z = \tau \sinh \eta. \tag{5.6}$$
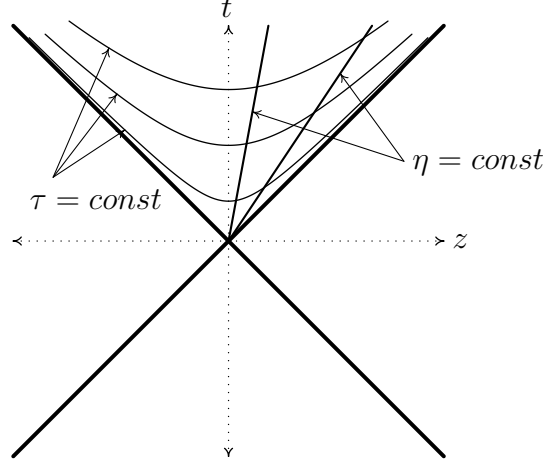
Figure 5.1: Illustration of proper time τ and space-time rapidity η.

The metric in the new comoving coordinates is diagonal with

$$g_{\tau\tau} = 1, \qquad g_{xx} = g_{yy} = -1, \qquad g_{\eta\eta} = -\tau^2. \tag{5.7}$$

We denote 4-vectors in comoving coordinates by an index from the beginning of the Greek alphabet $\tilde{X}^\alpha = (\tilde{x}^\tau, \tilde{x}^i, \tilde{x}^\eta) = (\tau, \tilde{x}^i, \eta)$, with $i = 1, 2$. Additionally we write a tilde over the vectors in τ, η- coordinates in this section to emphasize the distinction from cartesian coordinates. In later sections we will drop the tilde to avoid overloaded notation. Vectors in cartesian coordinates are denoted by indices $\mu, \nu, \ldots$

First we rewrite the Boltzmann-Vlasov equations in comoving coordinates. We note that the field strength tensor, being a two form $F = \mathrm{d}A - igA \wedge A$ and therefore with indices down, is given by

$$\tilde{F}_{\alpha\beta} = \tilde{\partial}_\alpha \tilde{A}_\beta - \tilde{\partial}_\beta \tilde{A}_\alpha - ig[\tilde{A}_\alpha, \tilde{A}_\beta]. \tag{5.8}$$

The indices can be lifted by the metric, but we point out that $\tilde{F}^{\alpha\beta}$ is not the same as $\tilde{\partial}^\alpha \tilde{A}^\beta - \tilde{\partial}^\beta \tilde{A}^\alpha - ig[\tilde{A}^\alpha, \tilde{A}^\beta]$. The covariant derivative is given by

$$\tilde{D}_\alpha = \tilde{\partial}_\alpha - ig[\tilde{A}_\alpha, \bullet]. \tag{5.9}$$

When we want to transform Maxwell's equation $D_\mu F^{\mu\nu} = j^\nu$ into comoving coordinates, we must take care of space-time derivatives and Christoffel symbols. To make things easier and in order to avoid confusion by space-time and gauge-covariant derivatives we write the additional terms coming from the Christoffel symbols explicitly. We do this in detail for $\tilde{j}^3$ and then state

the form of Maxwell's equation. The only non-vanishing Christoffel symbols for the metric in comoving coordinates are

$$\tilde{\Gamma}^0{}_{33} = \tau, \qquad \tilde{\Gamma}^3{}_{03} = \tilde{\Gamma}^3{}_{30} = \frac{1}{\tau}. \tag{5.10}$$

For $\nu = 3$ we obtain in τ, η coordinates

$$(\tilde{D}_0 + \tilde{\Gamma}^3{}_{30})\tilde{F}^{03} + \tilde{D}_1\tilde{F}^{13} + \tilde{D}_2\tilde{F}^{23} = \tilde{j}^3$$
$$(\tilde{D}_0 + \frac{1}{\tau})\tilde{F}^{03} + \tilde{D}_1\tilde{F}^{13} + \tilde{D}_2\tilde{F}^{23} = \tilde{j}^3. \tag{5.11}$$

Doing this for the other 3 components as well, Maxwell's equation can be compactly written as

$$\frac{1}{\tau}\tilde{D}_\alpha(\tau\tilde{F}^{\alpha\beta}) = \frac{1}{\tau}\tilde{D}_\alpha(\tau g^{\alpha\gamma}(\tau)g^{\beta\delta}(\tau)\tilde{F}_{\gamma\delta}) = \tilde{j}^\beta. \tag{5.12}$$

Furthermore we introduce a momentum rapidity $y = \text{atanh}\frac{p^z}{p^0}$ for massless particles such that

$$P^\mu = |p\bot|(\cosh y, \cos\phi, \sin\phi, \sinh y). \tag{5.13}$$

In comoving coordinates we get

$$\tilde{p}^\tau = \frac{\partial\tau}{\partial t}p^0 + \frac{\partial\tau}{\partial z}p^z = \cosh(\eta)p^0 - \sinh(\eta)p^z = p_\bot\cosh(y-\eta), \tag{5.14}$$

$$\tilde{p}^\eta = -\frac{\tilde{p}_\eta}{\tau^2} = -\frac{1}{\tau^2}\left(\frac{\partial t}{\partial\eta}p_0 + \frac{\partial z}{\partial\eta}p_z\right)$$

$$= -\frac{1}{\tau^2}(\tau\sinh(\eta)p_0 + \tau\cosh(\eta)p_z) = \frac{1}{\tau}p_\bot\sinh(y-\eta), \tag{5.15}$$

where from the above it can be seen that $tp^z - zp^0 = -\tilde{p}_\eta$. Therefore the momentum distribution function in (5.4) depends solely on $p_\bot$ and p_η in τ, η-coordinates. Additionally we define the new quantity

$$\tilde{V}^\alpha = \frac{\tilde{P}^\alpha}{p_\bot} = \left(\cosh(y-\eta), \cos\phi, \sin\phi, \frac{\sinh(y-\eta)}{\tau}\right). \tag{5.16}$$

Next we take a look at the expression of the current in comoving coordinates, which is

$$\tilde{j}^\beta = \frac{g}{2}\int\frac{d^2p_\bot dp'^z}{(2\pi)^3p'^0}\tilde{P}^\beta\delta f = -\frac{g}{2}\int\frac{d^2p_\bot d\tilde{p}_\eta}{(2\pi)^3\tau\tilde{p}^\tau}\tilde{P}^\beta\delta f = \frac{g}{2}\int\frac{d^2p_\bot dy}{(2\pi)^3}\tilde{P}^\beta\delta f \tag{5.17}$$

with $p'^0 = \gamma(p^0 - \beta p^z) = \tilde{p}^\tau$ and $p'^z = \gamma(p^z - \beta p^0) = -\tilde{p}_\eta/\tau$.

Finally we are able to write down the Boltzmann-Vlasov equations in comoving coordinates

$$\tilde{V} \cdot \tilde{D} \delta f^a|_{p^\mu} = g\tilde{V}^\alpha \tilde{F}^a_{\alpha\beta} \partial^\beta_{(P)} f_0(\mathbf{p}_\perp, \tilde{p}_\eta), \qquad (5.18)$$

$$\frac{1}{\tau} \tilde{D}_\alpha(\tau \tilde{F}^{\alpha\beta}) = \tilde{j}^\beta = \frac{g}{2} \int \frac{d^2 p_\perp dy}{(2\pi)^3} \tilde{P}^\beta \delta f \qquad (5.19)$$

It is important to note that the derivative of δf is taken at fixed P^μ and not at fixed $\tilde{P}^\alpha$[26]. In the following we will drop the tilde and denote comoving 4-vectors solely by indices from the beginning of the Greek alphabet as mentioned already before.

5.3 QCD Hamiltonian in comoving coordinates

Before solving the Boltzmann-Vlasov equations to obtain the time evolution of the soft gauge fields we digress from this topic for the moment and consider the QCD Lagrangian and Hamiltonian in comoving coordinates as well[1]. We will make use of the present discussion later when we consider the energy density of the expanding system for certain situations.

The pure gluonic part of the QCD action in general coordinates is of the form

$$S = -\frac{1}{2} \int d\tau d\eta dx_\perp \sqrt{-\det g_{\alpha\beta}} \text{Tr}[F_{\alpha\beta} g^{\alpha\gamma} g^{\beta\delta} F_{\gamma\delta}] = \int d\tau d\eta dx_\perp \mathcal{L}. \quad (5.20)$$

In τ, η-coordinates we have $\sqrt{-\det g_{\alpha\beta}} = \tau$. We adopt temporal gauge ($A^\tau = 0$) and then find for the Lagrangian

$$\mathcal{L} = \tau \text{Tr} \left[\frac{F^2_{\tau\eta}}{\tau^2} + F^2_{\tau i} - \frac{F^2_{\eta i}}{\tau^2} - \frac{F^2_{ij}}{2} \right] \qquad (5.21)$$

in comoving coordinates. From the Lagrangian we can obtain the conjugate momenta of the gauge fields which are

$$\Pi^i = \frac{\partial \mathcal{L}}{\partial(\partial_\tau A_i)} = \tau \partial_\tau A_i = \tau F_{\tau i} \qquad (5.22)$$

and

$$\Pi^\eta = \frac{\partial \mathcal{L}}{\partial(\partial_\tau A_\eta)} = \frac{1}{\tau} \partial_\tau A_\eta = \frac{1}{\tau} F_{\tau\eta}. \qquad (5.23)$$

---

[1]see also [29, 30]

We can use these to construct the Hamiltonian density

$$\mathcal{H} = 2\mathrm{Tr}\left[(\partial_\tau A_i)\Pi^i + (\partial_\tau A_\eta)\Pi^\eta\right] - \mathcal{L} = \mathrm{Tr}\left[\frac{(\Pi^i)^2}{\tau} + \frac{F_{\eta i}^2}{\tau} + \tau(\Pi^\eta)^2 + \frac{\tau}{2}F_{ij}^2\right].$$
(5.24)

Actually we find that the energy density differs from the Hamiltonian density by a factor $1/\tau$. Finally we obtain

$$\mathcal{E} = \frac{1}{\tau}\mathcal{H} = \mathcal{E}_{E_\perp} + \mathcal{E}_{B_\perp} + \mathcal{E}_{E_{||}} + \mathcal{E}_{B_{||}} =$$
$$= \mathrm{Tr}\left[\frac{(\Pi^i)^2}{\tau^2} + \frac{F_{\eta i}^2}{\tau^2} + (\Pi^\eta)^2 + \frac{F_{ij}^2}{2}\right],$$
(5.25)

where $\mathcal{E}_{E_{||}}$ and $\mathcal{E}_{E_\perp}$ is the energy density of electric fields in the z direction and perpendicular to the z direction, respectively[2]. The analog holds for the magnetic fields. From the energy density we can read off the expressions for electric and magnetic fields in terms of the gauge fields. Along the anisotropy we find

$$B_\eta = F_{xy}, \qquad E^\eta = \Pi^\eta$$
(5.26)

and perpendicular to it

$$B_1 = -\frac{1}{\tau}F_{\eta 2}, \qquad\qquad E^1 = \frac{1}{\tau}\Pi^1,$$
(5.27)

$$B_2 = \frac{1}{\tau}F_{\eta 1}, \qquad\qquad E^2 = \frac{1}{\tau}\Pi^2.$$
(5.28)

Due to the expansion the total energy density $\mathcal{E}$ is not conserved, but we find

$$\frac{d}{d\tau}\mathcal{E}\Big|_{j=0} = -\frac{2}{\tau}\mathcal{E}_T\Big|_{j=0}.$$
(5.29)

The condition $j = 0$ above indicates that this result is only true, if the induced current of the hard particles is zero. But in the presence of a plasma of hard particles this current does not vanish. To investigate the influence of the induced current we define the net energy gain rate [27]

$$R_{Gain} = \frac{d\mathcal{E}}{d\tau} + \frac{2}{\tau}\mathcal{E}_T,$$
(5.30)

which gives the rate of energy transfer from the free-streaming hard particles into the collective fields. This quantity can be negative which is the case when energy is transfered from the fields into the hard particles.

---

[2]We want to reserve the terms "longitudinal" and "transverse" to express directions along the wave vector of a collective mode or perpendicular to it.

5.4 Background distribution

After the short interlude on the QCD Hamiltonian in comoving coordinates in the preceding section, we come back to our task of describing the time evolution of gauge fields. We start by defining the background distribution of hard particles. We again consider a class of distribution functions that can be obtained from isotropic distributions by stretching or contracting along one direction, but this time the function will be non-stationary. We already saw that a distribution which satisfies the conditions mentioned in section 5.1 only depends on $p_\perp$ and p_η. When we assume the background distribution to be isotropic at proper time τ_{iso}, we can take [26]

$$f_0(p_\perp, p_\eta) = f_{iso}(\sqrt{p_\perp^2 + p_\eta^2/\tau_{iso}^2}). \tag{5.31}$$

The anisotropy parameter of chapter 4 is now a time dependent quantity and can be identified by

$$\xi(\tau) = \frac{\tau^2}{\tau_{iso}^2} - 1. \tag{5.32}$$

We find that the distribution is prolate for $\tau < \tau_{iso}$ and oblate for $\tau > \tau_{iso}$. Furthermore we note that the background distribution function gets more and more oblate as it evolves in time. We remark that a plasma description at arbitrarily early times does not make sense and therefore we must choose a starting time τ_0 for our considerations. In [26] only oblate distributions were studied and therefore τ_0 was set larger than τ_{iso}. We want to use the following treatment to study initially prolate cases as well and therefore do not make any restrictions on τ_0 for the moment.

5.5 Auxiliary fields W_α

Now we attempt to solve

$$\tilde{V} \cdot \tilde{D} \delta f^a|_{p^\mu} = g\tilde{V}^\alpha \tilde{F}_{\alpha\beta}^a \partial_{(P)}^\beta f_0(\mathbf{p}_\perp, \tilde{p}_\eta) \tag{5.33}$$

for the non-stationary background distribution we just introduced to get an expression for δf_a. Because

$$
\begin{aligned}
p^\tau \partial_\tau p_\eta(x)|_{y,\mathbf{p}_\perp} &= -p_\perp^2 \sinh(y-\eta)\cosh(y-\eta) \\
&= -p^\eta \partial_\eta p_\eta(x)|_{y,\mathbf{p}_\perp},
\end{aligned} \tag{5.34}
$$

we find that[3]

$$P \cdot \partial\left[\partial^\alpha_{(P)} f_0(\mathbf{p}_\perp, p_\eta)\right] = 0. \tag{5.35}$$

Therefore it is possible to solve (5.33) by introducing an auxiliary field $W_\alpha(\tau, x^i, \eta; \phi, y)$ that satisfies

$$\delta f(\mathbf{p}, x) = -g W_\alpha(\tau, x^i, \eta; \phi, y) \partial^\alpha_{(P)} f_0(p_\perp, p_\eta) \tag{5.36}$$

and

$$V \cdot D W_\alpha(\tau, x^i, \eta; \phi, y) = V^\beta F_{\alpha\beta}. \tag{5.37}$$

We want to solve the latter equation by the method of characteristics. We emphasize that we only consider the linear regime, which is valid as long as the gauge fields are weak enough to neglect them in the covariant derivative. It is then also appropriate to neglect self-interactions and therefore we are essentially dealing with an Abelian theory. We adopt the gauge condition $A^\tau = 0$ and can write

$$(V^\tau \partial_\tau + V^i \partial_i + V^\eta \partial_\eta) W_\alpha(\tau, x^i, \eta; \phi, y) = V^\beta F_{\alpha\beta} \tag{5.38}$$

Our background distribution is isotropic in the directions x^1 and x^2 (recall that the symbol y is already used for momentum rapidity), which allows us to choose the wave vector of the collective modes to lie in the plane spanned by $\hat{\mathbf{x}}^1$ and $\hat{\eta}$. Thus the modes and therefore the auxiliary fields W_α are independent of x^2 and we will from now on denote $x^1 = x$. Therefore (5.38) reduces to

$$(V^\tau \partial_\tau + V^\eta \partial_\eta + \cos\phi \partial_x) W_\alpha(\tau, x, \eta; \phi, y) = V^\beta F_{\alpha\beta}. \tag{5.39}$$

It is possible to solve this first-order partial differential equations by the method of characteristics where we introduce a parameter s such that

$$\frac{dW_\alpha}{ds} = \frac{\partial W_\alpha}{\partial_\tau}\frac{d\tau}{ds} + \frac{\partial W_\alpha}{\partial\eta}\frac{d\eta}{ds} + \frac{\partial W_\alpha}{\partial x}\frac{dx}{ds} = V^\beta F_{\alpha\beta}, \tag{5.40}$$

with

$$\frac{d\tau}{ds} = V^\tau = \cosh(y - \eta(s)), \tag{5.41}$$

$$\frac{d\eta}{ds} = V^\eta = \frac{1}{\tau(s)}\sinh(y - \eta(s)), \tag{5.42}$$

$$\frac{dx}{ds} = V^1 = \cos\phi. \tag{5.43}$$

---

[3]Here it is essential that the index of the partial differentiation with respect to the momentum is upstairs, since otherwise there would be additional τ's involved and (5.35) would not be valid.

Since $d\tau/ds > 0$ it is possible to use τ instead of s for the purpose of integrating (5.40). Writing $ds = d\tau'/V^\tau(\eta(\tau'))$ we get

$$W_\alpha(\tau, x, \eta; \phi, y) - W_\alpha(\tau_0, x_0, \eta_0; \phi, y) = \int_{\tau_0}^\tau d\tau' \frac{V^\beta F_{\alpha\beta}|_{\tau', x(\tau'), \eta(\tau')}}{V^\tau(\eta(\tau'))}, \quad (5.44)$$

where $x_0 = x(\tau' = \tau_0)$ and $\eta_0 = \eta(\tau' = \tau_0)$. The functions $x(\tau')$ and $\eta(\tau')$ are solutions of

$$\frac{dx(\tau')}{d\tau'} = \frac{\cos\phi}{\cosh(y - \eta(\tau'))}, \quad (5.45)$$

$$\frac{d\eta(\tau')}{d\tau'} = \frac{1}{\tau'} \tanh(y - \eta(\tau')), \quad (5.46)$$

with $x(\tau' = \tau) = x$ and $\eta(\tau' = \tau) = \eta$. The latter equation is solved by

$$\tau' \sinh(y - \eta(\tau')) = \tau \sinh(y - \eta) \quad (5.47)$$

as can be checked easily by differentiation with respect to τ'. More explicitly we find

$$\eta' \equiv \eta(\tau') = y - \operatorname{asinh}\left(\frac{\tau}{\tau'} \sinh(y - \eta)\right). \quad (5.48)$$

With this solution we can integrate (5.45) and obtain

$$\begin{aligned} x' \equiv x(\tau') &= x + [\tau' \cosh(y - \eta') - \tau \cosh(y - \eta)] \cos\phi \\ &= x + \left[\sqrt{\tau'^2 + \tau^2 \sinh^2(y - \eta)} - \tau \cosh(y - \eta)\right] \cos\phi, \quad (5.49) \end{aligned}$$

where we have inserted the expression for η' in the second line. After we have determined the characteristics we give the solution for the components of the W fields[4]

$$W_1 - W_1^0 = \int_{\tau_0}^\tau d\tau' \left[\partial_{\tau'} A^1 + \frac{\tanh(y - \eta')}{\tau'} (\partial_{x'} A_\eta + \partial_{\eta'} A^1)\right. \quad (5.50)$$

$$\left. - \frac{\sin\phi}{\cosh(y - \eta')} \partial_{x'} A^2\right],$$

$$W_2 - W_2^0 = \int_{\tau_0}^\tau d\tau' \left[\partial_{\tau'} + \frac{\tanh(y - \eta')}{\tau'} \partial_{\eta'} + \frac{\cos\phi}{\cosh(y - \eta')} \partial_{x'}\right] A^2, \quad (5.51)$$

$$W_\eta - W_\eta^0 = -\int_{\tau_0}^\tau d\tau' \left[\partial_{\tau'} A_\eta + \frac{V^i \partial_{\eta'} A^i + \partial_{x'} A_\eta}{\cosh(y - \eta')}\right]. \quad (5.52)$$

---

[4]We do not need the zero component of the W fields as can be seen in (5.36), because $\partial_{(P)}^\alpha f_0(p_\perp, p_\eta)$ does not depend on p_τ.

The dependencies of $A_\alpha(\tau', x', \eta')$ have been omitted above. We do not specify the W_α^0 here and postpone this task until the next chapter after we have seen why these terms turn out to be important to us[5].

5.6 Current conservation

At this point we pause in deriving the effective field equations for the soft modes and take a look at the conservation law for the current. From (5.2) and (5.36) it follows that the current in cartesian coordinates can be written as

$$J^\mu = -\frac{g^2}{2} \int \frac{d^3p}{(2\pi)^3} \frac{P^\mu}{p^0} W_\alpha \partial_{(P)}^\alpha f_0(p_\perp, p_\eta). \qquad (5.53)$$

Because $D_\mu P^\mu = P^\mu D_\mu = P^\alpha D_\alpha$ we obtain, by additionally changing the integration variables to comoving coordinates like in (5.17),

$$D \cdot J = \frac{g^2}{2} \int \frac{d^2p_\perp dp_\eta}{(2\pi)^3} \frac{1}{\tau p'^0} P \cdot D W_\alpha \partial_{(P)}^\alpha f_0(p_\perp, p_\eta). \qquad (5.54)$$

Now we can use (5.35), (5.37) and $p'^0 = \sqrt{p_\perp^2 + (p_z')^2}$ and end up with

$$D \cdot J = \frac{g^2}{2} \int \frac{d^2p_\perp dp_\eta}{(2\pi)^3} \frac{P^\beta}{\tau\sqrt{p_\perp^2 + p_\eta^2/\tau^2}} \left(F_{i\beta} \frac{\partial f_0(p_\perp, p_\eta)}{\partial p_i} + F_{\eta\beta} \frac{\partial f_0(p_\perp, p_\eta)}{\partial p_\eta} \right)$$
$$(5.55)$$

Finally for our class of background distribution functions, $\partial f_0/\partial p_i$ and $\partial f_0/\partial p_\eta$ are odd functions in p_i and p_η such that the current is conserved by symmetry. We now want to go on and find expressions for the components of the current and eventually obtain the equations of motion for the A fields.

---

[5]It turns out that keeping the initial W fields is the most important generalization compared to [26].

5.7 Time evolution of gauge fields

In a first step we want to to find an expression for the current in terms of the auxiliary fields. Therefore we insert (5.36) into (5.17) and obtain

$$
\begin{aligned}
J^\beta &= -\frac{g^2}{2} \int \frac{d^2 p_\perp dy}{(2\pi)^3} P^\beta W_\alpha \partial^\alpha_{(P)} f_0(p_\perp, p_\eta) \\
&= -\frac{g^2}{2} \int \frac{d^2 p_\perp dy}{(2\pi)^3} P^\beta \left(W_i \frac{p_i}{\sqrt{p_\perp^2 + p_\eta^2/\tau_{iso}^2}} + W_\eta \frac{p_\eta}{\tau_{iso}^2 \sqrt{p_\perp^2 + p_\eta^2/\tau_{iso}^2}} \right) \frac{\partial f_{iso}(p)}{\partial p} \\
&= -\frac{g^2}{2} \int_0^{2\pi} \frac{d\phi}{2\pi} \int_0^\infty \frac{dp_\perp}{(2\pi)^2} p_\perp^2 \int \frac{dy}{\sqrt{1+V_\eta^2/\tau_{iso}^2}} V^\beta \left(-V^i W_i + \frac{V_\eta}{\tau_{iso}^2} W_\eta \right) f'_{iso}(p) \\
&= -\frac{m_D^2}{2} \int_0^{2\pi} \frac{d\phi}{2\pi} \int \frac{dy}{(1+V_\eta^2/\tau_{iso}^2)^2} V^\beta \left(V^i W_i - \frac{V_\eta}{\tau_{iso}^2} W_\eta \right) \qquad (5.56)
\end{aligned}
$$

with

$$
m_D^2 = -g^2 \int_0^\infty \frac{dp}{(2\pi)^2} p^2 f'_{iso}(p) \qquad (5.57)
$$

and $p = p_\perp \sqrt{1 + V_\eta^2/\tau_{iso}^2}$.

Due to the linearity of Maxwell's equation and the expression for the W fields in the Abelian limit, we can study the time evolution of individual modes obtained by a Fourier decomposition

$$
A_\alpha(\tau, x, \eta) = \int \frac{dk}{2\pi} e^{ikx} \int \frac{d\nu}{2\pi} e^{i\nu\eta} \tilde{A}_\alpha(\tau; k, \nu) \qquad (5.58)
$$

and similarly for the currents.

To express the Fourier transformed current as functional of the gauge fields we note that the partial derivatives $\partial_{x'}$ and $\partial_{\eta'}$ in equations (5.50)-(5.52) will be replaced by factors ik and $i\nu$, respectively. The proper time integrals over the partial time derivative of the gauge fields $A_\alpha(\tau', x', \eta')$ can be partially integrated, yielding

$$
\begin{aligned}
\int_{\tau_0}^\tau d\tau' \partial_{\tau'} A_\alpha(\tau', x', \eta') &= \int_{\tau_0}^\tau d\tau' \int \frac{dk}{2\pi} e^{ikx'} \int \frac{d\nu}{2\pi} e^{i\nu\eta'} \partial_{\tau'} \tilde{A}_\alpha(\tau; k\nu) \\
&= \int \frac{dk}{2\pi} \int \frac{d\nu}{2\pi} \Big\{ e^{ikx} e^{i\nu\eta} \tilde{A}_\alpha(\tau; k, \nu) - e^{ikx_0} e^{i\nu\eta_0} \tilde{A}_\alpha(\tau_0; k, \nu) \\
&\quad - i \int_{\tau_0}^\tau d\tau' e^{ikx'} e^{i\nu\eta'} \Big[k \frac{\cos\phi}{\cosh(y-\eta')} + \nu \frac{\tanh(y-\eta')}{\tau'} \Big] \tilde{A}_\alpha(\tau'; k, \nu) \Big\}.
\end{aligned}
$$

$$(5.59)$$

We recall that x', x_0 and η', η_0 are given by (5.49) and (5.48), respectively, and therefore depend on x, η and τ. It remains to insert equations (5.50)-(5.52) and (5.59) into the expression for the current (5.56). The calculation is lengthy and involves quite many terms, therefore we will not present it explicitly here. We introduce new variables

$$\bar{y} \equiv y - \eta, \tag{5.60}$$

$$\bar{\eta}' \equiv \bar{\eta}(\tau') \equiv \eta(\tau') - \eta = \bar{y} - \text{asinh}\left(\frac{\tau}{\tau'} \sinh \bar{y}\right), \tag{5.61}$$

$$\chi' \equiv \chi(\tau') \equiv (x(\tau') - x)/\cos\phi = \sqrt{\tau'^2 + \tau^2 \sinh^2 \bar{y}} - \tau \cosh \bar{y} \tag{5.62}$$

with $\bar{\eta}_0 = \bar{\eta}(\tau_0)$ and $\chi_0 = \chi(\tau_0)$. The integration over the momentum space angle ϕ involves terms typically looking like

$$\int_0^{2\pi} \frac{d\phi}{2\pi} \cos^m \phi \; e^{ik\chi' \cos\phi} \qquad \text{and} \qquad \int_0^{2\pi} \frac{d\phi}{2\pi} \sin^m \phi \; e^{ik\chi' \cos\phi}, \tag{5.63}$$

with $m \in \mathbb{N}$. Their solution can be given in terms of Bessel functions of the first kind $J_n(k\chi)$. We also use the recurrence formula for the Bessel functions

$$J_{n+1}(x) = \frac{2n}{x} J_n(x) - J_{n-1}(x). \tag{5.64}$$

Eventually the expression for the 1 component of the current is

$$\tilde{j}^1 = -\frac{m_D^2}{2} \int \frac{d\bar{y}}{(1 + \frac{\tau^2 \sinh^2 \bar{y}}{\tau_{iso}^2})^2} \left\{ \frac{1}{2} \tilde{A}^1(\tau) \right. \tag{5.65}$$

$$+ e^{i\nu\bar{\eta}_0} \left[\frac{i\tau \sinh \bar{y}}{\tau_{iso}^2} J_1(k\chi_0) \tilde{A}_\eta(\tau_0) - \frac{1}{2}[J_0 - J_2](k\chi_0)\tilde{A}^1(\tau_0) \right]$$

$$+ \int_{\tau_0}^\tau d\tau' \frac{e^{i\nu\bar{\eta}'}}{\sqrt{1 + \frac{\tau^2 \sinh^2 \bar{y}}{\tau'^2}}} \left[\left(\frac{k}{4}[3J_1 - J_3](k\chi') - \frac{i\nu\tau \sinh \bar{y}}{2\tau_{iso}^2}[J_0 - J_2](k\chi') \right) \tilde{A}^1(\tau') \right.$$

$$\left. \left. + \frac{\tau \sinh \bar{y}}{\tau'^2} \left(\frac{ik}{2}[J_0 - J_2](k\chi') - \frac{\nu\tau \sinh \bar{y}}{\tau_{iso}^2} J_1(k\chi') \right) \tilde{A}_\eta(\tau') \right] \right\} + \tilde{j}_0^1(\tau).$$

The last term $\tilde{j}_0^1$ accounts for possible terms coming from the W_α^0 fields we have not specified yet. Similar terms show up for every component of the current. We refer to the τ'-integral as *memory* integral, because it depends

on the history of the gauge fields. For $\tilde{j}^\eta$ we find

$$\tilde{j}^\eta = -\frac{m_D^2}{2\tau} \int \frac{d\bar{y}\,\sinh\bar{y}}{(1 + \frac{\tau^2 \sinh^2 \bar{y}}{\tau_{iso}^2})^2} \left\{ -\frac{\tau \sinh\bar{y}}{\tau_{iso}^2} \tilde{A}_\eta(\tau) \right. \tag{5.66}$$

$$+ e^{i\nu\bar{\eta}_0} \left[\frac{\tau \sinh\bar{y}}{\tau_{iso}^2} J_0(k\chi_0)\tilde{A}_\eta(\tau_0) - i J_1(k\chi_0)\tilde{A}^1(\tau_0) \right]$$

$$+ \int_{\tau_0}^\tau d\tau' \frac{e^{i\nu\bar{\eta}'}}{\sqrt{1 + \frac{\tau^2 \sinh^2 \bar{y}}{\tau'^2}}} \left[\left(\frac{ik}{2}[J_2 - J_0](k\chi') + \frac{\nu\tau \sinh\bar{y}}{\tau_{iso}^2} J_1(k\chi') \right) \tilde{A}^1(\tau') \right.$$

$$\left. \left. + \frac{\tau \sinh\bar{y}}{\tau'^2} \left(\frac{i\nu\tau \sinh\bar{y}}{\tau_{iso}^2} J_0(k\chi') - k J_1(k\chi') \right) \tilde{A}_\eta(\tau') \right] \right\} + \tilde{j}_0^\eta(\tau).$$

We see that these components of the current only depend on $\tilde{A}^1$ and $\tilde{A}_\eta$. If either $k = 0$ or $\nu = 0$, the 1 and η components will decouple from each other. These will be two special cases we want to discuss in detail in the following chapter. On the other hand, $\tilde{j}^2$ is found to be a functional of $\tilde{A}^2$ only

$$\tilde{j}^2 = -\frac{m_D^2}{2} \int \frac{d\bar{y}}{(1 + \frac{\tau^2 \sinh^2 \bar{y}}{\tau_{iso}^2})^2} \left\{ \frac{1}{2}\tilde{A}^2(\tau) - \frac{1}{2}e^{i\nu\bar{\eta}_0}[J_0 + J_2](k\chi_0)\tilde{A}^2(\tau_0) \right.$$

$$- \int_{\tau_0}^\tau d\tau' \frac{e^{i\nu\bar{\eta}'}}{\sqrt{1 + \frac{\tau^2 \sinh^2 \bar{y}}{\tau'^2}}} \left[\frac{i\nu\tau \sinh\bar{y}}{2\tau_{iso}^2}[J_0 + J_2](k\chi') \right.$$

$$\left. \left. - \frac{k}{4}[J_1 + J_3](k\chi') \right] \tilde{A}^2(\tau') \right\} + \tilde{j}_0^2(\tau). \tag{5.67}$$

Finally, even though in temporal gauge there is no equation for the time evolution of the zeroth component of the gauge fields, we need $\tilde{j}^\tau$ to check the Gauss law. Therefore we continue and obtain

$$\tilde{j}^\tau = -\frac{m_D^2}{2} \int \frac{d\bar{y}\,\cosh\bar{y}}{(1 + \frac{\tau^2 \sinh^2 \bar{y}}{\tau_{iso}^2})^2} \left\{ e^{i\nu\bar{\eta}_0} \left[\frac{\tau \sinh\bar{y}}{\tau_{iso}^2} J_0(k\chi_0)\tilde{A}_\eta(\tau_0) - i J_1(k\chi_0)\tilde{A}^1(\tau_0) \right] \right.$$

$$+ \int_{\tau_0}^\tau d\tau' \frac{e^{i\nu\bar{\eta}'}}{\sqrt{1 + \frac{\tau^2 \sinh^2 \bar{y}}{\tau'^2}}} \left[\left(\frac{ik}{2}[J_2 - J_0](k\chi') + \frac{\nu\tau \sinh\bar{y}}{\tau_{iso}^2} J_1(k\chi')\tilde{A}^1(\tau') \right) \right.$$

$$\left. \left. + \frac{\tau \sinh\bar{y}}{\tau'^2} \left(\frac{i\nu\tau \sinh\bar{y}}{\tau_{iso}^2} J_0(k\chi') - k J_1(k\chi') \right) \tilde{A}_\eta(\tau') \right] \right\} + \tilde{j}_0^\tau(\tau), \tag{5.68}$$

which is again a functional of $\tilde{A}^1$ and $\tilde{A}_\eta$.

After we have found the expressions for the components of the current, we can write down the equations of motion for the soft gauge fields from Maxwell's equation

$$\frac{1}{\tau}\partial_\alpha\big(\tau g^{\alpha\gamma}(\tau)g^{\beta\delta}(\tau)F_{\gamma\delta}\big) = j^\beta. \tag{5.69}$$

We are interested in the Fourier transformed version, therefore we again replace the partial derivatives ∂_x and ∂_η by factors ik and $i\nu$. We find a coupled set of equations for $\tilde{A}^1$ and $\tilde{A}^\eta$

$$\Big(\frac{1}{\tau}\partial_\tau\tau\partial_\tau + \frac{\nu^2}{\tau^2}\Big)\tilde{A}^1(\tau;k,\nu) = \tilde{j}^1(\tau;k,\nu) - \frac{k\nu}{\tau^2}\tilde{A}_\eta(\tau;k,\nu), \tag{5.70}$$

$$\Big(\tau\partial_\tau\frac{1}{\tau}\partial_\tau + k^2\Big)\tilde{A}_\eta(\tau;k,\nu) = \tilde{j}_\eta(\tau;k,\nu) - k\nu\tilde{A}^1(\tau;k,\nu). \tag{5.71}$$

We observe that these equations decouple for either $k = 0$ or $\nu = 0$, since in these cases also $\tilde{j}^1$ and $\tilde{j}^\eta$ only depend on $\tilde{A}^1$ and $\tilde{A}_\eta$, respectively, as we have already seen. In terms of the conjugate momenta we defined in (5.22) and (5.23) we get

$$\frac{1}{\tau}\partial_\tau\tilde{\Pi}_1(\tau;k,\nu) = \tilde{j}^1(\tau;k,\nu) - \frac{\nu^2}{\tau^2}\tilde{A}^1(\tau;k,\nu) - \frac{k\nu}{\tau^2}\tilde{A}_\eta(\tau;k,\nu) \tag{5.72}$$

and

$$\frac{1}{\tau}\partial_\tau\tilde{\Pi}^\eta(\tau;k,\nu) = -\tilde{j}^\eta(\tau;k,\nu) - \frac{k^2}{\tau^2}\tilde{A}_\eta(\tau;k,\nu) - \frac{k\nu}{\tau^2}\tilde{A}^1(\tau;k,\nu), \tag{5.73}$$

where we used $\tilde{j}^\eta = -\tilde{j}_\eta/\tau^2$.

The equation of motion for the transverse mode $\tilde{A}^2(\tau;k,\nu)$ decouples for general k and ν and has the form

$$\Big(\frac{1}{\tau}\partial_\tau\tau\partial_\tau + k^2 + \frac{\nu^2}{\tau^2}\Big)\tilde{A}^2(\tau;k,\nu) = \tilde{j}^2(\tau;k,\nu) \tag{5.74}$$

or again in terms of the conjugate momenta

$$\frac{1}{\tau}\tilde{\Pi}_2(\tau;k,\nu) = \tilde{j}^2(\tau;k,\nu) - \Big(k^2 + \frac{\nu^2}{\tau^2}\Big)\tilde{A}^2(\tau;k,\nu). \tag{5.75}$$

Finally it only remains to find an expression for the Gauss law which can be obtained from the zeroth component of Maxwell's equation

$$\begin{aligned}
j^\tau(\tau,x,\eta) &= -\frac{1}{\tau}\partial_x(\tau F_{x\tau}) - \frac{1}{\tau}\partial_\eta\Big(\frac{1}{\tau}F_{\eta\tau}\Big) \\
&= -\partial_x\partial_\tau A^1(\tau,x,\eta) + \frac{1}{\tau}\partial_\eta\frac{1}{\tau}\partial_\tau A_\eta(\tau,x,\eta) \\
&= -\frac{1}{\tau}\partial_x\Pi_x(\tau,x,\eta) + \frac{1}{\tau}\partial_\eta\Pi^\eta(\tau,x,\eta). \tag{5.76}
\end{aligned}$$

The Fourier transformed version of the Gauss law constraint reads

$$\tilde{j}^{\tau}(\tau; k, \nu) = \frac{i}{\tau}\left(\nu\tilde{\Pi}^{\eta}(\tau; k, \nu) - k\tilde{\Pi}_1(\tau; k, \nu)\right). \tag{5.77}$$

At the end of this section we want to briefly discuss the need of the initial data for W-fields, which we have ignored so far. When the right side of (5.77) is not vanishing at initial time τ_0 we must have a non-vanishing τ component of the current at τ_0 in order to have a chance to satisfy the Gauss law constraint. Therefore let us take a closer look at $\tilde{j}^{\tau}(\tau_0)$. First we note that at $\tau = \tau_0$ we get $\bar{\eta}_0 = 0$ and $\chi_0 = 0$. The only non-vanishing Bessel function at 0 is $J_0(0) = 1$ which leaves us with

$$
\begin{aligned}
\tilde{j}^{\tau}(\tau_0; k, \nu) &= -\frac{m_D^2}{2}\int\frac{d\bar{y}\,\tau_0\cosh\bar{y}\sinh\bar{y}}{\tau_{iso}^2(1 + \frac{\tau_0^2\sinh^2\bar{y}}{\tau_{iso}^2})^2}\tilde{A}_{\eta}(\tau_0; k, \nu) + \tilde{j}_0^{\tau}(\tau_0; k, \nu)\\
&=\tilde{j}_0^{\tau}(\tau_0; k, \nu). \tag{5.78}
\end{aligned}
$$

As it should, the first term vanishes by symmetry, because we integrate an odd function in $\bar{y}$. Since we essentially need induced currents at τ_0 in some cases, it is also interesting to discuss the influence of such initial induced currents in general. This will be done in the following chapter, where our aim is to solve the integro-differential equations of motion for the soft gauge fields numerically.

Chapter 6

Results for the time evolution of gauge fields

Before we discuss our final results for the time evolution of the gauge fields in the weak-field approximation, let us briefly recapitulate what we did in the preceding chapter. Our starting point was the set of Boltzmann-Vlasov equations we first had obtained from kinetic theory in section 3.4 for stationary momentum distributions of the hard particles. We saw that under certain assumptions, which had to be satisfied by the distribution function, we were able to treat non-stationary situations as well. We adopted a convenient coordinate system and solved the Boltzmann-Vlasov equations by introducing auxiliary fields. In the end we obtained integro-differential equations which describe the time evolution of the collective modes we are interested in. It remains to solve these equations, which can only be done numerically, and to discuss certain interesting cases. This is done in the present chapter, where we encounter again stable and unstable modes like in the stationary case. We start by considering wave vectors with $k = 0$ and $\nu \neq 0$, hence parallel to the anisotropy direction which is the z or η direction in our case.

6.1   Wave vector parallel to anisotropy direction

In the stationary case and for an oblate momentum distribution we found that collective modes with wave vectors parallel to the anisotropy direction are unstable for transversally polarized fields and stable for longitudinally polarized ones. In the non-stationary situation we find that this does not change, but the frequency of the stable oscillations and the growth rate of the unstable modes become time dependent. At first we consider the stable

solutions and then turn to the more interesting instabilities.

6.1.1 Stable modes

In the case of longitudinal modes (gauge fields parallel to the wave vector) we need non-vanishing initial W fields whenever we choose the initial conjugate momentum to be non-zero due to the Gauss law constraint (5.77). In fact the numerical computation shows that initial A fields instead of initial Π fields only give constant solutions, which are not of interest to us. Therefore it is inevitable to introduce $W_\alpha^0 \neq 0$ at least in one spatial component. We need to choose the initial data such that the τ component of the current does not vanish at τ_0. A possible choice is

$$W_\eta^0(\tau_0, \eta_0; \phi, y) = K_1 \tanh(y - \eta_0) e^{i\nu\eta_0}, \qquad (6.1)$$

where K_1 is a constant and η_0 is given by (5.48) and depends on τ and η. At $\tau = \tau_0$ we have $\eta_0 = \eta$ and so (6.1) gives the non-vanishing term in $j^\tau(\tau_0)$

$$\begin{aligned}
j_0^\tau(\tau_0, \eta) &= \frac{m_D^2}{2} \int \frac{dy \cosh(y - \eta)}{(1 + \frac{\tau_0^2 \sinh^2(y-\eta)}{\tau_{iso}^2})^2} \frac{V_\eta}{\tau_{iso}^2} W_\eta^0(\tau_0; \nu, \phi, y) \\
&= -\frac{K_1 m_D^2 \tau_0}{2\tau_{iso}^2} \int \frac{d\bar{y} \sinh^2 \bar{y}}{(1 + \frac{\tau_0^2 \sinh^2 \bar{y}}{\tau_{iso}^2})^2} e^{i\nu\eta},
\end{aligned} \qquad (6.2)$$

where in the last step we used $\bar{y} = y - \eta$. However, our choice (6.1) is not unique, but every odd function in $\bar{y}$ can be used in principle. In the next step we fix the constant K_1 by requiring that the Gauss law constraint is satisfied at τ_0. We therefore Fourier transform (6.2) and obtain

$$\tilde{j}^\tau(\tau_0; \nu) = -\frac{2\pi K_1 m_D^2 \tau_0}{2\tau_{iso}^2} \int \frac{d\bar{y} \sinh^2 \bar{y}}{(1 + \frac{\tau_0^2 \sinh^2 \bar{y}}{\tau_{iso}^2})^2} = \frac{i\nu\tilde{\Pi}^\eta(\tau_0; \nu)}{\tau_0}. \qquad (6.3)$$

From above we read off the expression for the constant K_1

$$K_1 = -\frac{2i\tau_{iso}^2 \nu \tilde{\Pi}^\eta(\tau_0; \nu)}{2\pi m_D^2 \tau_0^2} \left(\int \frac{d\bar{y} \sinh^2 \bar{y}}{(1 + \frac{\tau_0^2 \sinh^2 \bar{y}}{\tau_{iso}^2})^2} \right)^{-1}. \qquad (6.4)$$

The τ component of the current coming from the initial W fields at arbitrary times $\tau > \tau_0$ is then given by

$$
\tilde{j}_0^\tau(\tau; \nu) = \frac{i\nu\tau^2\tilde{\Pi}^\eta(\tau_0; \nu)}{\tau_0^3} \left(\int \frac{d\bar{y} \sinh^2 \bar{y}}{(1 + \frac{\tau_0^2 \sinh^2 \bar{y}}{\tau_{iso}^2})^2} \right)^{-1} \times
$$
$$
\int \frac{d\bar{y} e^{i\nu\bar{\eta}_0} \cosh \bar{y} \sinh^2 \bar{y}}{(1 + \frac{\tau^2 \sinh^2 \bar{y}}{\tau_{iso}^2})^2 \sqrt{1 + \frac{\tau^2 \sinh^2 \bar{y}}{\tau_0^2}}}, \tag{6.5}
$$

with

$$
\bar{\eta}_0 \equiv \bar{y} - \mathrm{asinh}\left(\frac{\tau}{\tau_0} \sinh \bar{y} \right) \tag{6.6}
$$

according to (5.61).

The W_η^0 given in (6.1) does also contribute to $\tilde{j}^\eta$ and we eventually find

$$
\tilde{j}_0^\eta(\tau_0; \nu) = \frac{i\nu\tau\tilde{\Pi}^\eta(\tau_0; \nu)}{\tau_0^3} \left(\int \frac{d\bar{y} \sinh^2 \bar{y}}{(1 + \frac{\tau_0^2 \sinh^2 \bar{y}}{\tau_{iso}^2})^2} \right)^{-1} \times
$$
$$
\int \frac{d\bar{y} e^{i\nu\bar{\eta}_0} \sinh^3 \bar{y}}{(1 + \frac{\tau^2 \sinh^2 \bar{y}}{\tau_{iso}^2})^2 \sqrt{1 + \frac{\tau^2 \sinh^2 \bar{y}}{\tau_0^2}}}. \tag{6.7}
$$

As mentioned before the equations of motion of the gauge fields decouple for $k = 0$ and we therefore need to solve[1]

$$
\frac{1}{\tau}\partial_\tau\tilde{\Pi}^\eta(\tau; \nu) = -\tilde{j}^\eta(\tau; \nu) \tag{6.8}
$$

numerically. We discretize both the variable τ and τ' of the memory integral in $\tilde{j}^\eta$ and then apply a leap frog algorithm. It remains to fix the dimensionful parameters. We do this in the same way as in [26] in the framework of the color glass condensate. As a starting time for the plasma phase we choose $\tau_0 \simeq Q_s^{-1}$ with $Q_s \simeq 1$ and 3 GeV being the so called saturation scale for RHIC and LHC, respectively [31]. The only other dimensionful parameter is the Debye mass $m_D^2 \simeq 1.285/(\tau_0\tau_{iso})$ [2]. Because we intend to study oblate momentum distributions in this section, we choose $\tau_0 > \tau_{iso}$.

---

[1]Here, $\tilde{j}^\eta$ is the complete expression of the induced current as given in (5.66) and $\tilde{j}_0^\eta$ is just the part of it, that comes from initial W fields.

[2]The details on how to obtain these values are given in [26] and references therein. The value of the Debye mass chosen here corresponds to a gluon liberation factor $c = 2\ln 2$
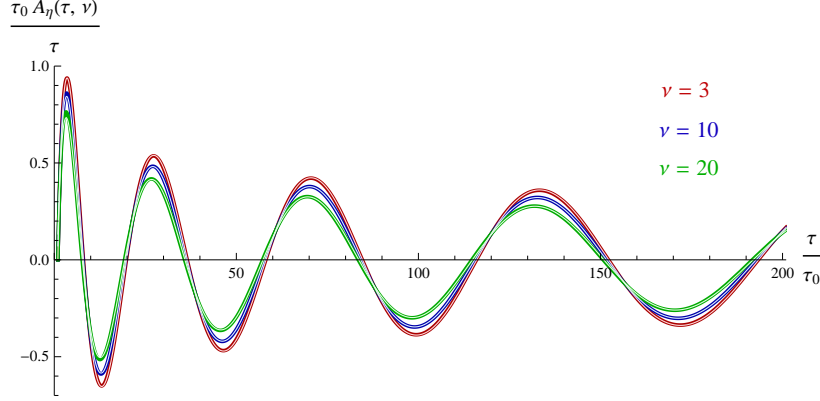
Figure 6.1: Longitudinal modes for $\tau_{iso}/\tau_0 = 0.01$. The thin light lines are the results from the analytic late time behavior (B.21), which are in good agreement with the numerical data (thick darker lines) even at early times.

In figure 6.1 we compare the late time behavior, which is obtained analytically in appendix B, with our numerical simulation. We notice that these modes are indeed stable. Finally we remark that we tested for Gauss law violations at $\tau > \tau_0$ and found that they decrease with increasing accuracy while the results in figure 6.1 remain the same. In the next section we turn to the more interesting case of unstable modes.

6.1.2 Unstable modes

From our analysis in section 4.3.3 we expect to find instabilities when we study transversely polarized fields and oblate distribution functions. Our aim is to consider various initial conditions and therefore we want to investigate the influence of initial induced currents too. In the present situation ($k = 0$ and $\Pi^\eta = 0$) the Gauss law constraint simply becomes $\tilde{j}^\tau = 0$ and hence by introducing appropriate non-vanishing initial data for the W fields we can choose a third parameter $\tilde{j}^i(\tau_0; \nu)$ besides $\tilde{\Pi}^i(\tau_0; \nu)$ and $\tilde{A}^i(\tau_0; \nu)$. We note that the equations of motion are the same for $\tilde{A}^1$ and $\tilde{A}^2$ when $k = 0$ as can be seen from (5.65) and (5.67) in section 5.7. As before for the longitudinal modes the choice of the W fields at τ_0 is not unique. We take[3]

$$W_i^0(\tau_0, \eta_0; \phi, y) = K_2 e^{i\nu\eta_0}, \tag{6.9}$$

---

[3]We studied different choices too, but the qualitative behavior turned out to be the same in all cases we considered.

where K_2 is again a constant. Next we investigate the expression for the current j^i at τ_0 taking into account (6.9) and find

$$j_0^i(\tau_0, \eta) = -\frac{K_2 m_D^2}{4} \int \frac{d\bar{y} e^{i\nu\eta}}{(1 + \frac{\tau_0^2 \sinh^2 \bar{y}}{\tau_{iso}^2})^2}, \tag{6.10}$$

where we used that $\eta_0 = \eta$ for $\tau = \tau_0$. From this expression we can write the constant K_2 in terms of the initial induced current. After performing a Fourier transformation we find for the term of the transverse current that comes from the initial W fields

$$\tilde{j}_0^i(\tau; \nu) = \tilde{j}^i(\tau_0; \nu) \left(\int \frac{d\bar{y}}{(1 + \frac{\tau_0^2 \sinh^2 \bar{y}}{\tau_{iso}^2})^2} \right)^{-1} \int \frac{d\bar{y} e^{i\nu\bar{\eta}_0}}{(1 + \frac{\tau^2 \sinh^2 \bar{y}}{\tau_{iso}^2})^2} \tag{6.11}$$

at arbitrary $\tau > \tau_0$.

Eventually we have to solve

$$\frac{1}{\tau}\partial_\tau \tilde{\Pi}_i(\tau; \nu) = \tilde{j}^i(\tau; \nu) - \frac{\nu^2}{\tau^2}\tilde{A}^i(\tau; \nu) \tag{6.12}$$

by applying a leap frog algorithm again. We fix the dimensionful parameters in exactly the same way as for the stable modes. In the left panel of figure 6.2 the solutions for 3 different values of ν are compared to their late time behavior, which is obtained in appendix B. Here, the starting conditions are $\tilde{\Pi}_i(\tau_0; \nu) = 1$ and $\tilde{A}^i(\tau_0; \nu) = \tilde{j}^i(\tau_0; \nu) = 0$ for all modes. For late times we notice that modes with a larger wave number ν also have larger growth rates. Actually we find for the analytical late time behavior of the transverse gauge fields obtained in appendix B that very infrared modes ($\nu \ll 1$) correspond indeed to oscillatory stable solutions.

In the left log-square root plot of figure 6.2 we additionally notice that there is a delay until the instabilities start to grow. For small τ the amplitudes even decrease. To clarify what this delay means we should discuss the time scales associated with it. From comparison of the experimental data from RHIC with results obtained from hydrodynamic simulations it has been concluded that the time the quark-gluon plasma needs to thermalize is of the order of or perhaps smaller than 1 fm/c.[4] In the way we fixed our dimensionful parameters, 1 fm/c corresponds to approximately $5\tau_0$ for RHIC and about $15\tau_0$ for LHC [27]. Due to this delay it would be unlikely that quark-gluon plasma instabilities contribute to the fast isotropization in heavy ion

---

[4]In [32] it has been argued that the hydrodynamic behavior observed experimentally does not require local thermodynamic equilibrium, but merely an isotropic momentum distribution.
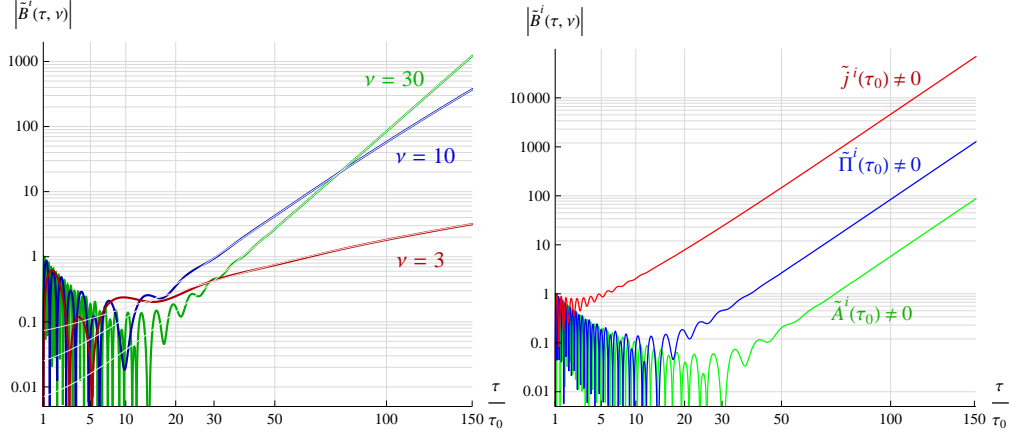
Figure 6.2: In the left panel transverse magnetic fields are compared for different wave numbers ν but equal initial conditions $\tilde{\Pi}^i(\tau_0) = 1$ and $\tilde{A}^i(\tau_0) = \tilde{j}^i(\tau_0) = 0$. The expected analytical late time behavior is indicated by the thin light lines. In the right plot the influence of different initial values is studied for modes with $\nu = 30$ (non-zero initial values are indicated in the plot). In both cases we assume an oblate momentum distribution from the beginning with $\tau_{iso}/\tau_0 = 0.01$.

collisions. However, we can still investigate other possible initial conditions. The result is shown in the right plot of figure 6.2 for $\nu = 30$. Whenever we choose the induced current to be zero at τ_0 we observe an uncomfortably long delay of the onset of the instabilities. The situation changes when we consider initial induced currents as can be seen clearly in the right panel of figure 6.2, where the amplitude of the magnetic field starts to rise almost immediately.

At this point we should mention how we normalize the modes for different starting conditions. Whenever we only have non-vanishing A and Π fields, but zero initial currents, we simply choose the total energy density of the fields (as defined in section 5.3) to be equal at the beginning. For initial currents only the energy density of the fields is zero at τ_0 and hence we must normalize these modes differently. We do this by setting the height of the first maximum in the amplitude of the A fields approximately equal to those of the other modes with non-zero initial values in the fields only. We also adopt this normalization when we study the energy density. Anyway the qualitative result that modes with $\tilde{j}^i(\tau_0; \nu) \neq 0$ start growing almost immediately does not depend on normalization issues.

When we consider the total energy density in figure 6.3, we find again that the delay of the onset of the instabilities is clearly reduced for modes
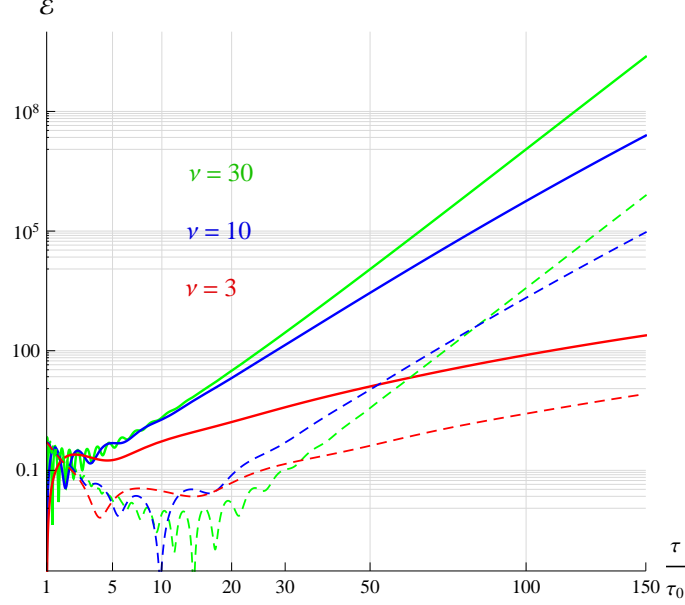
Figure 6.3: Total energy density for different wave numbers ν. The full lines correspond to $\tilde{j}^i(\tau_0; \nu) \neq 0$, while the dashed lines are the results for $\tilde{\Pi}^i(\tau_0; \nu) \neq 0$. $\tau_{iso}/\tau_0 = 0.01$.

with initial induced currents. However, let us quantify this result a bit. We stated already that plasma instabilities should have some important influence already around 1 fm/c in order to possibly describe the fast isotropization of the system, which takes place at this time scale. As mentioned before this would roughly correspond to $5\tau_0$ for RHIC, where the energy density for modes with $\tilde{j}^i(\tau_0; \nu) = 0$ is still decreasing. But also for the modes with non-vanishing initial currents the energy density has not grown significantly until $5\tau_0$. For LHC, where 1 fm/c $\approx 15\tau_0$, the situation becomes more promising, at least for modes with $\tilde{j}^i(\tau_0; \nu) \neq 0$. We should also mention that the actual isotropization takes place when the gauge fields have grown non-perturbatively large. Therefore this can not be studied in the hard loop approximation. Nevertheless, we can investigate the early evolution of the instabilities and therefore discuss the minimal time for isotropization.

When the total energy density is split into an electric and magnetic contribution, we find that the magnetic energy density accounts for almost all of the total energy density except at very early times. In figure 6.4 the gain rate as defined in (5.30), which gives the energy transfer from the hard particles to the soft collective modes, is plotted. It is exactly this transfered energy that drives the instability. In the beginning the gain rate actually becomes
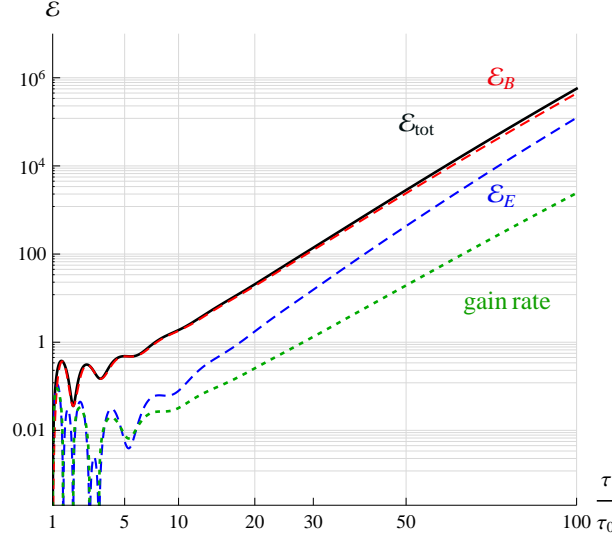
Figure 6.4: The total energy density $\mathcal{E}_{tot}$ for $\nu = 10$ and $\tilde{j}^i(\tau_0; \nu) \neq 0$ is split into the contributions from electric ($\mathcal{E}_E$) and magnetic fields ($\mathcal{E}_B$). Additionally the gain rate defined in (5.30) times τ_0 is shown.

negative. This indicates that the energy of hard particles increases at the expense of the collective modes. However, for late enough times we note that the energy transfer only takes place in direction to the soft gauge fields.

The important conclusion from this study is that taking into account initial values of W fields and, associated with this non-vanishing induced currents at starting time τ_0, modifies the dynamics of the system. Especially the long delay till the onset of the instabilities, which was found first in [26], is reduced drastically. This makes it at least more likely that plasma instabilities play some role in explaining the fast isotropization after heavy ion collisions[5].

6.2 Wave vector perpendicular to anisotropy direction

Next we discuss the second simple case where the equations for the time evolution of $\tilde{A}^1$ and $\tilde{A}^2$ decouple, which happens for $\nu = 0$. There we find 3

---

[5]We remind the reader that we only discuss the Abelian regime, but to draw conclusions for the quark-gluon plasma it is important to consider the non-Abelian case. However, the Abelian results can provide an upper bound for the behavior of non- Abelian plasma instabilities [27].

different modes, because the expressions for the gauge fields in the 1 and 2 direction are not the same this time. In this section we want to investigate the behavior for prolate distribution functions as well and therefore choose the starting time of our considerations τ_0 to be smaller than τ_{iso}. We only have to worry about the Gauss law constraint when we study the 1 direction, which refers to longitudinally polarized modes (the wave vector points in the 1 direction in this section). We again start by examining the stable solutions.

6.2.1 Stable modes

Let us first discuss the longitudinal modes. We must introduce initial W fields to be able to satisfy the Gauss law. This in done completely analogous to before. We choose the initial data of the W fields to be

$$W_1^0(\tau_0, x_0; \phi, y) = \frac{K_3 e^{ikx_0}}{\cos \phi}, \qquad (6.13)$$

where K_3 is again a constant that must be fixed in the following. This gives the non-vanishing contribution to $\tilde{j}^\tau(\tau_0; k)$ which reads

$$\tilde{j}^\tau(\tau_0; k) = -\frac{K_3 m_D^2 2\pi}{2} \int \frac{d\bar{y}\cosh\bar{y}}{(1 + \frac{\tau_0^2 \sinh^2 \bar{y}}{\tau_{iso}^2})^2}. \qquad (6.14)$$

We obtain the expression for K_3 from the Gauss law constraint

$$\tau_0 \tilde{j}^\tau(\tau_0; k) = -ik\tilde{\Pi}_1(\tau_0; k). \qquad (6.15)$$

Eventually we find

$$\tilde{j}_0^\tau(\tau; k) = -\frac{ik\tilde{\Pi}_1(\tau_0; k)}{\tau_0} \left(\int \frac{d\bar{y}\cosh\bar{y}}{(1 + \frac{\tau_0^2 \sinh^2 \bar{y}}{\tau_{iso}^2})^2} \right)^{-1} \int \frac{d\bar{y} J_0(k\chi_0)\cosh\bar{y}}{(1 + \frac{\tau^2 \sinh^2 \bar{y}}{\tau_{iso}^2})^2} \quad (6.16)$$

for $\tau > \tau_0$, where χ_0 is a function of both τ and $\bar{y}$. It remains to find the contribution to $\tilde{j}^1$, which is

$$\tilde{j}_0^1(\tau; k) = \frac{k\tilde{\Pi}_1(\tau_0; k)}{\tau_0} \left(\int \frac{d\bar{y}\cosh\bar{y}}{(1 + \frac{\tau_0^2 \sinh^2 \bar{y}}{\tau_{iso}^2})^2} \right)^{-1} \int \frac{d\bar{y} J_1(k\chi_0)}{(1 + \frac{\tau^2 \sinh^2 \bar{y}}{\tau_{iso}^2})^2}. \quad (6.17)$$

Finally we have all the ingredients we need in order to solve the equation of motion for $\tilde{A}^1$

$$\frac{1}{\tau}\partial_\tau \tilde{\Pi}_1(\tau; k) = \tilde{j}^1(\tau; k) \qquad (6.18)$$
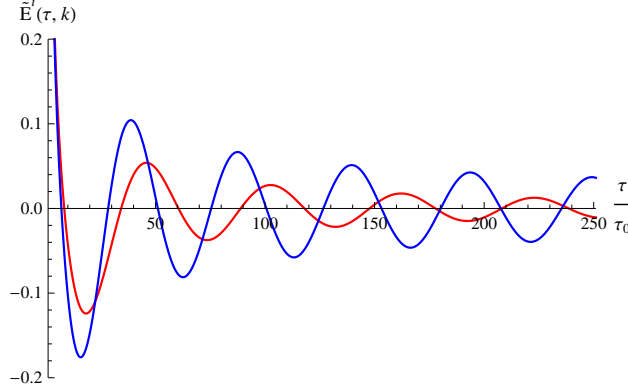
Figure 6.5: Stable modes for wave vectors perpendicular to the anisotropy direction. The red and the blue line correspond to $\tilde{E}^1$ and $\tilde{E}^2$, respectively. The parameters are $m_D^2 = 1.285/(\tau_{iso}\tau_0)$, $\tau_{iso}/\tau_0 = 100$ and $k = 0.1$. The initial conditions are such that there is only a non-vanishing conjugate momentum $\tilde{\Pi}_i(\tau_0; k) = 1$.

consistently. Since we want to study prolate and oblate momentum distributions, we fix $\tau_{iso} = 100\tau_0$. The class of momentum distribution functions we defined in section 5.4 gets more and more oblate in time. Therefore we simply choose the final time of our simulation to be larger than τ_{iso} such that we can investigate the behavior in the oblate case as well. In figure 6.5 we plot the electric field corresponding to a mode with $k = 0.1$.

For wave vectors perpendicular to the anisotropy direction we additionally find stable modes that are transversally polarized, namely in the 2 direction. There is no need for any initial W fields to satisfy the Gauss law and, because we are more interested in instabilities, we skip the task of introducing initial induced currents in the present case[6]. Therefore we simply solve

$$\frac{1}{\tau}\partial_\tau\tilde{\Pi}_2(\tau; k) = \tilde{j}^2(\tau; k) - k^2\tilde{A}^2(\tau; k), \tag{6.19}$$

with $\tilde{j}_0^2(\tau; k) = 0$ in (5.67). The electric field in the 2 direction is compared to the longitudinal electric field in figure 6.5. The parameters are the same in both cases. We notice that the modes are stable for prolate and oblate momentum distribution functions.

---

[6]Possible initial data would be $W_2^0(\tau_0, x_0; \phi, y) = Ke^{ikx_0}$ (with K being constant), but the solution turns out to be qualitatively similar for initial induced currents too.

6.2.2 Unstable modes

We still need to examine the time evolution of $\tilde{A}^\eta$. To study the influence of induced currents at τ_0 we introduce

$$W_\eta^0(\tau_0, x_0; \phi, y) = K_4 e^{ikx_0}. \tag{6.20}$$

With this initial data we have the freedom to set the value of the current at τ_0. We proceed in the same way as before and end up with

$$\tilde{j}_0^\eta(\tau; k) = \tilde{j}^\eta(\tau_0; k) \left(\int \frac{d\bar{y} \sinh^2 \bar{y}}{(1 + \frac{\tau_0^2 \sinh^2 \bar{y}}{\tau_{iso}^2})^2} \right)^{-1} \int \frac{d\bar{y} J_0(k\chi_0) \sinh^2 \bar{y}}{(1 + \frac{\tau^2 \sinh^2 \bar{y}}{\tau_{iso}^2})^2}. \tag{6.21}$$

The integro-differential equation we intend to solve is

$$\frac{1}{\tau} \partial_\tau \tilde{\Pi}^\eta(\tau; k) = -\tilde{j}^\eta(\tau; k) - \frac{k^2}{\tau^2} \tilde{A}_\eta(\tau; k). \tag{6.22}$$

As for the stable modes we choose $\tau_0 < \tau_{iso}$ such that the momentum distribution is prolate at the initial time. We again stop our simulation only after the momentum distribution function became oblate. Unfortunately the solutions show little activity for physically reasonable mass parameters m_D. Therefore we want to consider the solutions for a very high Debye mass $m_D^2 = 1000/(\tau_0 \tau_{iso})$ at first and comment on the situation for physical parameters later.

The gauge fields for different wave numbers are shown in the left plot of figure 6.6. We note that the corresponding magnetic fields point in the 2 direction. We see that there exists an instability for prolate distributions. However, the modes get stable for $\tau \geq \tau_{iso}$. We again show the solutions for different initial conditions, but this time the difference is not as significant as before. For completeness we mention that this time modes with non-vanishing initial currents are normalized such that the oscillations in the stable region have approximately the same amplitude. When we consider the energy density of one mode, we again find that the magnetic fields account for most of the total energy density. This can be seen in the logarithmic plot on the right side of figure 6.6. The energy transfer between hard particles and soft modes takes place in the following way (we note that the gain rate is not shown in figure 6.6). At early times energy is transfered to the gauge fields, such that the instability can evolve. At about $5.5\tau_0$ the gain rate changes sign and in the following the energy density for the collective modes decreases rapidly. Eventually the gain rate oscillates with a small amplitude around zero in the region where the momentum distribution is oblate.
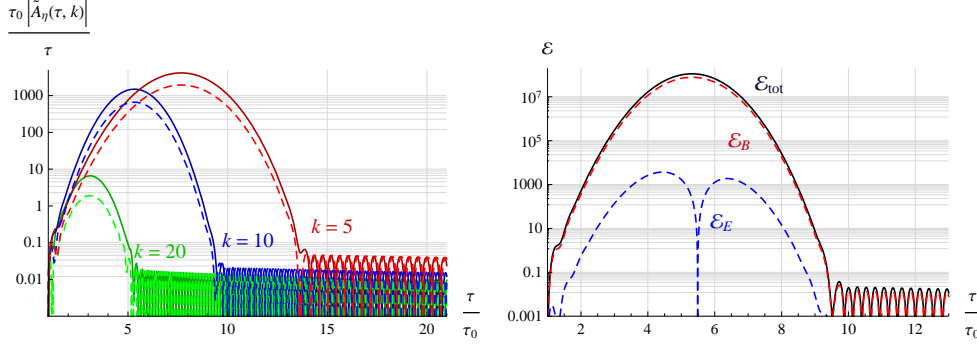
Figure 6.6: Unstable modes for prolate momentum distributions for different wave numbers and initial conditions (left). The dashed lines correspond to $\tilde{\Pi}^{\eta}(\tau_0; k) \neq 0$ and the full lines to $\tilde{j}^{\eta}(\tau_0; k) \neq 0$. In the right panel the total energy density and its contributions from electric and magnetic fields are shown for $k = 10$ and $\tilde{j}^{\eta}(\tau_0; k) \neq 0$. The remaining parameters in both plots are $m_D^2 = 1000/(\tau_{iso}\tau_0)$ and $\tau_{iso}/\tau_0 = 10$.

Now we turn to a more reasonable Debye mass $m_D^2 = 1.285/(\tau_{iso}\tau_0)$. We must consider small wave numbers $k < 1$ and strongly elongated momentum distributions to find an instability. We choose $\tau_{iso}/\tau_0 = 100$. In figure 6.7 the energy density for $k = 0.1$ is shown. Again we split the total energy density into contributions coming from magnetic and electric fields. We emphasize that the plot is not logarithmic this time. To get a better insight we consider the gain rate too. We find that it is positive in the very beginning, which indicates that energy is transfered from the hard particles to the soft fields. However, after about $30\tau_0$ it becomes negative for the first time. The gain rate then rises again, but after $70\tau_0$ it becomes negative for a second time. After the distribution function becomes isotropic at $100\tau_0$ and thereafter increasingly oblate the gain rate simply oscillates around zero. As for the bigger Debye mass we see that there is only an instability for prolate momentum distributions.

6.3 General wave vectors

Up to now we considered two special situations, where the integro-differential equations for $\tilde{A}^1$ and $\tilde{A}^{\eta}$ decoupled. In this section we intend to examine cases, where both k and ν are non-zero. Due to the expansion the wave vector is not constant in time. From dimensional analysis we find that the
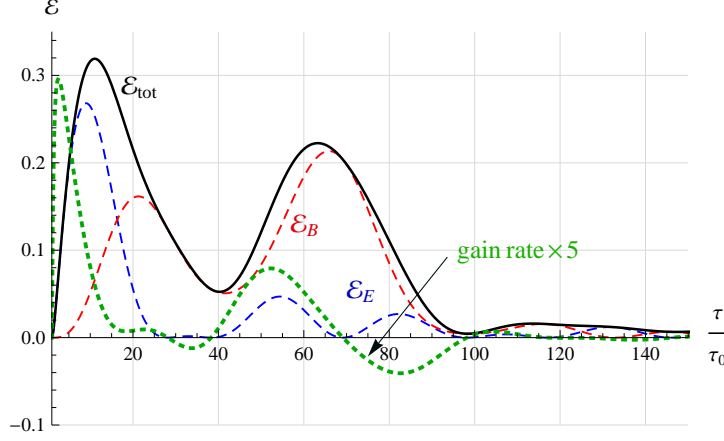
Figure 6.7: Total, electric and magnetic energy densities for a physically more reasonable Debye mass $m_D^2 = 1.285/(\tau_{iso}\tau_0)$. The gain rate is increased by a factor 5 to make it better visible. The only non-vanishing initial data is for the induced current. The remaining parameters are $k = 0.1$ and $\tau_{iso}/\tau_0 = 100$.

wave vector can be written as

$$\mathbf{k} = k\hat{\mathbf{x}}^1 + \frac{\nu}{\tau}\hat{\eta}. \tag{6.23}$$

We see that the angle $\mathbf{k}$ makes with the η (or z) axis increases as time passes by. At first we solve the coupled equations and return to the task of determining the time evolution of $\tilde{A}^2$ at the end of this section. The Gauss law constraint reads

$$\tau\tilde{j}^\tau(\tau;k,\nu) = i\big(\nu\tilde{\Pi}^\eta(\tau;k,\nu) - k\tilde{\Pi}_1(\tau;k,\nu)\big) \tag{6.24}$$

and we must take care that it is satisfied at τ_0 by introducing initial W fields. This can be done in various ways. We choose the initial data such that it equals (6.1) for $k = 0$ and take

$$W_\eta^0(\tau_0, x_0, \eta_0; \phi, y) = K_5 \tanh(y - \eta_0)e^{i\nu\eta_0}e^{ikx_0}, \tag{6.25}$$

where x_0 and η_0 are given by (5.49) and (5.48), respectively. The constant K_5 is found by demanding the Gauss law constraint at τ_0. We have performed analogous calculations above and therefore only state the final result for the

part of $\tilde{j}^\tau(\tau; k, \nu)$ that comes from non-vanishing initial W fields

$$
\tilde{j}_{0I}^\tau(\tau; k, \nu) = \frac{i\tau^2}{\tau_0^3} \left(\nu \tilde{\Pi}_0^\eta - k \tilde{\Pi}_1^0 \right) \left(\int \frac{d\bar{y} \sinh^2 \bar{y}}{(1 + \frac{\tau_0^2 \sinh^2 \bar{y}}{\tau_{iso}^2})^2} \right)^{-1} \times
$$
$$
\int \frac{d\bar{y} J_0(k\chi_0) e^{i\nu\bar{\eta}_0} \cosh \bar{y} \sinh^2 \bar{y}}{(1 + \frac{\tau^2 \sinh^2 \bar{y}}{\tau_{iso}^2})^2 \sqrt{1 + \frac{\tau^2 \sinh^2 \bar{y}}{\tau_0^2}}}, \tag{6.26}
$$

where $\tilde{\Pi}_0^\eta = \tilde{\Pi}^\eta(\tau_0; k, \nu)$ and $\tilde{\Pi}_1^0 = \tilde{\Pi}_1(\tau_0; k, \nu)$. It is easy to check that this does indeed give the Gauss law constraint for $\tau = \tau_0$.

The W field in (6.25) does also contribute to the currents in the 1 and η direction. Eventually we find

$$
\tilde{j}_{0I}^1(\tau; k, \nu) = \frac{\tau^2}{\tau_0^3} \left(k \tilde{\Pi}_1^0 - \nu \tilde{\Pi}_0^\eta \right) \left(\int \frac{d\bar{y} \sinh^2 \bar{y}}{(1 + \frac{\tau_0^2 \sinh^2 \bar{y}}{\tau_{iso}^2})^2} \right)^{-1} \times
$$
$$
\int \frac{d\bar{y} J_1(k\chi_0) e^{i\nu\bar{\eta}_0} \sinh^2 \bar{y}}{(1 + \frac{\tau^2 \sinh^2 \bar{y}}{\tau_{iso}^2})^2 \sqrt{1 + \frac{\tau^2 \sinh^2 \bar{y}}{\tau_0^2}}} \tag{6.27}
$$

and

$$
\tilde{j}_{0I}^\eta(\tau; k, \nu) = \frac{i\tau}{\tau_0^3} \left(\nu \tilde{\Pi}_0^\eta - k \tilde{\Pi}_1^0 \right) \left(\int \frac{d\bar{y} \sinh^2 \bar{y}}{(1 + \frac{\tau_0^2 \sinh^2 \bar{y}}{\tau_{iso}^2})^2} \right)^{-1} \times
$$
$$
\int \frac{d\bar{y} J_0(k\chi_0) e^{i\nu\bar{\eta}_0} \sinh^3 \bar{y}}{(1 + \frac{\tau^2 \sinh^2 \bar{y}}{\tau_{iso}^2})^2 \sqrt{1 + \frac{\tau^2 \sinh^2 \bar{y}}{\tau_0^2}}}. \tag{6.28}
$$

However, these expressions vanish at τ_0. When we want to take initial induced currents in the τ and η component into account, we need to introduce further W fields at τ_0. For example

$$
W_\eta^0(\tau_0, x_0, \eta_0; \phi, y) = K_6 e^{i\nu\eta_0} e^{ikx_0} \tag{6.29}
$$

gives only a non-vanishing contribution at τ_0 in the η component and hence K_6 turns out to be proportional to $\tilde{j}^\eta(\tau_0; k, \nu)$. At arbitrary time $\tau > \tau_0$ (6.29) contributes to $\tilde{j}^\tau$, $\tilde{j}^1$ and $\tilde{j}^\eta$. The expressions are quite lengthy and we therefore collect them in appendix C. In the same way we can fix initial values for $\tilde{j}^1(\tau_0; k, \nu)$ after introducing

$$
W_1^0(\tau_0, x_0, \eta_0; \phi, y) = K_7 e^{i\nu\eta_0} e^{ikx_0}. \tag{6.30}
$$

The corresponding contributions to the various currents for $\tau > \tau_0$ can again be found in the appendix. In total we add 3 terms coming from initial W fields to the current

$$\tilde{j}_0^1(\tau; k, \nu) = \tilde{j}_{0I}^1(\tau; k, \nu) + \tilde{j}_{0II}^1(\tau; k, \nu) + \tilde{j}_{0III}^1(\tau; k, \nu), \qquad (6.31)$$

where $\tilde{j}_{0II}^1$ and $\tilde{j}_{0III}^1$ are associated with (6.29) and (6.30), respectively. The same is true for the η and τ component.

We can now solve the coupled integro-differential equations for $\tilde{A}^1$ and $\tilde{A}^\eta$, given in (5.70) and (5.71), numerically. Before we proceed, we discuss in which directions the resulting physical electric and magnetic fields point. At first we examine magnetic fields. We notice that the gauge fields and the wave vector all lie in the plane spanned by $\hat{\mathbf{x}}^1$ and $\hat{\eta}$ and it follows from $\mathbf{B} = \text{rot}\mathbf{A}$ that the corresponding B field must point in the direction perpendicular to that plane, hence in the 2 direction. On the other side the electric field has a longitudinal and a transversal component with respect to the wave vector. The projection of $\mathbf{E}$ parallel to the wave vector yields

$$E_L = \frac{k\tilde{\Pi}^1 + \nu\tilde{\Pi}^\eta}{\sqrt{k^2\tau^2 + \nu^2}}. \qquad (6.32)$$

This expression gives the correct form for the limiting cases $k = 0$ and $\nu = 0$. In the following we are interested in the energy density of the longitudinal electric fields. The reason is that in the previous sections we only encountered transversal instabilities, but from our analysis of the stationary plasma in section 4.3 we expect to find an electric instability for wave vectors within an angle of $45°$ to the η axis. However, this is complicated by the fact that in the non-stationary case the angle between the wave vector and the η axis increases in time. Therefore we study situations where the 1 component of the wave vector is initially small compared to the η component.

In figure 6.8 the energy density for $k = 1$ and $\nu = 10$ is shown. This means after $10\tau_0$ there can not be an electric instability anymore according to our analysis before. Again we consider a larger mass parameter $m_D^2 = 10/(\tau_{iso}\tau_0)$ to find more significant results and indeed we notice that the total energy density rises initially and has its maximum at about $4\tau_0$. In the following it decreases and only takes on comparably small values after $\tau = 10\tau_0$. Additionally we remark that the electric energy density in the longitudinal direction contributes a big fraction of the total energy density this time, while the transversal electric energy density is still almost negligible.

To conclude our analysis we finally consider the time evolution of the transverse gauge fields $\tilde{A}^2$. We once more introduce initially non-vanishing W fields to be able to examine the influence of initial currents. We take

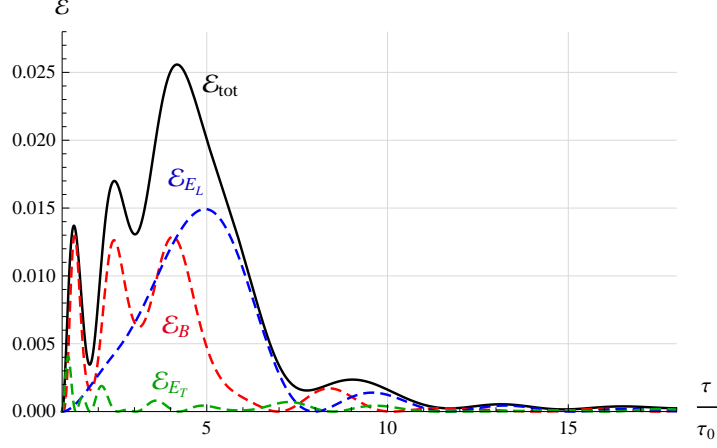$$W_2^0(\tau_0, x_0, \eta_0; \phi, y) = K_8 e^{i\nu\eta_0} e^{ikx_0}. \qquad (6.33)$$

Figure 6.8: Total, magnetic and electric energy densities for $k = 1$ and $\nu = 10$. The electric energy density is split into a longitudinal and a transverse part. The remaining parameters are $m_D^2 = 10/(\tau_{iso}\tau_0)$, $\tau_{iso}/\tau_0 = 0.1$ and $\tilde{j}^1(\tau_0; k, \nu) \neq 0$.

After a short calculation we find that K_8 is proportional to $\tilde{j}^2(\tau_0; k, \nu)$ and end up with

$$\tilde{j}^2(\tau_0; k, \nu) = \tilde{j}^2(\tau_0; k, \nu) \left(\int \frac{d\bar{y}}{(1 + \frac{\tau_0^2 \sinh^2 \bar{y}}{\tau_{iso}^2})^2} \right)^{-1} \times$$
$$\int \frac{d\bar{y} \big(J_2(k\chi_0) + J_0(k\chi_0) \big) e^{i\nu\bar{\eta}_0}}{(1 + \frac{\tau^2 \sinh^2 \bar{y}}{\tau_{iso}^2})^2} \tag{6.34}$$

It turns out that there is again a significant difference whether we examine initial induced currents or not. With vanishing currents at τ_0 the total energy density decreases already from the beginning. Contrary to this for $\tilde{j}^2(\tau_0; k, \nu) \neq 0$ we find a maximum in the energy density between 6 and $7\tau_0$ (see figure 6.9). We also notice that the magnetic fields account again for most of the total energy density and the electric contribution is almost negligible.
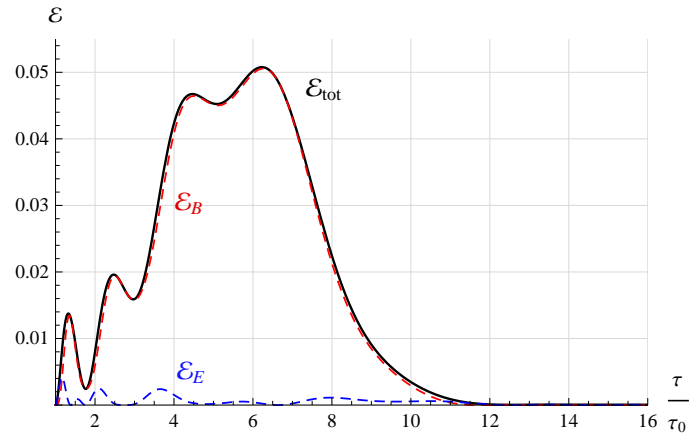
Figure 6.9: Energy density and its electric and magnetic contributions for $k = 1$ and $\nu = 10$. The parameters are $m_D^2 = 10/(\tau_{iso}\tau_0)$, $\tau_{iso}/\tau_0 = 0.1$ and $\tilde{j}^2(\tau_0; k, \nu) \neq 0$.

Chapter 7

Conclusion

In the last chapters we studied the collective behavior of an ultrarelativistic plasma. Even though our motivation was connected to the physics of heavy ion collisions we only studied effectively Abelian systems, since the full nonlinear dynamics of large gauge fields requires real-time lattice simulations [23, 24, 25, 33, 34, 35]. However, it has been noted in [27] that the Abelian solutions provide an upper bound to the late time behavior of non-Abelian plasma instabilities. We started by considering the collective behavior present in isotropic plasmas. Then we introduced an anisotropic momentum distribution and found that additionally to the stable collective modes instabilities arise. The stationary anisotropic plasma and the instabilities associated with it are considered in the context of heavy ion collisions and the quark-gluon plasma in various papers. However, to be able to describe realistic situations we argued that we must take the expansion of the system after the collision into account. This leads to modified dynamics of the gauge fields.

In chapter 5 we set the framework to discuss the collective behavior in an anisotropically expanding plasma. The expansion takes place in the z direction only, which should be a good approximation for the initial stage of a parton gas produced by colliding heavy nuclei. The study is based on a paper by Romatschke and Rebhan from 2006 [26], which we generalized in certain aspects. The probably most fundamental detail of this thesis is that initial data for the auxiliary W fields is inevitable to describe modes that are restricted by the Gauss law consistently, although this is not an issue for the unstable modes considered in [26]. Nevertheless, in chapter 6 we found that this initial W fields give us the possibility to discuss a wider class of initial conditions, which turned out to be very interesting for unstable modes. By examining the influence of non-vanishing initial currents we noticed that the delay in the onset of growth of instabilities that was found in [26] reduces

drastically. Furthermore we generalized the treatment of modes parallel to the anisotropy direction and presented results for arbitrary orientation of wave vectors with respect to the direction of anisotropy. We were therefore able to discuss a fully 3+1 dimensional situation, where we again investigated stable and unstable collective modes.

However, to understand the dynamics of a weakly coupled quark-gluon plasma after a heavy ion collision non-Abelian studies are inevitable. Especially in the context of instabilities nonlinear effects occur eventually, when the modes have grown such that non-Abelian interactions become important. The important issue of saturation of the unstable modes is therefore beyond the scope of this study.

On the experimental side the LHC will probably shed some light on the properties of a realistic quark-gluon plasma at unprecedented high energy densities. This is especially interesting in the case of non-Abelian plasma instabilities, since they do not seem to play an important role at RHIC. However, as we have argued in chapter 6 there is a possibility that plasma instabilities will contribute to the fast isotropization at LHC, which appears more likely in the light of our results on general initial conditions.

Appendix A

Sufficient conditions for instabilities

We recall that an instability is associated with a zero eigenvalue of

$$(\Delta^{-1}(Q))^{ij} = (q^2 - \omega^2)\delta^{ij} - q^i q^j + \Pi^{ij}(\omega, \mathbf{q}), \tag{A.1}$$

for some ω with Im $\omega > 0$. The above equation was already obtained in section 3.4. It is possible to justify the conditions from section 4.3.1 by continuity arguments which we want to explain in the following [15].

A.1 Condition 1

The spatial part of the self energy is given by

$$\Pi^{ij}(\omega, \mathbf{q}) = g^2 \int \frac{d^3p}{(2\pi)^3} \partial_k^{(p)} f(\mathbf{p}) \left[-v^i \delta^{kj} + \frac{v^i v^j q^k}{-\omega + \mathbf{q} \cdot \mathbf{v}} \right], \tag{A.2}$$

where we simply absorbed the $i\epsilon$ prescription into the value of the complex frequency ω and $\mathbf{v} = \mathbf{p}/|\mathbf{p}|$. We can change the integration variable $\mathbf{p} \to -\mathbf{p}$ which implies $\Pi^{ij}(\omega) = \Pi^{ij}(-\omega)$ because $f(\mathbf{p})$ is parity symmetric. We can also consider the complex conjugate of the polarization tensor and then find

$$\Pi^{ij} = [\Pi^{ij}(-\omega^*)]^*. \tag{A.3}$$

For purely imaginary $\omega = i\gamma$ (γ is real) we obtain

$$\Pi^{ij}(i\gamma) = [\Pi^{ij}(i\gamma)]^* \tag{A.4}$$

indicating that $\Pi^{ij}(i\gamma)$ is a real matrix and since it is symmetric too it has real eigenvalues. $\Pi^{ij}(i\gamma, \mathbf{q})$ is bounded for $\gamma \to \infty$ and thus

$$\lim_{\gamma \to \infty} \left[\Delta^{-1}(Q)\right]^{ij} = \lim_{\gamma \to \infty} \gamma^2 \delta^{ij}. \tag{A.5}$$
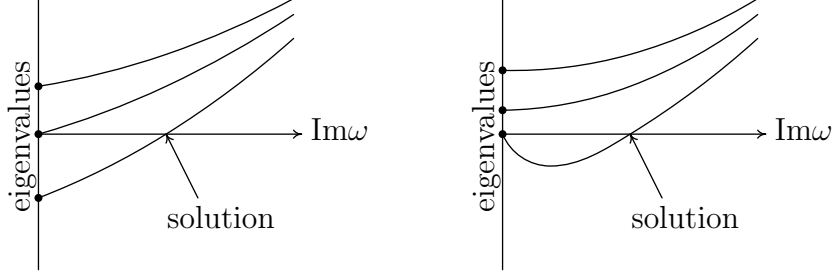
71

Figure A.1: Illustration of the continuity argument for condition 1 (left) and condition 2 (right).

Thus, for large enough γ the eigenvalues are always positive. Lets assume we find a negative eigenvalue for $\gamma = 0$. Then, by continuity of the real eigenvalues of $\mathbf{\Delta}^{-1}(Q)$ as γ goes from 0 to ∞, we eventually find a γ associated with an zero eigenvalue and thus an instability. But for $\gamma = 0$ we obtain

$$\left[\Delta^{-1}(0, \mathbf{q})\right]^{ij} = q^2 \delta^{ij} - q^i q^j + \Pi^{ij}(0, \mathbf{q}) \tag{A.6}$$

and therefore we found condition 1.

A.2 Condition 1-b

To motivate condition 1-b, we first show that non-vanishing $\Pi^{ij}(0, \hat{\mathbf{q}})$ implies a magnetic instability. To do so we consider the trace of the spatial part of the polarization tensor averaged over the direction of $\hat{\mathbf{q}}$

$$\langle \Pi^{ii}(0, \mathbf{q}) \rangle_{\hat{\mathbf{q}}} = \frac{g^2}{2} \int \frac{d^3 p}{(2\pi)^3} \partial_k^{(p)} f(\mathbf{p}) \left(-v^k + v^2 \left\langle \frac{q^k}{\mathbf{v} \cdot \hat{\mathbf{q}} - i\epsilon} \right\rangle_{\hat{\mathbf{q}}} \right), \tag{A.7}$$

where

$$\left\langle \frac{q^k}{\mathbf{v} \cdot \hat{\mathbf{q}} - i\epsilon} \right\rangle_{\hat{\mathbf{q}}} = \frac{v^k}{v^2}. \tag{A.8}$$

Hence we find that

$$\langle \Pi^{ii}(0, \mathbf{q}) \rangle_{\hat{\mathbf{q}}} = 0. \tag{A.9}$$

This expression states that the sum of the eigenvalues of Π^{ij}, which is the same as the trace, averaged over all directions of $\hat{\mathbf{q}}$ is zero. Therefore we find two possibilities. Either all eigenvalues are identically zero, or in some direction there must be a negative eigenvalue indicating an instability according to condition 1.

In a next step we show that anisotropic $\mathcal{M}(\hat{\mathbf{p}})$ as defined in (4.33) implies a non-vanishing trace $\Pi^{ii}(0, \mathbf{q})$ for some $\hat{\mathbf{q}}$. Therefore we note that we can write

$$\Pi^{ii}(0, \mathbf{q}) = \left\langle \mathcal{M}(\hat{\mathbf{p}}) \Big(1 + \frac{1}{(\hat{\mathbf{p}} \cdot \hat{\mathbf{q}} - i\epsilon)^2} \Big) \right\rangle_{\hat{\mathbf{p}}}. \tag{A.10}$$

Decomposing $\mathcal{M}(\hat{\mathbf{p}})$ into spherical harmonics gives

$$\mathcal{M}(\hat{\mathbf{p}}) = \sum_{lm} \alpha_{lm} Y_{lm}(\hat{\mathbf{p}}). \tag{A.11}$$

For $\Pi^{ii}(0, \hat{\mathbf{q}})$ we then find

$$\Pi^{ii}(0, \hat{\mathbf{q}}) = \sum_{lm} \kappa_l \alpha_{lm} Y_{lm}(\hat{\mathbf{q}}), \tag{A.12}$$

with

$$\kappa_l \equiv 4\pi \left\langle Y_{lm}^*(\hat{\mathbf{q}}) \Big(1 + \frac{1}{(\hat{\mathbf{p}} \cdot \hat{\mathbf{q}} - i\epsilon)^2} \Big) Y_{lm}(\hat{\mathbf{p}}) \right\rangle_{\hat{\mathbf{p}},\hat{\mathbf{q}}}, \tag{A.13}$$

which does not depend on m because of rotational invariance.

At this point we note that for an anisotropic $\mathcal{M}(\hat{\mathbf{p}})$ at least one of the α_{lm} with $l > 0$ can not vanish. Additionally, from our assumptions that $f(\mathbf{p})$ is parity symmetric, we conclude that l must be even. However, the only way (A.12) vanishes for all $\hat{\mathbf{q}}$ is that $\kappa_l \alpha_{lm}$ is zero. Therefore it remains to check, whether $\kappa_l = 0$ for all even $l > 0$.

To obtain κ_l we choose $m = 0$ in (A.13) and use the Wigner D functions to write the spherical harmonic $Y_{l0}(\hat{\mathbf{p}})$, which is defined with respect to a fixed z axis, in terms of spherical harmonics $Y_{lm'}^{(\hat{\mathbf{q}})}(\hat{\mathbf{p}})$ with respect to the direction $\hat{\mathbf{q}}$. The corresponding identity reads

$$Y_{lm}(\hat{\mathbf{p}}) = \sum_{m'} D_{mm'}^l(\hat{\mathbf{q}}) Y_{lm'}^{(\hat{\mathbf{q}})}(\hat{\mathbf{p}}). \tag{A.14}$$

Let θ_p be the angle between $\hat{\mathbf{p}}$ and $\hat{\mathbf{q}}$, then we can write

$$\left\langle \Big(1 + \frac{1}{(\hat{\mathbf{p}} \cdot \hat{\mathbf{q}} - i\epsilon)^2} \Big) Y_{l0}(\hat{\mathbf{p}}) \right\rangle_{\hat{\mathbf{p}}} = D_{00}^l(\hat{\mathbf{q}}) \left\langle \Big(1 + \frac{1}{(\cos\theta_p - i\epsilon)^2} \Big) Y_{l0}^{(\hat{\mathbf{q}})}(\hat{\mathbf{p}}) \right\rangle_{\hat{\mathbf{p}}}. \tag{A.15}$$

By noting that

$$D_{00}^l(\hat{\mathbf{q}}) = \sqrt{\frac{4\pi}{2l+1}}Y_{l0}(\hat{\mathbf{q}}), \qquad Y_{l0}^{(\hat{\mathbf{q}})}(\hat{\mathbf{p}}) = \sqrt{\frac{2l+1}{4\pi}}P_l(\cos\theta_p), \qquad (A.16)$$

we eventually obtain

$$\kappa_l = 4\pi\left\langle Y_{l0}^*(\hat{\mathbf{q}})Y_{l0}(\hat{\mathbf{q}})\left(1 + \frac{1}{(\cos\theta_p - i\epsilon)^2}\right)P_l(\cos\theta_p)\right\rangle_{\hat{\mathbf{p}},\hat{\mathbf{q}}}$$

$$= \frac{1}{2}\int_{-1}^{1}d(\cos\theta_p)\left(1 + \frac{1}{(\cos\theta_p - i\epsilon)^2}\right)P_l(\cos\theta_p). \qquad (A.17)$$

After performing the remaining integral we end up with [15]

$$\kappa_l = \delta_{l0} - \frac{(-1)^{l/2}\sqrt{\pi}\left(\frac{l}{2}\right)!}{\Gamma\left(\frac{l+1}{2}\right)}, \qquad (A.18)$$

which does not vanish for any even $l > 0$. Therefore we have shown that anisotropic $\mathcal{M}(\hat{\mathbf{p}})$ implies magnetic instabilities.

We only state that the converse can also be proven. That means, if $\mathcal{M}(\hat{\mathbf{p}})$ is isotropic, there is, except from possible normalization factors, no difference to equilibrium distributions and thus there exists no instability.

A.3 Condition 2

The longitudinal polarization of $\mathbf{\Delta}^{-1}$ has always a zero eigenvalue at $\gamma = 0$, because of the Ward identity ($\Pi^{\hat{\mathbf{q}}\nu}(0,\mathbf{q}) = 0$). However this does not rule out the existence of an instability, because there can still be negative eigenvalues for small but non vanishing $\gamma > 0$. For small $\omega = i\gamma$ we obtain

$$\mathbf{\Delta}^{-1}(\omega,\mathbf{q}) = \begin{pmatrix} -\omega^2 + \Pi^{\hat{\mathbf{q}}\hat{\mathbf{q}}}(\omega,\mathbf{q}) & \Pi^{\hat{\mathbf{q}}\top}(\omega,\mathbf{q}) \\ \Pi^{\top\hat{\mathbf{q}}}(\omega,\mathbf{q}) & q^2 - \omega^2 + \mathbf{\Pi}^{\top\top}(\omega,\mathbf{q}) \end{pmatrix}$$

$$\simeq \begin{pmatrix} -\omega^2 + \frac{\omega^2}{q^2}\Pi^{00}(0,\mathbf{q}) & \frac{\omega}{q}\Pi^{0\top}(0,\mathbf{q}) \\ \frac{\omega}{q}\Pi^{\top 0}(0,\mathbf{q}) & q^2 + \mathbf{\Pi}^{\top\top}(0,\mathbf{q}) \end{pmatrix}, \qquad (A.19)$$

with $\top$ denoting the two directions perpendicular to the wave vector. In the last step we set $\omega = 0$ where the leading contribution is not proportional to ω. The small eigenvalue λ of such a matrix is given by

$$\lambda \simeq \frac{\omega^2}{q^2}\left[-q^2 + \Pi^{00} - \Pi^{0\top}[q^2 + \mathbf{\Pi}^{\top\top}]^{-1}\Pi^{\top 0}\right]_{\omega\to i0^+}, \qquad (A.20)$$

where $[q^2 + \mathbf{\Pi}^{\top\top}]^{-1}$ denotes the inverse 2×2 matrix $q^2 + \mathbf{\Pi}^{\top\top}$. The condition for λ to be negative can be written in the form of condition 2 in section 4.3.1.

Appendix B

Analytical late time behavior

For modes with $k = 0$ and $\nu \neq 0$ it is possible to obtain expressions for the late time behavior of single modes analytically, when we expand the expression in the memory integral around $\tau' = \tau$. [26].

B.1 Transversal modes

The expressions for the currents are the same in the 1 and 2 direction when we specialize on modes, whose wave vector is parallel to the anisotropy direction. In this limit we find

$$
\tilde{j}^i(\tau;\nu) = -\frac{m_D^2}{4} \int \frac{d\bar{y}}{(1 + \frac{\tau^2 \sinh^2 \bar{y}}{\tau_{iso}^2})^2} \left\{ \tilde{A}^i(\tau;\nu) - e^{i\nu\bar{\eta}_0} \tilde{A}^i(\tau_0;\nu) \right.
$$
$$
\left. - \int_{\tau_0}^{\tau} d\tau' \frac{i\nu\tau e^{i\nu\bar{\eta}'} \sinh \bar{y}}{\tau_{iso}^2 \sqrt{1 + \frac{\tau^2 \sinh^2 \bar{y}}{\tau'^2}}} \tilde{A}^i(\tau';\nu) \right\}. \tag{B.1}
$$

For simplicity we set $\tilde{A}^i(\tau_0;\nu) = 0$. We then expand the integrand of the memory integral around $\tau' = \tau$, which gives

$$
\frac{i\nu\tau e^{i\nu\bar{\eta}'} \sinh \bar{y}}{\tau_{iso}^2 \sqrt{1 + \frac{\tau^2 \sinh^2 \bar{y}}{\tau'^2}}} = \frac{i\nu\tau}{\tau_{iso}^2} \left(\tanh \bar{y} + i\nu \tanh^2 \bar{y} \left(1 - \frac{\tau}{\tau'}\right) \right.
$$
$$
\left. + \tanh^3 \bar{y} \left(1 - \frac{\tau}{\tau'}\right) + O\left[\left(1 - \frac{\tau}{\tau'}\right)^2\right] \right). \tag{B.2}
$$

We neglect higher orders and, since the integration with respect to $\bar{y}$ is symmetric, the terms odd in $\bar{y}$ give no contribution. Therefore the transverse

current becomes

$$\tilde{j}^i(\tau;\nu) \simeq -\frac{m_D^2}{4} \int \frac{d\bar{y}}{(1+\frac{\tau^2 \sinh^2 \bar{y}}{\tau_{iso}^2})^2} \left\{ \tilde{A}^i(\tau;\nu) \right.$$
$$\left. + \int_{\tau_0}^{\tau} d\tau' \frac{\nu^2 \tau \tanh^2 \bar{y}}{\tau_{iso}^2} \left(1-\frac{\tau}{\tau'}\right) \tilde{A}^i(\tau';\nu) \right\}. \qquad (B.3)$$

In a next step we perform the $\bar{y}$ integral. For the first term we find

$$\int \frac{d\bar{y}}{(1+\frac{\tau^2 \sinh^2 \bar{y}}{\tau_{iso}^2})^2} = \frac{(x^{-2}-2)\arctan(\sqrt{x^{-2}-1})}{(x^{-2}-1)^{3/2}} + \frac{1}{x^{-2}-1}, \qquad (B.4)$$

with $x = \tau_{iso}/\tau \neq 1$. We are interested in the late time behavior when $\tau_{iso} \ll \tau$ such that x is a small quantity. In this limit we obtain

$$\frac{(x^{-2}-2)\arctan(\sqrt{x^{-2}-1})}{(x^{-2}-1)^{3/2}} + \frac{1}{x^{-2}-1} = \frac{\pi x}{2} - \frac{\pi x^3}{4} + O(x^4). \qquad (B.5)$$

For the second term in (B.3) the $\bar{y}$ integration yields

$$\int \frac{d\bar{y} \tanh^2 \bar{y}}{(1+\frac{\tau^2 \sinh^2 \bar{y}}{\tau_{iso}^2})^2} = \frac{(2+x^{-2})\arctan(\sqrt{x^{-2}-1})}{(x^{-2}-1)^{5/2}} - \frac{3}{(x^{-2}-1)^2}$$
$$= \frac{\pi x^3}{2} + O(x^4) \qquad (B.6)$$

for $\tau \gg \tau_{iso}$.

Finally the transverse current becomes

$$\tilde{j}^i(\tau;\nu) \simeq -\frac{\mu}{\tau} \tilde{A}^i(\tau;\nu) - \frac{\mu\nu^2}{\tau^2} \int_{\tau_0}^{\tau} d\tau' \tilde{A}^i(\tau';\nu)\left(1-\frac{\tau}{\tau'}\right), \qquad (B.7)$$

where $\mu = m_D^2 \pi \tau_{iso}/8$ and only terms of order 1 in τ_{iso}/τ have been kept. The equation of motion for the transverse gauge fields are

$$\left(\frac{1}{\tau}\partial_\tau \tau \partial_\tau + \frac{\nu^2}{\tau^2}\right) \tilde{A}^i(\tau;\nu) = \tilde{j}^i(\tau;\nu) \qquad (B.8)$$

and acting with $\partial_\tau^2 \tau^2$ on it we eventually obtain an ordinary differential equation for each mode ν

$$\left(\partial_\tau^2 \tau \partial_\tau \tau \partial_\tau + \nu^2 \partial_\tau^2 + \mu \partial_\tau^2 \tau - \frac{\mu\nu^2}{\tau}\right) \tilde{A}^i(\tau;\nu) \simeq 0. \qquad (B.9)$$

Unfortunately easy expressions for the gauge fields are only found for very infrared modes $\nu \ll 1$, where all terms proportional to ν can be neglected, or for high momentum modes $\nu \gg 1$, where only those terms proportional to ν contribute. We find

$$\tilde{A}^i(\tau; \nu \ll 1) \simeq c_1 J_0(2\sqrt{\mu\tau}) + c_2 Y_0(2\sqrt{\mu\tau}), \tag{B.10}$$

which is a stable oscillatory solution ($J_n(x)$ and $Y_n(x)$ are Bessel functions of the first and second kind, respectively), and

$$\tilde{A}^i(\tau; \nu \gg 1) \simeq c_1 \sqrt{\tau} I_1(2\sqrt{\mu\tau}) + c_2 \sqrt{\tau} K_1(2\sqrt{\mu\tau}), \tag{B.11}$$

with $c_{1,2}$ being constants. The modified Bessel functions K_n and I_n have the asymptotic behavior $K_n(x) \simeq \exp(-x)/\sqrt{2\pi x}$ and $I_n(x) \simeq \exp(x)/\sqrt{2\pi x}$, where the latter describes a rapidly growing mode. Therefore we expect that large ν modes will be dominant at sufficiently late times with a behavior of

$$\tilde{A}^i(\tau) \sim \tau^{1/4} \exp(2\sqrt{\mu\tau}). \tag{B.12}$$

The same behavior is found qualitatively in [29]. For $\nu \sim 1$ the expressions are more complicated, but in [26] it was found that it is possible to write them in terms of generalized hypergeometric functions $_2F_3$ and a Meijer G function. The dominant contribution is

$$\tilde{A}^i(\tau; \nu) \sim \tau_2 F_3 \Big(\frac{3 - \sqrt{1 + 4\nu^2}}{2}, \frac{3 + \sqrt{1 + 4\nu^2}}{2}; 2, 2 - i\nu, 2 + i\nu, -\mu\tau \Big). \tag{B.13}$$

B.2 Longitudinal modes

In this section we want to obtain the late time behavior for longitudinally polarized gauge fields analytically. We proceed similarly to before. When we check for the contribution of the $\tilde{j}_0^\eta$ term numerically, we notice that at late times the contribution is negligible compared to the rest of the current, as can be seen in figure B.1. Therefore we may omit terms proportional to $\tilde{\Pi}^\eta(\tau_0; \nu)$ for the present discussion.

For $k = 0$ and $\nu \neq 0$ the expression for the longitudinal expression is

$$\tilde{j}^\eta(\tau; \nu) = \frac{m_D^2}{2\tau_{iso}^2} \int \frac{d\bar{y}\, \sinh^2 \bar{y}}{(1 + \frac{\tau^2 \sinh^2 \bar{y}}{\tau_{iso}^2})^2} \Bigg\{ \tilde{A}_\eta(\tau; \nu)$$
$$- \int_{\tau_0}^{\tau} d\tau' \frac{i\nu\tau e^{i\nu\bar{\eta}'} \sinh \bar{y}}{\tau'^2 \sqrt{1 + \frac{\tau^2 \sinh^2 \bar{y}}{\tau_{iso}}}} \tilde{A}_\eta(\tau'; \nu) \Bigg\}, \tag{B.14}$$
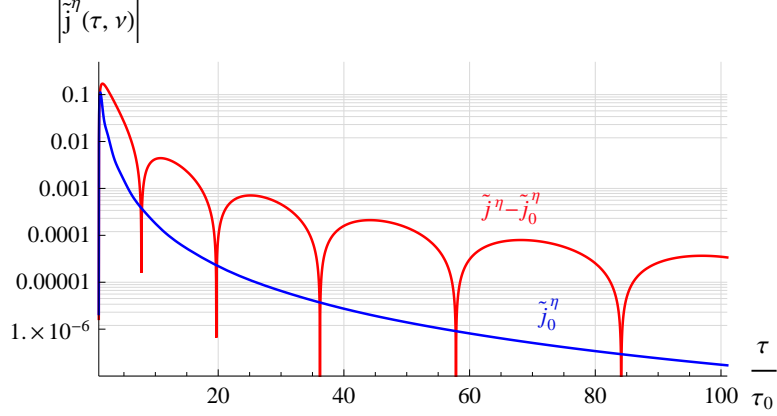
Figure B.1: The contribution from to the current proportional to the initial conjugate momentum $\tilde{j}_0^\eta$ is negligible compared to the rest at late times. This data is for $\nu = 10$ and $\tau_{iso}/\tau_0 = 0.01$.

where we omitted the term proportional to $\tilde{A}_\eta(\tau_0; \nu)$ also. When we replace the factor $1/\tau_{iso}^2$ by $1/\tau'^2$ in (B.2) we can make use of the same expansion and find

$$\tilde{j}^\eta(\tau; \nu) \simeq \frac{m_D^2}{2\tau_{iso}^2} \int \frac{d\bar{y} \sinh^2 \bar{y}}{(1 + \frac{\tau^2 \sinh^2 \bar{y}}{\tau_{iso}^2})^2} \left\{ \tilde{A}_\eta(\tau; \nu) \right.$$
$$\left. + i\nu \tanh^2 \bar{y} \int_{\tau_0}^\tau d\tau' \tilde{A}_\eta(\tau'; \nu) \frac{1}{\tau'^2} \left(1 - \frac{\tau}{\tau'} \right) \right\}. \qquad (B.15)$$

Here, we again neglected higher orders. As before we can perform the $\bar{y}$ integral by finding a function of $x = \tau_{iso}/\tau$, which gives the correct values everywhere except for $x = 1$. For small x we get

$$\int \frac{d\bar{y} \sinh^2 \bar{y}}{(1 + \frac{\tau^2 \sinh^2 \bar{y}}{\tau_{iso}^2})^2} = \frac{\pi x^3}{2} + O(x^4) \qquad (B.16)$$

and

$$\int \frac{d\bar{y} \sinh^2 \bar{y} \tanh^2 \bar{y}}{(1 + \frac{\tau^2 \sinh^2 \bar{y}}{\tau_{iso}^2})^2} = 2x^4 + O(x^5). \qquad (B.17)$$

Eventually the current is given by

$$\tilde{j}^\eta(\tau; \nu) \simeq \frac{2\mu}{\tau^3} \tilde{A}_\eta(\tau; \nu) + \frac{8\mu\nu^2 \tau_{iso}}{\pi \tau^3} \int_{\tau_0}^\tau d\tau' \tilde{A}_\eta(\tau'; \nu) \frac{1}{\tau'^2} \left(1 - \frac{\tau}{\tau'} \right). \qquad (B.18)$$

By acting with $\partial_\tau^2 \tau^2$ on the current we find

$$\partial_\tau^2 \big(\tau^2 \tilde{j}^\eta(\tau; \nu)\big) \simeq 2\mu \partial_\tau^2 \Big(\frac{\tilde{A}_\eta(\tau; \nu)}{\tau}\Big) - \frac{8\mu\nu^2 \tau_{iso}}{\pi \tau^4} \tilde{A}_\eta(\tau; \nu), \tag{B.19}$$

where we can neglect the second part for very large τ. When we only use the first part of the longitudinal current, the equation of motion for the gauge fields eventually becomes

$$\Big(\partial_\tau \frac{1}{\tau} \partial_\tau + \frac{2\mu}{\tau^2}\Big) \tilde{A}_\eta(\tau; \nu) \simeq 0. \tag{B.20}$$

Finally the late time behavior of the longitudinal fields is given by

$$\frac{\tilde{A}_\eta(\tau; \nu)}{\tau} \simeq c_1 J_2(2\sqrt{2\mu\tau}) + c_2 Y_2(2\sqrt{2\mu\tau}). \tag{B.21}$$

This corresponds to stable and oscillatory solutions.

Appendix C

Induced currents

In this appendix we collect the expressions for the induced currents associated with the two initial W fields given in (6.29) and (6.30) in section 6.3. For the first we find

$$
\tilde{j}_{0II}^{\tau}(\tau; k, \nu) = \tau \tilde{j}^{\eta}(\tau_0; k, \nu) \left(\int \frac{d\bar{y} \sinh^2 \bar{y}}{(1 + \frac{\tau_0^2 \sinh^2 \bar{y}}{\tau_{iso}^2})^2} \right)^{-1} \times
$$
$$
\int \frac{d\bar{y} J_0(k\chi_0) e^{i\nu\bar{\eta}_0} \cosh \bar{y} \sinh \bar{y}}{(1 + \frac{\tau^2 \sinh^2 \bar{y}}{\tau_{iso}^2})^2}, \tag{C.1}
$$

$$
\tilde{j}_{0II}^{1}(\tau; k, \nu) = i\tau \tilde{j}^{\eta}(\tau_0; k, \nu) \left(\int \frac{d\bar{y} \sinh^2 \bar{y}}{(1 + \frac{\tau_0^2 \sinh^2 \bar{y}}{\tau_{iso}^2})^2} \right)^{-1} \int \frac{d\bar{y} J_1(k\chi_0) e^{i\nu\bar{\eta}_0} \sinh \bar{y}}{(1 + \frac{\tau^2 \sinh^2 \bar{y}}{\tau_{iso}^2})^2} \tag{C.2}
$$

and

$$
\tilde{j}_{0II}^{\eta}(\tau; k, \nu) = \tilde{j}^{\eta}(\tau_0; k, \nu) \left(\int \frac{d\bar{y} \sinh^2 \bar{y}}{(1 + \frac{\tau_0^2 \sinh^2 \bar{y}}{\tau_{iso}^2})^2} \right)^{-1} \int \frac{d\bar{y} J_0(k\chi_0) e^{i\nu\bar{\eta}_0} \sinh^2 \bar{y}}{(1 + \frac{\tau^2 \sinh^2 \bar{y}}{\tau_{iso}^2})^2}. \tag{C.3}
$$

It is easy to check that the τ and 1 component vanish at $\tau = \tau_0$. For the W field defined in (6.30) the components of the currents are given by

$$
\tilde{j}_{0III}^{\tau}(\tau; k, \nu) = 2i\tilde{j}^{1}(\tau_0; k, \nu) \left(\int \frac{d\bar{y}}{(1 + \frac{\tau_0^2 \sinh^2 \bar{y}}{\tau_{iso}^2})^2} \right)^{-1} \int \frac{d\bar{y} J_1(k\chi_0) e^{i\nu\bar{\eta}_0} \cosh \bar{y}}{(1 + \frac{\tau^2 \sinh^2 \bar{y}}{\tau_{iso}^2})^2}, \tag{C.4}
$$

$$\tilde{j}^1_{0III}(\tau; k, \nu) = \tilde{j}^1(\tau_0; k, \nu) \left(\int \frac{d\bar{y}}{(1 + \frac{\tau_0^2 \sinh^2 \bar{y}}{\tau_{iso}^2})^2} \right)^{-1} \times$$
$$\int \frac{d\bar{y} \big(J_0(k\chi_0) - J_2(k\chi_0) \big) e^{i\nu\bar{\eta}_0}}{(1 + \frac{\tau^2 \sinh^2 \bar{y}}{\tau_{iso}^2})^2} \qquad (C.5)$$

and

$$\tilde{j}^\eta_{0III}(\tau; k, \nu) = \frac{2i}{\tau} \tilde{j}^1(\tau_0; k, \nu) \left(\int \frac{d\bar{y}}{(1 + \frac{\tau_0^2 \sinh^2 \bar{y}}{\tau_{iso}^2})^2} \right)^{-1} \int \frac{d\bar{y} J_1(k\chi_0) e^{i\nu\bar{\eta}_0} \sinh \bar{y}}{(1 + \frac{\tau^2 \sinh^2 \bar{y}}{\tau_{iso}^2})^2}.$$
$$(C.6)$$

Bibliography

[1] J. I. Kapusta and C. Gale, *Finite-Temperature Field Theory: Principles and Applications.* Cambridge Univ. Press, Cambridge, second ed., 2006.

[2] M. LeBellac, *Thermal Field Theory.* Cambridge Univ. Press, Cambridge, paperback ed., 2000.

[3] A. Schmitt, "Thermal Field Theory, WS08/09." Lecture at Vienna University of Technology, 2009.
`http://hep.itp.tuwien.ac.at/~aschmitt/thermal.pdf`.

[4] A. Rebhan, "Thermal gauge field theories," *Lect. Notes Phys.* **583** (2002) 161–208, `arXiv:hep-ph/0105183`.

[5] M. E. Peskin and D. V. Schroeder, *An Introduction to Quantum Field Theory.* Addison-Wesley, Reading, Mass., 1995.

[6] C. Itzykson and J.-B. Zuber, *Quantum Field Theory.* MacGraw-Hill, New York, 1985.

[7] S. Pokorski, *Gauge Field Theories.* Cambridge Univ. Press, Cambridge, second ed., 2000.

[8] A. Rebhan, "HTL perturbation theory and QCD thermodynamics," `arXiv:hep-ph/0111341`.

[9] E. Braaten and R. D. Pisarski, "Soft Amplitudes in Hot Gauge Theories: A General Analysis," *Nucl. Phys.* **B337** (1990) 569.

[10] H. A. Weldon, "Covariant Calculations at Finite Temperature: The Relativistic Plasma," *Phys. Rev.* **D26** (1982) 1394.

[11] J.-P. Blaizot and E. Iancu, "The quark-gluon plasma: Collective dynamics and hard thermal loops," *Phys. Rept.* **359** (2002) 355–528, `arXiv:hep-ph/0101103`.

[12] R. Kobes, G. Kunstatter, and A. Rebhan, "Gauge dependence identities and their application at finite temperature," *Nucl. Phys.* **B355** (1991) 1–37.

[13] P. Romatschke and M. Strickland, "Collective Modes of an Anisotropic Quark-Gluon Plasma," *Phys. Rev.* **D68** (2003) 036004, `arXiv:hep-ph/0304092`.

[14] P. Romatschke and M. Strickland, "Collective modes of an anisotropic quark-gluon plasma. II," *Phys. Rev.* **D70** (2004) 116006, `arXiv:hep-ph/0406188`.

[15] P. Arnold, J. Lenaghan, and G. D. Moore, "QCD plasma instabilities and bottom-up thermalization," *JHEP* **08** (2003) 002, `arXiv:hep-ph/0307325`.

[16] M. Strickland, "Thermalization and plasma instabilities," *Nucl. Phys.* **A785** (2007) 50–57, `arXiv:hep-ph/0608173`.

[17] N. A. Krall and A. W. Trivelpiece, *Principles of plasma physics*. MacGraw-Hill, New York, 1973.

[18] R. C. Davidson, "Kinetic waves and instabilities in a uniform plasma," in *Basic Plasma Physics*, A. A. Galeev and R. N. Sudan, eds. North Holland, Amsterdam, paperback ed., 1989.

[19] F. F. Chen, *Introduction to Plasma Physics and controlled Fusion, Vol. 1*. Springer, New York, second ed., 1983.

[20] E. S. Weibel, "Spontaneously Growing Transverse Waves in a Plasma Due to an Anisotropic Velocity Distribution," *Phys. Rev. Lett.* **2** (1959) 83–84.

[21] S. Mrowczynski, "Plasma instability at the initial stage of ultrarelativistic heavy ion collisions," *Phys. Lett.* **B314** (1993) 118–121.

[22] S. Mrowczynski, "Color collective effects at the early stage of ultrarelativistic heavy ion collisions," *Phys. Rev.* **C49** (1994) 2191–2197.

[23] A. Rebhan, P. Romatschke, and M. Strickland, "Hard-loop dynamics of non-Abelian plasma instabilities," *Phys. Rev. Lett.* **94** (2005) 102303, `arXiv:hep-ph/0412016`.

[24] P. Arnold, G. D. Moore, and L. G. Yaffe, "The fate of non-abelian plasma instabilities in 3+1 dimensions," *Phys. Rev.* **D72** (2005) 054003, `arXiv:hep-ph/0505212`.

[25] A. Dumitru and Y. Nara, "QCD plasma instabilities and isotropization," *Phys. Lett.* **B621** (2005) 89–95, `arXiv:hep-ph/0503121`.

[26] P. Romatschke and A. Rebhan, "Plasma Instabilities in an Anisotropically Expanding Geometry," *Phys. Rev. Lett.* **97** (2006) 252301, `arXiv:hep-ph/0605064`.

[27] A. Rebhan, M. Strickland, and M. Attems, "Instabilities of an anisotropically expanding non-Abelian plasma: 1D+3V discretized hard-loop simulations," *Phys. Rev.* **D78** (2008) 045023, `arXiv:0802.1714 [hep-ph]`.

[28] J. D. Bjorken, "Highly Relativistic Nucleus-Nucleus Collisions: The Central Rapidity Region," *Phys. Rev.* **D27** (1983) 140–151.

[29] P. Romatschke and R. Venugopalan, "The unstable Glasma," *Phys. Rev.* **D74** (2006) 045011, `arXiv:hep-ph/0605045`.

[30] K. Fukushima, F. Gelis, and L. McLerran, "Initial Singularity of the Little Bang," *Nucl. Phys.* **A786** (2007) 107–130, `arXiv:hep-ph/0610416`.

[31] E. Iancu and R. Venugopalan, "The color glass condensate and high energy scattering in QCD," `arXiv:hep-ph/0303204`.

[32] P. Arnold, J. Lenaghan, G. D. Moore, and L. G. Yaffe, "Apparent thermalization due to plasma instabilities in quark gluon plasma," *Phys. Rev. Lett.* **94** (2005) 072302, `arXiv:nucl-th/0409068`.

[33] A. Rebhan, P. Romatschke, and M. Strickland, "Dynamics of quark-gluon plasma instabilities in discretized hard-loop approximation," *JHEP* **09** (2005) 041, `arXiv:hep-ph/0505261`.

[34] P. Arnold and G. D. Moore, "Non-Abelian Plasma Instabilities for Extreme Anisotropy," *Phys. Rev.* **D76** (2007) 045009, `arXiv:0706.0490 [hep-ph]`.

[35] D. Bodeker and K. Rummukainen, "Non-abelian plasma instabilities for strong anisotropy," *JHEP* **07** (2007) 022, `arXiv:0705.0180 [hep-ph]`.

[36] P. Arnold, "Quark-Gluon Plasmas and Thermalization," *Int. J. Mod. Phys.* **E16** (2007) 2555–2594, `arXiv:0708.0812 [hep-ph]`.

[37] A. Rebhan, "Hard loop effective theory of the (anisotropic) quark gluon plasma," *Prog. Part. Nucl. Phys.* **62** (2009) 518–528, `arXiv:0811.0457 [hep-ph]`.

[38] S. Mrowczynski and M. H. Thoma, "What do electromagnetic plasmas tell us about quark-gluon plasma?," *Ann. Rev. Nucl. Part. Sci.* **57** (2007) 61–94, `arXiv:nucl-th/0701002`.